Soluble HLA-G binds to dendritic cells which likely suppresses anti-tumour immune responses in regional lymph nodes in ovarian carcinoma

Lösliches HLA-G wird von dendritischen Zellen gebunden, was beim Ovarialkarzinom zur Hemmung von Immunraktionen in regionalen Lymphknoten führen kann

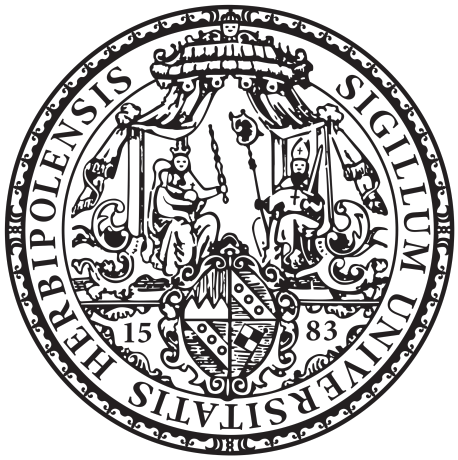

Doctoral thesis for a doctoral degree
at the Department for Gynaecology and Obstetrics,
University hospital Würzburg
and Graduate School of Life Sciences,
Julius-Maximilians-Universität Würzburg
Section: Infection and immunity

submitted by
Valentin Stefan Bruttel
from
Villingen-Schwenningen

Würzburg, 2015

Submitted on: .....

Members of the *Promotionskomitee:*

Chairperson: Prof. Dr. Thomas Hünig

Primary Supervisor: Prof. Dr. Jörg Wischhusen

Supervisor (Second): Prof. Dr. Thomas Rudel

Supervisor (Third): Dr. Thomas Joos

Date of Public Defence: .....

Date of receipt of Certificates: .....

For Anna, Linus, Elea & Jorin

Table of contents

Abbreviations

ACD-A	acid citrate dextrose solution A
ALDH	aldehyde dehydrogenase
APC	antigen presenting cells
APC	allophycocyanin
APS	ammonium peroxodisulfate
BHQ	black hole quencher
Bp, kb	base pair(s); kilo base pairs
BRCA	breast cancer susceptibility protein
BSA	bovine serum albumin
CD	cluster of differentiation
cDNA	complementary DNA
Da	dalton
DAPI	4', 6-diamidino-2-phenylindole
DC	dendritic cells
DMSO	dimethyl sulfoxide
DNA	deoxyribonucleic acid
ECL	enhanced chemiluminescence
EDTA	Ethylenediaminetetraacetic acid
FAM	6-FAM phosphoramidite
FCS	fetal calf serum
FFPE	formalin-fixed, paraffin-embedded
FIGO	International Federation of Gynaecology and Obstetrics
FITC	fluorescein isothiocyanate
GM-CSF	granulocyte-macrophage colony-stimulating factor
H&E stain	hematoxylin and eosin stain
hAB	human serum from blood group AB donor
HER2	human epidermal growth factor receptor 2
HLA	human leukocyte antigen
HRP	horseradish peroxidase
IDO	indoleamine-2,3-dioxygenase
IF	immunofluorescence
IFN	interferon
IHC	immunohistochemistry
IL	interleukin
ILT	immunoglobulin-like transcript
ITIM	immunoreceptor tyrosine-based inhibitory motif
KIR	killer cell immunoglobulin-like receptor

Lck	Lymphocyte-specific protein tyrosine kinase
LILR	leukocyte immunoglobulin-like receptor
LN	lymph node
LPS	lipopolysaccharide
MHC	major histocompatibility complex
mRNA	messenger RNA
NK cell	natural killer cell
Nll	nodi lymphatici (lymph nodes)
PBL	peripheral blood lymphocyte
PBMC	peripheral blood mononuclear cells
PBS	phosphate buffered saline
PCR	polymerase chain reaction
PE	phycoerythrin
PFA	Paraformaldehyde
PHA	phytohaemagglutinin (here phytohaemagglutinin L or leucoagglutinin)
RB1	retinoblastoma protein
rh	rekombinant human
RNA	Ribonucleic acid
RPMI	Roswell Park Memorial Institute, developed RPMI1640 medium
scHLA-G5	single-chain HLA-G5
SDS-PAGE	sodium dodecyl sulfate polyacrylamide gel electrophoresis
sHLA-G	soluble HLA-G
SN	supernatant
TAMRA	carboxytetramethylrhodamine
TMA	tissue microarray
T_{reg}	regulatory T cell
WB	Western Blot
β2m	β2-microglobulin

Zusammenfassung

Einleitung

HLA-G, ein nicht-klassisches HLA bzw. MHC Klasse Ib Molekül, kann sowohl als membrangebundenes als auch als lösliches Molekül verschiedenste Immunzellpopulationen effektiv inhibieren. Unter physiologischen Bedingungen wird HLA-G vor allem in der Plazenta exprimiert, wo es dazu beiträgt den semiallogenen Embryo vor einer Abstoßung durch das mütterliche Immunsystem zu beschützen. Außerdem wird HLA-G in einer Vielzahl von Tumoren wie zum Beispiel in Ovarialkarzinomen überexprimiert. Ziel dieser Arbeit war es besonders die Rolle von löslichem HLA-G im Ovarialkarzinom und die Expression von HLA-G in verschiedenen Subtypen des Ovarialkarzinoms genauer zu untersuchen.

Ergebnisse

Anhand eines Tissue Microarrays wurde bestätigt dass HLA-G unter physiologischen Bedingungen nur in sehr wenigen Geweben wie Plazenta oder Testes exprimiert wird. Außerdem wurden erstmals auch im Nebennierenmark hohe Expressionslevel detektiert. Im Gegensatz zur physiologischen Expression wurde HLA-G in serösen, muzinösen, endometrioiden und Klarzellkarzinomen und somit in Tumoren aller untersuchten Subtypen des Ovarialkarzinoms detektiert. Am häufigsten war HLA-G in hochgradigen serösen Karzinomen überexprimiert. Hier konnte gezeigt werden dass auf Genexpressionslevel in Ovarialkarzinomen die Expression des immunsuppressiven HLA-G mit der Expression von klassischen MHC Molekülen wie HLA-A, -B oder -C hochsignifikant korreliert. Außerdem konnte in Aszitesproben von Patientinnen mit Ovarialkarzinomen hohe Konzentrationen von löslichem HLA-G nachgewiesen werden. Auch auf metastasierten Tumorzellen in regionalen Lymphknoten war HLA-G nachweisbar. Überraschenderweise wurde aber besonders viel HLA-G auf Dendritischen Zellen in Lymphknoten detektiert. Da in Monozyten und Dendritischen Zellen von gesunden Spendern durch IL-4 oder IL-10 im Gegensatz zu Literatur keine Expression von HLA-G induzierbar war, untersuchten wir ob Dendritische Zellen lösliches HLA-G binden. Es konnte gezeigt werden, dass besonders Dendritische Zellen die in Gegenwart von IL-4, IL-10 und GM-CSF aus Monozyten generiert wurden (DC-10) effektiv

lösliches HLA-G über ILT Rezeptoren binden. In Abhängigkeit von ihrer Beladung mit HLA-G hemmen auch fixierte DC-10 Zellen noch die Proliferation von zytotoxischen $CD8^+$ T Zellen. Zudem wurden regulatorische T Zellen induziert.

Schlussfolgerungen

Besonders in den am häufigsten diagnostizierten hochgradigen serösen Ovarialkarzinomen ist HLA-G in den meisten Fällen überexprimiert. Durch die Expression immunsuppressiver MHC Klasse Ib Moleküle wie HLA-G können wahrscheinlich auch Tumore wachsen, die noch klassische MHC Moleküle exprimieren und aufgrund ihrer Mutationslast eigentlich vom Immunsystem erkannt und eliminiert werden müssten. Lösliches HLA-G könnte zudem lokal Immunantworten gegen Tumorantigene unterdrücken indem es an Dendritische Zellen in regionalen Lymphknoten bindet. Diese Zellen präsentieren nomalerweise zytotoxischen T Zellen Tumorantigene und spielen daher eine entscheidende Rolle in der Entstehung von protektiven Immunantworten. Mit löslichem HLA-G beladene Dendritische Zellen hemmen jedoch die Proliferation von $CD8^+$ T Zellen und induzieren regulatorische T Zellen. Dadurch könnten Ovarialkarzinome “aus der Ferne” auch in metastasenfreien Lymphknoten die Entstehung von gegen den Tumor gerichteten Immunantworten unterdrücken. Dieser erstmals beschriebene Mechanismus könnte auch in anderen malignen Erkrankungen eine Rolle spielen, da lösliches HLA-G in einer Vielzahl von Tumorindikationen nachgewiesen wurde.

Abstract

Background

HLA-G is a non-classical MHC class I molecule which exerts strong immunosuppressive effects on various immune cells. Several membrane-bound and soluble isoforms are known. Physiologically, HLA-G is predominantly expressed in the placenta, where it contributes to protecting the semi-allogeneic embryo from rejection by the maternal immune system. However, HLA-G is also often upregulated during tumourigenesis, such as in ovarian cancer. The aim of this thesis is to investigate how soluble HLA-G may contribute to local immunosuppression in ovarian carcinomas, and to characterize HLA-G expression in different ovarian carcinoma subtypes and metastases.

Results

As reported by others, physiological HLA-G expression is restricted to few tissues, such as placenta and testes. Here, HLA-G was also detected in the medulla of the adrenal gland. In contrast, HLA-G expression was frequently detected in tumours of all assessed subtypes of ovarian carcinomas (serous, mucinous, endometrioid and clear cell). Highest expression levels were detected in high-grade serous carcinomas. In primary tumours, expression of HLA-G correlated with expression of classical MHC class I molecules HLA-A, -B and -C. Surprisingly, high levels of HLA-G were also detected on dendritic cells in local lymph nodes. As no expression of HLA-G was inducible in monocytes or dendritic cells from healthy donors in response to IL-10 or IL-4, we speculated that tumour-derived soluble HLA-G might be transferred to dendritic cells via the lymphatic system. Accordingly, high levels of tumour-derived soluble HLA-G were detected in ovarian cancer ascites samples. In vitro, dendritic cells expanded in the presence of IL-4, IL-10 and GM-CSF (DC-10) were particularly prone to binding high amounts of soluble HLA-G via ILT receptors. Furthermore, HLA-G loaded DC-10 cells inhibited the proliferation of CD8 effector cells and induced regulatory T cells, even when the DC-10 cells had been fixed with paraformaldehyde.

Conclusion

The immunosuppressive molecule HLA-G is overexpressed in high-grade serous ovarian carcinomas, which account for the majority of ovarian cancers. In particular tumours with a high mutational burden and intact expression of classical, immunogenic MHC class Ia molecules may use HLA-G to escape from immunosurveillance. Additionally, tumour-derived soluble HLA-G may inhibit adaptive immune responses by binding to dendritic cells in local lymph nodes. Dendritic cells usually play a decisive role in the initiation of adaptive anti-tumour immune responses by presenting tumour antigens to cytotoxic T cells. In contrast, dendritic cells loaded with soluble HLA-G inhibit the proliferation of effector T cells and promote the induction of regulatory T cells. Thus, soluble HLA-G that is transferred to dendritic cells via lymphatic vessels may enable ovarian carcinomas to remotely suppress anti-tumour immune responses in local lymph nodes. This novel immune-escape mechanism may also exist in other solid tumours that express HLA-G.

1 Introduction

1.1 Ovarian cancer

1.1.1 Epidemiology, staging and risk factors

220 000 women are diagnosed with ovarian cancer each year, and although treatment methods are continuously improving, 60% of these patients will die from the malignancy (Jayson *et al.* 2014). In the US, ovarian cancer is the most common cancer of the reproductive tract and the fifth most common cause of cancer related deaths in women (CDC cancer statistics 1999-2011, www.cdc.gov/uscs). This equals to a lifetime risk of about 1.7% in more developed nations (Jemal *et al.* 2011). The median age at diagnosis is 63 (Jayson, Kohn et al. 2014). It has been shown that the use of oral contraception and pregnancies reduce the risk for developing ovarian cancer, possibly due to a reduced number of ovulations (Tsilidis *et al.* 2011). Factors that increase the risk for some ovarian cancer subtypes include obesity, menopausal hormone therapy (Yang *et al.* 2012), smoking (Collaborative Group on Epidemiological Studies of Ovarian *et al.* 2012) and hereditary risk factors such as BRCA mutations (Miki *et al.* 1994, Wooster *et al.* 1995). Ovarian cancer is most often staged by the FIGO (International Federation of Gynaecology and Obstetrics) system (Shepherd 1989). Here, spreading of the primary tumour (T) and metastases in lymph nodes (N) and distant organs (M) are taken into account. Briefly, stage I tumours are confined to the ovaries or fallopian tubes, stage II tumours have metastasized within the pelvis, stage III tumours have metastasized to retroperitoneal or extra-pelvic areas and stage IV tumours have metastasized to extra peritoneal organs, such as lungs, spleen or liver (Prat and Oncology 2014). Historically, well differentiated, moderately differentiated, poorly differentiated or undifferentiated ovarian carcinomas were graded from G1 to G4, respectively (Shepherd 1989). More recently, the World Health Organisation has adopted an alternative classification for ovarian carcinomas. Accordingly, ovarian carcinomas are classified either as low-grade, less aggressive type I and high grade, more aggressive type II tumours based on morphological markers and commonly detected mutations (Shih Ie and Kurman 2004). This system may be particularly useful for predicting the response to chemotherapeutic agents (Silverberg 2000).

1.1.2 Histopathological subtypes

About 90% of ovarian cancers in woman age 20 or older are classified as adenocarcinomas or surface-epithelial-stromal tumours (Ries 2007). Other ovarian cancers include undefined carcinomas or sex cord-stromal tumours, mullerian tumours and germ cell tumours. Due to the high prevalence of adenocarcinomas, this thesis focuses on these subtypes.

Most ovarian carcinomas are serous ovarian carcinomas, accounting for about 75% (70% high-grade, 5% low grade) of all cases (Prat 2012). About 10% each are diagnosed as endometrioid or clear cell carcinomas (Prat 2012), the latter being almost exclusively high-grade tumours (Tan and Kaye 2007). Mucinous tumours account for about 3% of ovarian carcinomas and are more frequently confined to the ovaries, however, usually less chemosensitive (Harrison *et al.* 2008, Prat 2012). Examples of H&E stained ovarian carcinoma subtypes are shown in Figure 1, a graphical overview of common ovarian carcinoma subtypes, frequencies and associated mutations is given in Figure 2.

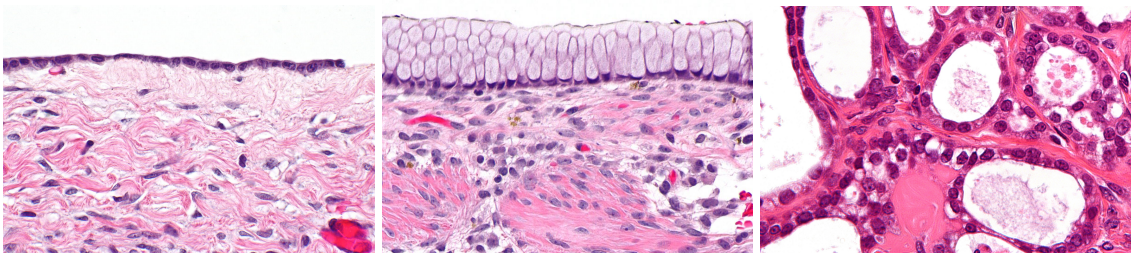

Figure 1: H&E stained serous, mucinous and clear cell ovarian carcinomas
Micrographs of haematoxylin and eosin stained formalin-fixed, paraffin-embedded (FFPE) sections of serous (left), mucinous (centre) and clear cell (right) ovarian carcinomas (copyright © 2011 „Nephron“, published under GNU creative commons licence).

1.1.3 Molecular pathogenesis

Low grade serous, mucinous and clear cell ovarian carcinomas may develop in a step-wise manner from benign to borderline to malignant ovarian cysts (Kurman 2013). Here, genes such as *BRAF, KRAS* and *ERBB2* (also known as *HER2/neu*) that code for proteins involved in signalling pathways are frequently mutated or amplified (Vang *et al.* 2009). In comparison to high grade ovarian carcinomas, these tumours are genetically more stable (Kurman 2013). High-grade ovarian carcinomas are thought to originate from the fallopian tube (Lee *et al.* 2007, Shaw *et al.* 2009). In most of these genetically less stable tumours, mutations in the tumour suppressor gene *TP53* are detectable, and mutations in *BRCA1* or *2* or *RB1* genes are also mostly found in this subtype (Banerjee and Kaye 2013, Kurman 2013). Further genes frequently mutated in different ovarian cancer subtypes are listed in Figure 2.

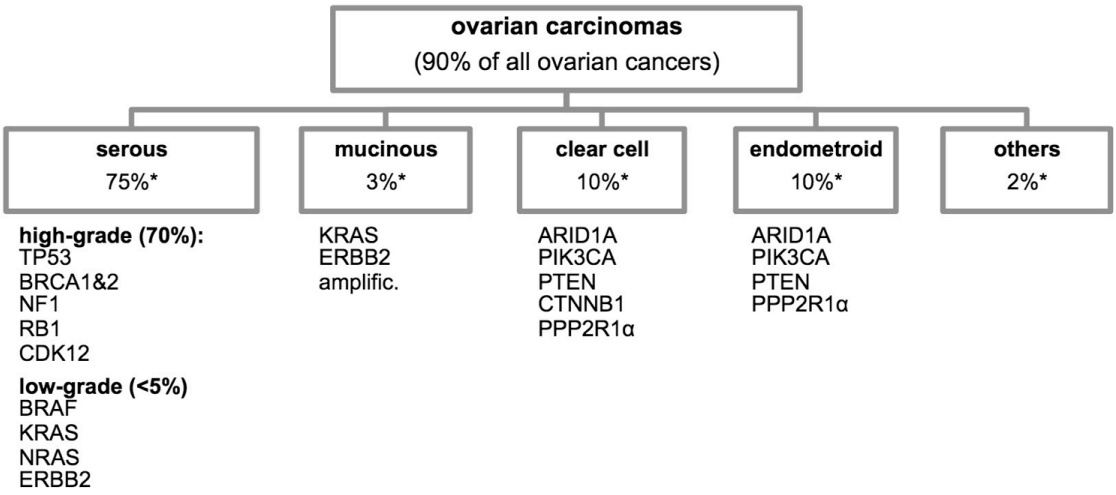

Figure 2: Common subtypes of ovarian carcinomas and associated genetic alterations
About 90% of all ovarian cancers are carcinomas. Among these, serous carcinomas are the most common subtype, followed by endometrioid, clear cell and mucinous carcinomas. As depicted, different genetic alterations typically occur in histologically different subtypes or low-grade and high-grade tumours (%* = percentage of ovarian carcinomas, not all ovarian cancers, frequencies slightly vary depending on source, adapted from (Banerjee and Kaye 2013), frequencies from (Prat 2012)).

1.1.4 Diagnosis and treatment

If detected at early stages, ovarian carcinomas are mostly curable (Jayson, Kohn *et al*. 2014). However, due to a lack of specific early symptoms, ovarian cancer has been termed the "silent" or "whispering" disease (Goff 2012, Smith 2006). Thus, most patients are only diagnosed in late stages of tumour development (mostly FIGO stage III) (Jayson, Kohn *et al*. 2014, Prat and Oncology 2015). Even yearly screening programs based on ultrasound and measuring serum concentrations of the tumour marker CA-125 have failed to reduce ovarian cancer associated mortality (Buys *et al.* 2011). Instead, it was found that such screening (Partridge *et al.* 2009) gives rise to numerous unnecessary surgical interventions and should not be recommended (Clarke-Pearson 2009). In addition to distant metastases, most primary serous high-grade tumours already have a diameter of more than 15 cm when ovarian cancer is diagnosed (Levy and Purcell 2013).

Irrespective of the tumour subtype, ovarian carcinomas are usually treated surgically, with chemotherapeutics, in some cases with radiotherapy (Jayson, Kohn *et al*. 2014) and with anti-VEGF antibodies. Usually, the ovaries, fallopian tubes, the uterus, the omentum majus and as much of the detectable tumour mass as possible are surgically removed (debulking) (Eisenkop *et al.* 1998, King *et al.* 2003). First line chemotherapy for advanced tumours most commonly consists of DNA-crosslinking platinum-based chemotherapeutics (carboplatin or cisplatin) in combination with taxanes (paclitaxel or docetaxel) that disrupt microtubule formation (Jayson, Kohn *et al*. 2014). Radiation therapy has only been proven to be effective for certain subtypes of low-grade ovarian cancer (Hoskins *et al.* 2012) as well as for palliative treatment of metastases (Rodriguez *et al.* 1992). More recent clinical studies have shown that anti-VEGF antibodies (Bevacizumab) can prolong progression free survival for a few months (Aghajanian *et al.* 2012, Garcia and Singh 2013, Perren *et al.* 2011, Pujade-Lauraine *et al.* 2014).

1.2 Ovarian cancer and immune escape

1.2.1 Mechanisms of tumour suppression

Like any other cancer, ovarian carcinomas are caused by accumulating genetic alterations that promote cell growth and survival and prevent cell cycle arrest or the induction of apoptosis. It has been estimated that more than one million molecular lesions occur in each cell every day (Lodish H *et al.* 2004). Most of these are instantly repaired or not affecting the malignant potential of a cell. However, if several decisive pathways and intracellular control mechanisms (or hallmarks of cancer (Hanahan and Weinberg 2000)) are altered within one cell, this cell may finally initiate a tumour.

However, these control mechanisms are not limited to intracellular proteins and pathways. As included in a recent update to the hallmarks of cancer (Hanahan and Weinberg 2011), cancer cells must also escape from immunosurveillance. This concept was first systematically introduced by Burnet in the 70s of the last century (Burnet 1970). It has become evident that the innate immune system can be seen as a first line of defence against malignant cells, which initiates adaptive immune responses (Diefenbach and Raulet 2002) that in most cases contain malignant cells in microscopic lesions for a lifetime. Such oncogenic stress can induce the upregulation of innate natural killer (NK) cell receptors (Raulet and Guerra 2009). Furthermore, non-silent mutations that accumulate in protein-coding regions lead to the emergence of novel tumour-specific peptides that are presented to adaptive T cells via major histocompatibility complex (MHC) molecules (Diefenbach and Raulet 2002, Schumacher and Schreiber 2015, Sensi and Anichini 2006).

1.2.2 Tumour immune escape

Many researchers have addressed the question why these sophisticated control mechanisms sometimes fail to prevent tumours from growing into organ-sized masses as frequently observed particular in ovarian cancer. Here, it has been shown that cancer cells may adapt in an evolutionary manner to immunological assaults. This involves two key processes: the upregulation of immunosuppressive molecules (immunosubversion) and

the loss of immunogenic targets on tumour cells (immunoediting) (reviewed by Zitvogel *et al.* 2006). These processes have been integrated into a model that nicely correlates with clinical observations and describes three phases of tumour immune escape: elimination, equilibrium, and escape. Briefly, it proposes that malignant cells that are not detected and destroyed by the innate or adaptive immune system in the elimination phase may still be contained in equilibrium over prolonged periods of time. During this time, they may accumulate further mutations that may finally enable them to escape from immunosurveillance (Dunn *et al.* 2002, Dunn *et al.* 2004, Mittal *et al.* 2014).

The existence of tumour latency has also been demonstrated in a mouse study where low doses of carcinogens usually induced a small number of stable malignant cells, that only started growing into clinically detectable tumours when T cells were depleted (Koebel *et al.* 2007). These microtumours may be contained by similar processes as during tumour dormancy, the period spanning the depletion of all clinically detectable tumour masses and recurrence, which can also last for decades. (Aguirre-Ghiso 2007). However, this model does not satisfyingly explain why malignant cells that can be constrained by the immune system are not immediately eliminated, or why cells that are not eliminated during the equilibrium do not immediately grow into overt tumours.

1.2.3 Cancer stem cells in tumour immune escape

We have suggested that the equilibrium phase may be maintained by immune-privileged, yet niche-restricted premalignant cancer stem cells (Bruttel and Wischhusen 2014). In ovarian cancer, different markers including CD133 (Baba *et al.* 2009), ALDH1 (Landen *et al.* 2010) and CD44 (Zhang *et al.* 2008) have been associated with the cancer stem cell phenotype. Stem cells are usually rare, exceptionally long-lived and highly resistant towards chemotherapeutic agents and have thus long been suspected to be the culprits of tumour development or recurrence (reviewed by Lobo *et al.* 2007, Reya *et al.* 2001). However, at least physiological stem cells are constrained to defined niches (Li and Neaves 2006). Additionally, stem cells and cancer stem cells possess unique immunological properties, which may explain why cancer stem cells may not be immunologically eliminated during the early phases of tumourigenesis (Bruttel and Wischhusen 2014). Thus, as depicted in Figure 3, cancer stem cells may play a decisive role in tumour development and immune escape in ovarian carcinomas.

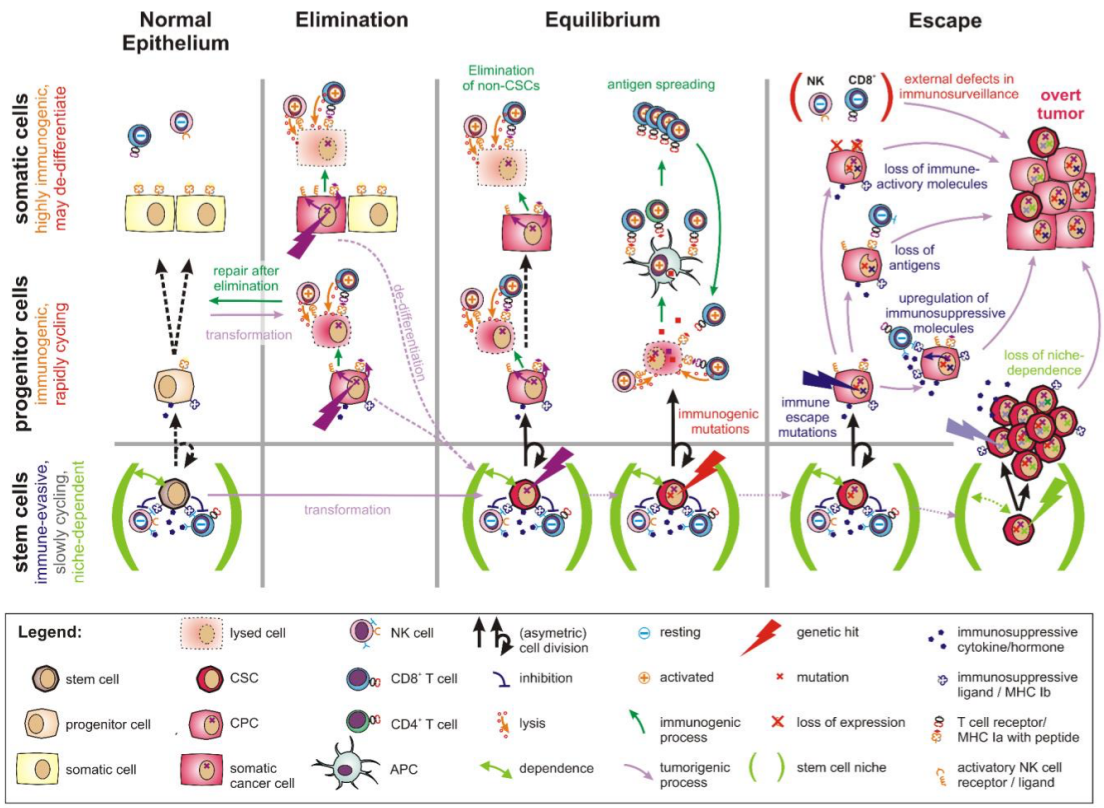

Figure 3: Cellular and molecular processes in tumour immune escape

Tissue homeostasis in **normal epithelium**. During organogenesis or in response to tissue damage, rare stem cells are activated to undergo asymmetric divisions that produce more differentiated progenitor cells. Progenitor cells regenerate tissue through symmetric cell divisions. The resulting daughter cells further differentiate and acquire organ-specific functions while their ability to re-enter the cell cycle is gradually lost. When healthy cells acquire mutations, malignant transformation can occur as a multi-step process that can be divided into different phases:

Elimination. Malignant mutations occurring in somatic cells or progenitor cells are likely to be detected by the immune system due to oncogenic stress-induced ligands for activator NK cell receptors and tumour antigen presentation via MHC class Ia. These cells are subsequently eliminated, resulting in the restoration of normal epithelium. However, mutated cells may in some cases escape from immunosurveillance by de-differentiating into less immunogenic stem cells.

Equilibrium. If an oncogenic mutation occurs in an immune-evasive stem cell, this cell may not be eliminated by the immune system due to its low expression of immunostimulatory and high expression of immunosuppressive molecules. However, such premalignant stem cells may not immediately grow into overt tumours as they cycle slowly, depend on stem cell niches and naturally undergo only asymmetric divisions. Their more immunogenic daughter cells, however, may constantly be eliminated by the adaptive immune system. Over decades, such mutated stem cells can accumulate further genetic alterations. Thus, novel tumour-specific antigens may emerge, which can be taken up and presented by APCs to induce activation and expansion of tumour-specific T cells. This would lead to antigen spreading which strengthens tumour immunosurveillance and stabilizes the equilibrium.

Escape. Immune escape mutations occurring in CSCs or premalignant daughter cells may finally lead to tumour outgrowth. Particular risks may be associated with genetic alterations leading to the loss of immune-activatory molecules (like MHC molecules or NK cell receptor ligands), or to loss of immunogenic tumour antigens or to the upregulation of immunosuppressive factors. Furthermore, immunosenescence or therapeutically induced immunosuppression may limit immunosurveillance and thus enable more immunogenic tumours to grow. Alternatively, poorly immunogenic CSCs may lose their niche dependence and expand to form poorly differentiated tumours. (Figure and Figure legend: (Bruttel and Wischhusen 2014)).

1.2.4 Immune escape mechanisms in ovarian cancer

Numerous immune escape mechanisms have been reported to occur in ovarian cancer. Ovarian cancer derived macrophage migration inhibitory factor (MIF), for example, induces the downregulation of activatory NK cell receptors (Krockenberger *et al.* 2008). Furthermore, immunosuppressive cytokines TGF-β and IL-10 are frequently detected in the tumour microenvironment (Loercher *et al.* 1999, Zitvogel, Tesniere *et al*. 2006). Prostaglandin E2 not only inhibits immune effector cells such as macrophages (Harris *et al.* 2002), but may also promote metastasis (Spinella *et al.* 2004). Vascular endothelial growth factor (VEGF) may not only promote vascularisation, but also suppress immune effector cells (Kandalaft *et al.* 2011). Furthermore, ovarian carcinoma cells express the immunosuppressive surface molecules CD200 (Siva *et al.* 2008) and indoleamine-2,3-dioxygenase (IDO), which arrests T cell proliferation (Qian *et al.* 2009). The ectonucleotidases CD39 and CD73 that generate immunosuppressive adenosine are also overexpressed in ovarian cancer (Hausler *et al.* 2011). Classical human leukocyte antigens (HLA) class Ia molecules or proteins of the antigen processing machinery are often not detectable in late stage ovarian carcinomas, which correlates with a poor prognosis (Han *et al.* 2008, Vitale *et al.* 2005). In contrast, the immunosuppressive, nonclassical MHC Ib molecule HLA-G is frequently expressed in ovarian cancer (Sheu and Shih Ie 2007). The important role of HLA-G in ovarian carcinoma will subsequently be discussed in detail.

Combined, these effects generate an immunosuppressive tumour microenvironment that locally promotes immunological tolerance towards ovarian cancer cells (Yigit *et al.* 2010). Accordingly, immunosuppressive regulatory T cells are frequently detected in late-stage ovarian cancers (Woo *et al.* 2001), and myeloid derived suppressor cells (Yigit, Massuger *et al*. 2010) are associated with an unfavourable clinical outcome. On the other hand, tumour-infiltrating $CD8^+$ effector T cells (Sato *et al.* 2005) and dendritic cells (Eisenthal *et al.* 2001) are indicators of a good prognosis. Immunosuppressive molecules expressed by ovarian cancer cells as well as affected immune cells are also shown in Figure 4.

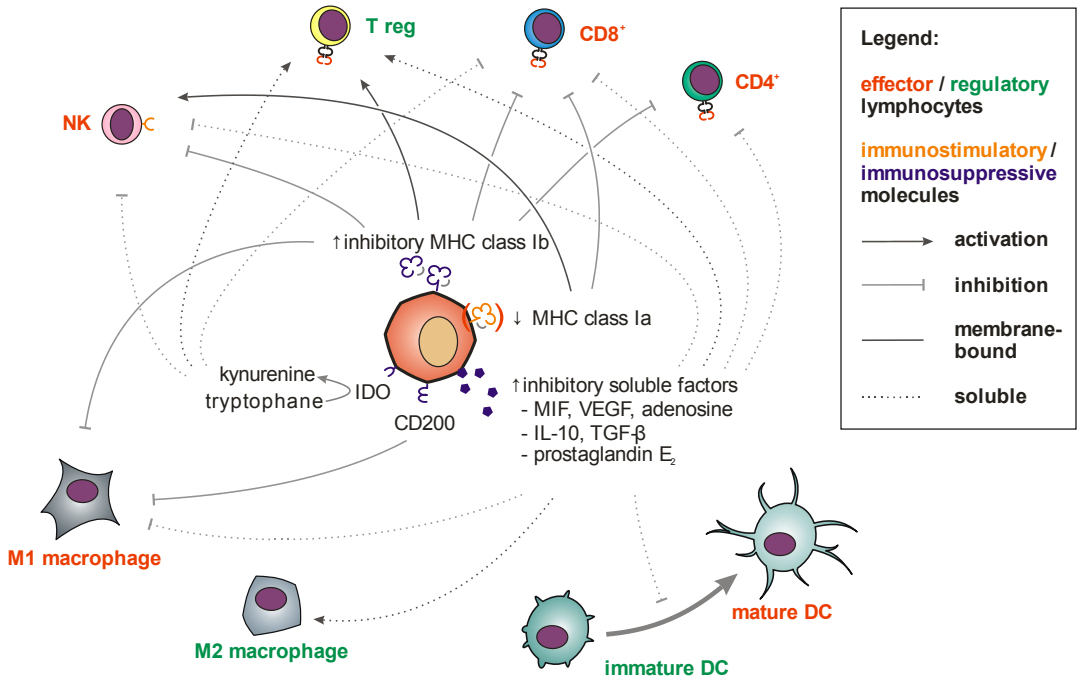

Figure 4: Immune escape mechanisms in ovarian cancer and affected immune cells
Immunosuppressive molecules secreted by or expressed on the surface of ovarian carcinoma cells (red cell, centre) and intratumoral immune cell subpopulations that are affected by these molecules are shown. See main text for references.

1.3 HLA-G

1.3.1 MHC molecules

HLA-G is a non-classical major histocompatibility complex (MHC) class Ib molecule. In humans, genes coding for antigen-presenting molecules such as HLA-A, -B, -C, -E, -F and -G are clustered in the MHC class I region, while genes coding for HLA-DP, HLA-DQ and HLA-DR belong the MHC class II region. The MHC class III complex genes code for cytokines, heat shock proteins and components of the complement system (Horton *et al.* 2004). More recently, it was suggested that this complex could be subdivided in class III and IV genes (Gruen and Weissman 2001). All human MHC genes are located in an approximately 3.6 mega base, gene-dense region on chromosome 6 (6p21.31) (Horton, Wilming *et al*. 2004, MHC sequencing consortium 1999).

MHC class II molecules consist of an alpha and a beta chain with each 2 extracellular domains of which α1 and β1 form the peptide-binding cleft. MHC class II molecules are mostly expressed on antigen presenting cells and present linear peptides of 15 to 24 amino acids that are derived from phagocytosed proteins. MHC class II proteins have a high affinity for CD4 that is expressed on T helper and regulatory T cells.

MHC class Ia molecules HLA-A, -B and -C are expressed on almost all nucleated cells. They comprise an alpha chain with three extracellular domains that is non-covalently linked to a beta2-microglobulin. The peptide-binding groove is made up from the α1 and α2 domain. The presented peptides are 8 to 10 amino acids long and contain defined anchor residues that stabilize the peptide within the cleft. These peptides are usually derived from intracellular proteins (MHC peptide presentation has been comprehensively reviewed by Neefjes *et al.* 2011). The α3 domain and beta2-microglobulin bind CD8. Thus, $CD8^+$ cytotoxic T cells that express T cell receptors recognizing pathogenic peptides can detect and eliminate malignant or virally infected cells. MHC class Ia and class II molecules are highly polymorphic. Thus, within a population, a huge variety of peptides can be immunologically detected, which reduces the risk that non-detectable pathogens rapidly spread through a population. Interestingly, it has been shown that MHC phenotypes influence body odour, and that animals and humans may preferentially

select mates with divergent MHC subsets, which would enable the offspring to react to a greater variety of pathogens (Consuegra and Garcia de Leaniz 2008, O'Dwyer and Nevitt 2009).

1.3.2 MHC class Ib molecules

In contrast to MHC class Ia molecules, non-classical MHC class 1b molecules HLA-E, -F and -G display very low polymorphism, particularly in the peptide-binding domains. They structurally resemble MHC Ia molecules, bind β2-microglobulins and HLA-G and -E present peptides (Bhutta 2007, Chaix *et al.* 2008). They do, however, have a shortened cytoplasmic segment (O'Callaghan and Bell 1998, Rodgers and Cook 2005). As discussed in detail below, HLA-E and -G inhibit NK cell and T cell functions, while the precise role of HLA-F is still unclear. It has recently been shown that HLA-F does not present peptides but interacts with inhibitory receptors on NK cells (Goodridge *et al.* 2013). Additionally, MHC class Ib molecules have a very restricted expression pattern. The physiological and pathological relevance of MHC Ib molecules will be discussed on the example of HLA-G, which has first been described by Gerathy *et al.* in 1987 as HLA-6.0 (Geraghty *et al.* 1987).

1.3.3 Physiological expression of HLA-G

Physiologically, highest levels of HLA-G are expressed during embryonic development. It was first detected on cytotrophoblast cells within the placenta (Geraghty, Koller *et al.* 1987), but later studies revealed that it is already expressed in fertilized oocytes and detectable in cleavage-stage embryos and blastocysts (McMaster *et al.* 1995). Furthermore, HLA-G is detectable in spermatogenic testicular tissues and seminal plasma (Verloes *et al.* 2011, Yao *et al.* 2014). The immunosuppressive effects on both the adaptive and innate immune system (see 1.3.5) and the expression on the feto-maternal interface suggest that HLA-G may play an important role in protecting the semi-allogeneic embryo from the maternal immune system (Dahl *et al.* 2014, Yao, Shu *et al.* 2014). The finding that embryos originating from assisted reproduction techniques that secrete more soluble HLA-G (sHLA-G) have a significantly increased chance to lead to successful pregnancies after transplantation supports this view (Rizzo *et al.* 2011).

HLA-G has also been detected in the thymus (Rebmann *et al.* 2010), specifically on medullary thymic epithelial cells (Crisa *et al.* 1997) which play a decisive role during central tolerance induction (Mallet *et al.* 1999). Furthermore, HLA-G is expressed in the immune-privileged cornea (Passos *et al.* 2015) and in pancreatic islets (Le Discorde *et al.* 2003).

1.3.4 Immune cell receptors interacting with HLA-G

The immunosuppressive effects of HLA-G are mediated via various receptors expressed on immune cells. Best characterized are interactions with immunoglobulin-like transcript (ILT) receptors 2 and 4 and the killer-cell immunoglobulin-type receptor KIR2DL4 (Cirulli *et al.* 2006). Furthermore, CD160, which is expressed by endothelial cells, may also interact with HLA-G (Fons *et al.* 2006).

ILT receptors have also been referred to as leukocyte Ig-like receptors (LIR), HM/HL transcripts or monocyte/macrophage Ig-like receptors (MIR) (Allan *et al.* 2000). ILT2 (CD85j) and ILT4 (CD85d) possess 4 extracellular Ig domains (Allan, McMichael et al. 2000), of which the first two interact with the α3 domain of MHC class I molecules and beta2-microglobulin (Clements *et al.* 2005), or, in the case of ILT4, also with beta2-microglobulin-free HLA-G (Gonen-Gross *et al.* 2005). Here, ILT2 and 4 compete with CD8 for the same MHC class I structures, but while CD8 has a higher affinity for MHC Ia molecules, ILT2 and 4 preferentially bind HLA-G (Shiroishi *et al.* 2003). CD8 promotes T cell activation through the associated lymphocyte-specific protein tyrosine kinase (Lck) (Artyomov *et al.* 2010, Barber *et al.* 1989, Delon *et al.* 1998). In contrast, ILT 2 and 4 inhibit immune cells via several immunoreceptor tyrosine-based inhibitory motif (ITIM)-related sequences (Allan, McMichael *et al*. 2000). While ILT4 is only expressed on myeloid cells such as monocytes, macrophages and dendritic cells, (Allan, McMichael *et al*. 2000, Colonna *et al.* 1998), ILT2 is also expressed on lymphoid lineages such as T cells, NK cells and B cells (Allan, McMichael *et al*. 2000, Colonna *et al.* 1997, Cosman *et al.* 1997).

KIR2DL4 (CD185d) also contains only one intracellular ITIM (Yusa *et al.* 2002) and its only known ligand is HLA-G (Rajagopalan and Long 1999). It is expressed on some $CD8^+$ T cells all NK cells (Rajagopalan and Long 1999) while highest levels are detected on $CD56^{bright}$ NK cells (Goodridge *et al.* 2003). $CD56^{bright}$ NK cells most frequently occur

in the uterus (Cooper *et al.* 2001). Some reports suggest an inhibitory function for this receptor (Goodridge, Witt *et al*. 2003, Yusa, Catina *et al*. 2002), others suggest that it may activate NK cells which could promote angiogenesis during early pregnancy (Rajagopalan and Long 2012). A recent report even suggested that effects of HLA-G on KIR2DL4 may be indirect and due to contaminations (Le Page *et al.* 2014).

HLA-G has also been reported to upregulate the expression of ILT2, 3 and 4 and KIR2DL4 in immune cells (Braud *et al.* 1999).

1.3.5 HLA-G mediated immunosuppressive effects

By activating these receptors HLA-G inhibits various immune effector cells. Effects of HLA-G on different immune cell subsets have been comprehensively reviewed by Carosella *et al*. (Carosella *et al.* 2008) and are displayed in Table 1.

Table 1: Direct HLA-G mediated effects on immune effector cells

Immune cell subset / effect of HLA-G	Receptors involved
$CD8^+$ T cells	
Inhibition of cytotoxic function	unknown
Inhibition of proliferation	ILT2
Generation of $CD8^{low}$ regulatory T cells	unknown
Apoptosis	CD8
$CD4^+$ T cells	
Inhibition of alloreactivity	ILT2, ILT4
Inhibition of proliferation	ILT2
Up-regulation of inhibitory receptors	unknown
Generation of regulatory T cells, which include $CD4^{low}$ T cells	unknown
NK cells	
Inhibition of cytotoxic function	ILT2, KIR2DL4
Inhibition of proliferation	ILT2
Up-regulation of inhibitory receptors	unknown
Apoptosis	CD8
Increased proliferation and IFNγ production	KIR2DL4
Increased secretion of pro-angiogenic factors	Internalized KIR2DL4
Inhibition of trans-endothelial migration	ILT2
Inhibition of cytotoxic function	ILT2, KIR2DL4
APC	
Inhibition of DC maturation, antigen presentation, trafficking, and induction of regulatory T cells	ILT4
Up-regulation of inhibitory receptors	unknown

Adapted from (Carosella, Favier *et al*. 2008), all references see (Carosella, Favier *et al*. 2008).

1.3.5 Structure and isoforms of HLA-G

The HLA-G gene comprises 8 exons und 7 introns, of which exons 1 to 6 code for the mature protein. Exon 1 codes for the 5' untranslated region and the leader peptide. Exon 2, 3 and 4 code for the α1, α2 and α3 domains, respectively. Exon 5 codes for the transmembrane domain and exon 6 for a short intracellular tail and the stop codon. Alternative splicing processes can lead to 7 different isoforms of HLA-G. Membrane-

bound HLA-G2, 3 and 4 isoforms lack the α2 and/or α3 domain due to exon skipping during transcription. Soluble isoforms emerge due to intron retention of intron 2 (HLA-G7) or intron 4 (HLA-G5 and 6), which contain alternative stop codons (Carosella, Favier *et al*. 2008, Carosella *et al.* 2003). Alternatively, soluble isoforms such as shed HLA-G1 (sHLA-G1) (Moreau *et al.* 1995) can result from proteolytic cleavage of membrane-bound isoforms through matrix metalloproteinases (MMP) such as MMP-2 (Rizzo *et al.* 2013). All known isoforms of HLA-G are displayed in Figure 5.

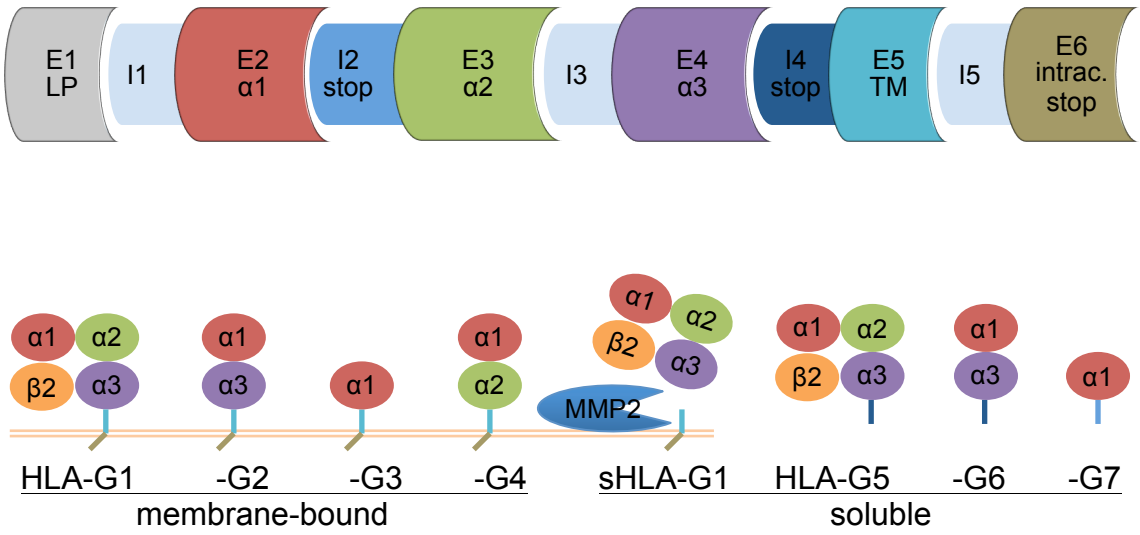

Figure 5: Structure of the HLA-G gene and HLA-G isoforms
The HLA-G gene comprises 6 protein-coding exons (E1-E6, I = intron). Alternative splicing yields 7 distinct protein isoforms, of which HLA-G1-4 are membrane-bound and HLA-G5-7 are soluble. Proteolytic cleavage of all membrane-bound HLA-G isoforms through MMP2 may also generate soluble HLA-G. Exons and corresponding domains are displayed in matching colours. Figure adapted from (Carosella, Favier *et al*. 2008, Carosella, Moreau *et al*. 2003).

Dimers of HLA-G which result from disulphide bonds involving cysteine residues at positions 42 and 147 may be particularly effective in activating HLA-G receptors (Shiroishi *et al.* 2006). These have been detected both in soluble (Juch *et al.* 2005) and membrane-bound forms (Boyson *et al.* 2002).

1.3.6 Transfer of HLA-G

As discussed, the physiological expression of HLA-G is restricted to a few tissues. However, matters are complicated by mechanisms which transfer HLA-G proteins from one cell to another.

One mechanism that has been studied in detail is trogocytosis (reviewed by Davis 2007, Joly and Hudrisier 2003). Upon cell-cell contact, both T or NK cells temporarily acquire cell membrane patches from APC or tumour cells which include membrane-bound HLA-G. This alters effector cells to become transiently tolerant (Caumartin *et al.* 2007, LeMaoult *et al.* 2007).

Another mechanism of HLA-G transfer is via exosomes. Exosomes are extracellular vesicles of 50-90 nm in diameter in which surface proteins have the same orientation as in a cell and that enclose small amounts of cytoplasm. They are generated in larger, intracellular multivesicular bodies, which fuse with the cell membrane in order to release exosomes (reviewed by Fevrier and Raposo 2004). Exosomes bearing HLA-G molecules have been detected in tumour cell line supernatants as well as in pleural exudates and ascites from cancer patients (Alegre *et al.* 2013, Riteau *et al.* 2003).

1.4 Role of HLA-G in ovarian carcinoma

1.4.1 HLA-G expression in malignant diseases

HLA-G expression has been detected in a large variety of malignancies. Interestingly, the frequencies at which HLA-G positive tumours are detected within investigated entities vary from 0% (uveal melanoma) to 100% (hydratiform moles, which originate from the placenta) (reviewed by Amiot *et al.* 2011). HLA-G expression has also been detected in some of the most frequent malignancies including breast cancer, lung cancer, colorectal cancer, prostate cancer and melanoma (comprehensively reviewed by Carosella *et al.* 2008, Rouas-Freiss *et al.* 2005).

The choriocarcinoma cell line Jeg-3 stably expresses HLA-G (Burt *et al.* 1991). However, other cell lines generated from primary tumour cells that initially express HLA-G lose expression when cultured over prolonged periods of time (Rouas-Freiss *et al.* 2005). This may explain why, in some entities, it is difficult to study the relevance of HLA-G expression for tumourigenesis *in vitro*. Nevertheless, some initially negative tumour cell lines upregulate HLA-G when treated with inflammatory cytokines like tumour necrosis factor alpha (TNF-α) or interferon gamma (IFN-γ) (Wiendl *et al.* 2002).

1.4.2 HLA-G expression in ovarian carcinoma

HLA-G has been detected in about 60 to 70% of high-grade serous carcinomas but only rarely in low-grade serous carcinomas (Menier *et al.* 2009, Singer *et al.* 2003). Soluble HLA-G was detected in 25 of 25 high-grade serous ascites samples (Singer, Rebmann *et al*. 2003). This clearly indicates that HLA-G and particularly soluble HLA-G may play a role in ovarian cancer progression.

This is further supported by findings showing that HLA-G expression in primary ovarian cancer cells protects these cells from NK cell mediated lysis (Lin *et al.* 2013, Lin *et al.* 2007). Besides, HLA-G expression may induce matrix metalloproteinases and thus increase tumour invasiveness and metastases formation (Lin, Xu *et al*. 2013). The relevance of HLA-G in tumour progression has also been demonstrated by overexpressing HLA-G in ovarian cancer cell lines. Nude mice inoculated with HLA-G

transfected ovarian cancer cell lines suffered from more widespread metastases and survived significantly shorter as compared to mice inoculated with parental cells (Lin *et al.* 2012).

HLA-G has been suggested as a biomarker for ovarian carcinomas (Menier, Prevot *et al.* 2009). HLA-G expression may also predict susceptibility towards certain chemotherapeutic agents (Davidson *et al.* 2005).

Jung *et al.* found that HLA-G expression in high and low grade carcinomas correlates with disease progression and inversely correlates with patient survival (Jung *et al.* 2009). In contrast, a tissue microarray (TMA) based study in which only high-grade tumours were analysed showed that elevated expression of HLA-G correlated with improved patient survival (Rutten *et al.* 2014).

1.4.3 Induction of HLA-G in ovarian carcinoma

The HLA-G gene is physiologically silenced in epithelial and other tissues due to hypermethylation of CpG sites (Mouillot *et al.* 2005). Thus, these tumours must undergo cis-acting epigenetic changes in order to express HLA-G. Correspondingly, methylation patterns in the 5' region of the *HLA-G* gene were significantly different in malignant ovarian carcinoma cells as compared to benign or normal ovarian surface epithelium (Menendez *et al.* 2008). However, HLA-G transcription may also be enabled by demethylating agents which have been used in ovarian cancer trials (Brown *et al.* 2014).

The transcriptional regulation of the HLA-G gene is unique even among MHC class Ib molecules (Gobin and van den Elsen 2000). Numerous environmental factors have been shown to induce or increase the expression of HLA-G in tissues or tumours in which the HLA-G gene is accessible. These include hypoxia (Mouillot *et al.* 2007), stress, cytokines such as GM-CSF, IL-10, interferons and leukaemia inhibitory factor (Bamberger *et al.* 2000), hormones such as progesterone (Ivanova-Todorova *et al.* 2009) or glucocorticoids (Moreau *et al.* 2001) (reviewed by Carosella, Moreau et al. 2003).

Elevated concentrations of IL-10 have also been detected both in serum and ascites of ovarian cancer patients (Gotlieb *et al.* 1992, Mustea *et al.* 2006). Furthermore, some ovarian cancer cell lines secrete IL-10 (Berger *et al.* 2001). High levels of IL-10

frequently correlate with HLA-G expression in different tumour entities (Urosevic and Dummer 2003).

Interestingly, IL-10 in combination with IL-4 and GM-CSF has been reported to induce dendritic cells which express HLA-G and induce tolerogenic T cells (Gregori *et al.* 2010). During pregnancy, IL-4 may also induce the expression of HLA-G5 in T cells (Lombardelli *et al.* 2013).

1.5 Aims of this thesis

While expression of HLA-G has been well documented in high-grade serous ovarian carcinoma cells, HLA-G expression in clear cell, mucinous or endometrioid ovarian carcinomas has only been investigated in one study with 2, 5 and 6 samples, respectively (Menier, Prevot *et al*. 2009). Therefore, one aim of this thesis was to investigate the frequency of HLA-G expression in these ovarian carcinoma subtypes.

As discussed, HLA-G is a potent immunosuppressive molecule and may thus promote tumour growth. However, in high-grade carcinomas, its expression correlates with a favourable clinical outcome (Rutten, Dijk *et al*. 2014). Interestingly, Gajewski *et al.* have suggested that two immunological groups of solid tumours may exist. One subset of tumours is infiltrated by immune cells, but actively suppresses them. In contrast, immune-ignorant or immunoedited tumours may emerge because cancer cells stop expressing immunogenic proteins (Gajewski *et al.* 2013). If this is the case in ovarian carcinomas, immunosubversive tumours that express MHC Ib molecules such as HLA-G could grow despite expressing classical MHC Ia molecules. In contrast, HLA-G negative tumours should have evolved alternative immune-escape mechanisms including downregulation of classical MHC molecules. In order to test if these distinct immune escape strategies may be observable in ovarian carcinomas, published gene-expression datasets from ovarian carcinomas were screened for mRNAs expressed in correlation with HLA-G mRNA.

Furthermore, we set out to investigate whether tumour-derived cytokines may induce the expression of HLA-G in immune cells in primary lesions or regional lymph nodes.

Finally, the relevance of soluble HLA-G during tumourigenesis in this malignancy should be further elucidated. As discussed, ovarian carcinomas frequently accumulate numerous

mutations (Hunt *et al.* 2006) and grow into large solid tumours without causing specific symptoms. Here, membrane-bound HLA-G may clearly help to suppress immune effector cells infiltrating the tumour. In contrast, soluble HLA-G should be constantly transported out of the tumour microenvironment via the lymph and then diluted and distributed via circulation throughout the body. Thus, it is unclear how soluble HLA-G may contribute to regional immunosuppression. It has been shown that soluble HLA-G induces apoptosis in T and NK cells (Contini *et al.* 2003, Lindaman *et al.* 2006, Pistoia *et al.* 2007). However, if this occurs on a systemic rather than local level, patients should experience severe immune-related symptoms including opportunistic infections. These are not typically observed during "silent" ovarian tumourigenesis. Thus, it remains unclear how soluble HLA-G may promote local tumour immune escape.

2 Material and methods

2.1 Material

If not directly indicated, company locations are listed in Supplements, Table 6

2.1.1 Software

Use	Software & Manufacturer
Confocal image acquisition	ImagePro Plus, Leica, Germany
Data handling	Microsoft Excel 2010 & 2011, Microsoft Cooperation
ELISA data analysis	Magellan, Tecan Trading AG
Figure compilation	Corel Draw X4, Corel Corporation
Flow Cytometry	Attune cytometry software v2.1.0, Thermo Fisher Scientific Inc.
Gene expression analysis	R2 genomics analysis and visualization platform (www.r2.amc.nl)
Graphs & charts	GraphPad Prism 6, GraphPad Software, Inc.
Image and blot analysis	ImageJ, Wayne Rasband (NIH)
Image handling	Photoshop CS3, Adobe Systems Inc.
Real-time PCR analysis	7500 Software, Applied Biosystems Inc.
Statistical analysis	GraphPad Prism 6, GraphPad Software, Inc.
TaqMan design	Primer3, http://primer3.ut.ee/
Text editor	Microsoft Word 2010 & 2011, Microsoft Cooperation
Citation manager	EndNote X4, Thompson Reuters

2.1.2 Important devices

Device	Model & Manufacturer
Absorbance reader	Sunrise, Tecan Trading AG
Agarose gel electrophoresis apparatus	MupidexU, Eurogentec GmbH, Cologne, Germany
Autoclave	H P Labortechnik AG, Oberschleißheim, Germany
Centrifuges	5810 R, 5424 R: Eppendorf, Hamburg, Germany Jouan C4i, Heraus Megafuge 16: Thermo Electron GmbH, Dreieich, Germany
CO_2 incubator	Thermo Electron GmbH
Confocal microscope	laser-scanning microscope TCS SP5 II, Leica
Digital camera	Canon, USA
Electronic balance	Sartorius AG, Göttingen, Germany
Flow cytometer	Attune Flow Cytometer, Thermo Fisher Scientific Inc.
Freezers (-20°C, -86°C)	Liebherr, Germany; Thermo Electron GmbH Philipp Kirsch GmbH, Offenburg, Germany
Inverted microscope	Leica, Solms, Germany
Laminar flow hood	Heraeus, Hanau, Germany
Photometer	Thermo Electron GmbH
Real-Time PCR cycler	7500Fast Real-Time PCR System, Applied Biosystems
Western blotting system	Mini-Protean® Tetra Cell, Bio-Rad Laboratories, Inc.

2.1.3 Consumables

Consumable	Specification & Manufacturer
96-well PCR plate	ABITaqMan-Plate, Fisher Scientific GmbH
Cell culture flasks (25, 75 or 150 cm^2)	TPP Techno Plastic Products AG
Cell culture plates (6, 12, 24 or 96 well flat or round bottom)	TPP Techno Plastic Products AG
ELISA plates	Nunc (Maxisorp), Roskilde, Denmark
Falcon tubes (15 ml, 50 ml)	Greiner Bio One International GmbH
Fixer & developer	Eastman Kodak
LS magnetic columns	Miltenyi Biotec GmbH

Consumable	Specification & Manufacturer
Lumox dishes, 35 mm, soft bottom	Sarstedt AG & Co, Nümbrecht, Germany
Micro test tubes	Greiner Bio One International GmbH
PVDF membrane, 0.2 µm pores	Roti®-Fluoro PVDF, Carl Roth GmbH + Co. KG
SuperFrost microscope slides & cover slips	Carl Roth GmbH + Co. KG
TaqMan design	Primer3, http://primer3.ut.ee/
X-ray films	Fisher Scientific GmbH

2.1.4 Cells, cell lines and supernatants

Biological material	Source
Jeg-3 choriocarcinoma cell line	ATCC Manassas, VA, USA
Peripheral blood mononuclear cells (PBMCs)	Healthy blood donors
LCL-HLA-G5B2M (scHLA-G5) supernatant	Supernatant from LCL 721.221 cells transfected with a pRc-RSV vector containing human beta2-microglobulin, a $(4GS)_4$ linker and human HLA-G5. The soluble HLA-G concentration is 0.87µg/ml. Kind gift from Dr. Joël LeMaoult, Hôpital Saint Louis, Paris.
LCL-RSV (ctrl) supernatant	Supernatant from mock transfected LCL 721.221 cells (empty pRc-RSV vector), no HLA-G detectable. Kind gift from Dr. Joël LeMaoult, Hôpital Saint Louis, Paris.

2.1.5 Tumour and ascites samples

Sample	Source
Ascites samples	Ascites from ovarian cancer patients was drained for symptoms relief by doctors of the Universitäts-Frauenklinik Würzburg and provided for scientific purposes anonymized and with informed consent.
FFPE serous ovarian carcinoma and lymph node sections	FFPE tumour samples were anonymized and provided by the Institute of Pathology, University of Würzburg. All patients had signed a form indicating their informed consent regarding the use of surgical specimens for scientific purposes.
Healthy control FFPE tissue microarray	The CHTN Norm2 normal adult FFPE tissue microarray was bought from the Cooperative Human Tissue Network via the university of Virginia….

Sample	Source
	…Central nervous system tissues were obtained from autopsy specimens within 36 hours after death. All other tissues were obtained from surgical resections and fixed within one hour with 3.7% formaldehyde. Three 1mm cores from each tissue were combined into a tissue microarray, which was sectioned on charged glass slides at 4 µm. For each tissue, donor age and sex are listed below.
Ovarian carcinoma FFPE tissue microarray	The CHTN OvCa1 ovarian carcinoma FFPE tissue microarray was also bought from the Cooperative Human Tissue Network. Four 0.6mm cores from each tumour were combined into a tissue microarray, which was sectioned on charged glass slides at 4 µm. Patient characteristics are listed in Table 2

2.1.6 Cell culture reagents

Reagent	Manufacturer
Phosphate-buffered saline (PBS)	Sigma-Aldrich Co. LLC
RPMI-1640	Sigma-Aldrich Co. LLC
Penicillin (10kU/ml) and streptomycin (10mg/ml) (P/S)	Sigma-Aldrich Co. LLC
Sodium pyruvate (100mM)	Sigma-Aldrich Co. LLC
Human AB serum (hAB)	Serum from human serotype AB donors, PAA Laboratories, GE Healthcare
Fetal calf serum (FCS)	GE Healthcare
Acid citrate dextrose (ACD-A)	Haemonetics Corporation
Accutase	PAA Laboratories, GE Healthcare
Biocoll separation solution	Biochrom GmbH
Trypsin EDTA	PAA Laboratories, GE Healthcare
Cell Proliferation Dye eFluor 670	eBioscience, Inc.
Phytohemagglutinin (PHA)	Biochrom GmbH

2.1.7 Chemicals & solution reagents

Reagent	Manufacturer
37%-formaldehyde	Sigma-Aldrich Co. LLC
40% Acrylamide/Bis solution	Bio-Rad Laboratories, Inc.
Agarose	Carl Roth GmbH + Co. KG
Ammonium peroxodisulfate (APS)	Carl Roth GmbH + Co. KG
Aprotinin	Carl Roth GmbH + Co. KG
Bovine serum albumin (BSA)	AppliChem GmbH
Bovines Serum Albumin (BSA)	AppliChem GmbH
Bradford reagent Roti-Quant	Carl Roth GmbH + Co. KG
Bromophenol blue	Carl Roth GmbH + Co. KG
Chloroform	Sigma-Aldrich Co. LLC
Diaminobenzidine (DAB)	Dako, Agilent Technologies, Inc.
Dimethylsulfoxid (DMSO)	Carl Roth GmbH + Co. KG
Ethylenediaminetetraacetic acid (EDTA)	AppliChem GmbH
GelRed	Biotium Inc.
Glacial acetic acid	Carl Roth GmbH + Co. KG
Glycerol	Carl Roth GmbH + Co. KG
Glycine	Carl Roth GmbH + Co. KG
Leupeptin	Carl Roth GmbH + Co. KG
Sodium chloride (NaCl)	Carl Roth GmbH + Co. KG
NP-40	AppliChem GmbH
Phenylmethanesulfonylfluoride (PMSF)	Carl Roth GmbH + Co. KG
Phorbol 12-myristoyl 13-acetate (PMA)	Sigma-Aldrich Co. LLC
Ponceau S	Carl Roth GmbH + Co. KG
Potassium (di) hydrogen phosphate	Carl Roth GmbH + Co. KG
Potassium chloride	Carl Roth GmbH + Co. KG
Skimmed milk powder	Merck KGaA
Sodium chloride (NaCl)	Carl Roth GmbH + Co. KG
Sodium dodecyl sulfate (SDS)	Carl Roth GmbH + Co. KG
Sodium fluoride (NaF)	AppliChem GmbH
Sodium hydroxide	Carl Roth GmbH + Co. KG
Sodium orthovanadate ($NaVO_5$)	AppliChem GmbH
Sodium(di)hydrogen phosphate	Carl Roth GmbH + Co. KG

Reagent	Manufacturer
Streptavidin-HRP	Dako, Agilent Technologies, Inc.
Tetramethylethylenediamine (TEMED)	Carl Roth GmbH + Co. KG
TRI Reagent (TriZol)	Sigma-Aldrich Co. LLC
Trichloroacetic acid	Carl Roth GmbH + Co. KG
Tris-HCL	Carl Roth GmbH + Co. KG
Tween20	Carl Roth GmbH + Co. KG
Sodium acetate	Carl Roth GmbH + Co. KG
H_2O_2 30%	Carl Roth GmbH + Co. KG
Na_2CO_3	Carl Roth GmbH + Co. KG
VitroClud	Langenbrinck, Emmendingen, Germany
β-mercaptoethanol	Carl Roth GmbH + Co. KG

2.1.8 Buffers, solutions and media

Buffer/Solution	Composition
1 x MOPS buffer	10% 10 x MOPS buffer, 2% 37%-formaldehyde, 88% H_2O
10 x MOPS buffer	400 mM MOPS, 100 mM NaAc, 10 mM EDTA, pH 7
50 x TAE	2 M Tris, 0.6 M EDTA, 0.57% glacial acetic acid
Antibody Diluent	Dako REAL
Complete RPM1640 5% hAB serum	93.5% RPMI 1640, 5% human AB serum, 1% P/S, 0.5% sodium pyruvate
Complete RPMI1640 10% FCS	88.5% RPMI 1640, 10% FCS, 1% P/S, 0.5% sodium pyruvate
ELISA blocking buffer	PBS, 4% BSA
ELISA coating buffer	100 mM Na_2CO_3, pH9.6
ELISA dilution buffer	PBS, 1% BSA
ELISA sodium acetate solution	0.1 M sodium acetate, pH 6.0
ELISA TMB solution	TMB substrate kit, Biolegend
ELISA washing buffer	PBS, 0,.05% Tween20
FACS buffer	PBS, 2% FCS
Fluoromount G	Southern Biotech
Freezing medium	70% FCS, 20% Complete RPMI1640 10% FCS, 10% DMSO
Hematoxylin solution	Carl Roth GmbH + Co. KG

Lysis buffer P	H_2O, 50 mM Tris-HCl, pH 8, 120 mM NaCl, 5mM EDTA, 0.5% NP-40
MACS-Buffer	PBS pH 7.2, 0.5% BSA, 2 mM EDTA
PBS	37 mM NaCl, 2.7 mM KCl, 80 mM Na_2HPO_4, 1.8 M KH_2PO_4, pH 7.4
TBS	10 mM Tris-HCl, 150 mM NaCl, pH 7.5
TBS-T	TBS, 0.05% Tween20
TRIS buffer	TRIS 0.1M, pH 7.6
WB 5x protein loading buffer	100 mM Tris-HCl pH 6.8, 4% SDS, 0.2% bromophenol blue, 20% glycerol, 10% β-mercaptoethanol
WB blocking buffer	TBS-T, 5% skim milk powder
WB ECL solution A	50 mg luminol in 200 ml 0.1 M Tris-HCl, pH 6.8
WB ECL solution B	11 mg para-hydroxycoumarinic acid in 10 ml of DMSO
WB lysis buffer	Lysis buffer P, 2 µg/ml Aprotinin, 10µg/ml Leupeptin, 100 µg/ml PMSF, 50 mM NaF, 200 µM $NaVO_5$
WB neutralizing buffer	1.5 M Tris-Base pH 7.4
WB Ponceau S solution	0.2% Ponceau S in 3% trichloroacetic acid
WB running buffer	25 mM Tris, 193 mM glycine, 0.5% SDS, pH 8.8
WB stripping buffer	0.2 M glycine, 0.5 M NaCl, pH 2.8
WB transfer buffer	25 mM Tris, 192 mM glycine, 20% methanol

WB = Western Blot

2.1.9 Cytokines

Cytokine	Manufacturer
rhIL-2	PeproTech, Inc.
rhIL-4	Immunotools GmbH
rhIL-10	Miltenyi Biotec GmbH
rhGM-CSF	Immunotools GmbH
rhTGF-β	PeproTech, Inc.

rh = recombinant human

2.1.10 Antibodies and labelling agents

Antigen	Clone	Source/isotype	Label	Use	Manufacturer
Biotin	Streptavidin	-	HRP	ELISA	ImmunoTools
HLA-G	Mem-G9	mouse	-	ELISA	ExBio
β2-microglobulin	B2M-01	mouse	biotin	ELISA	ExBio
CD11c	MJ4-27G12	mouse IgG2b	FITC	FC	Miltenyi Biotec
CD14	MEM-18	mouse	FITC	FC	ImmunoTools
CD3	BW264/56	mouse	PE or FITC	FC	Immunotools
CD3	BW264/56	mouse	APC-Vio770	FC	Miltenyi Biotec
CD4	MEM-241	mouse IgG1	PE	FC	ImmunoTools
CD56	N901	mouse IgG1	APC	FC	Immunotech
CD86	IT2.2	mouse IgG2b, κ	APC	FC	BioLegend
CD8b	SIDI8BEE	mouse IgG1, κ	PE-Cy7	FC	eBioscience
HLA-DR	LT-DR	Mouse IgG2a	PE	FC	ImmunoTools
HLA-G	Mem-G9	mouse	FITC or APC	FC	Life technologies
ILT4	42D1	rat IgG2a	PE	FC	eBioscience
Isotype	RTK2758	rat IgG2a, κ	PE	FC	Biolegend
Isotype	MOPC-21	mouse IgG1	FITC/PE	FC	BioLegend
Mouse IgG	Poly4053	goat	APC	FC	BioLegend
Rat IgG	Poly4054	goat	FITC	FC	BioLegend
FoxP3	PCH101	mouse	APC	FC	eBioscience
HLA-G	87G	mouse IgG2a κ	-	FN	BioLegend
ILT2	HP-F1	mouse IgG1 κ	-	FN	eBioscience
ILT4	27D6	rat IgM	-	FN	eBioscience
Isotype	eBM2a	mouse IgG2a κ	-	FN	eBioscience
KIR2DL4	mAB33	mouse IgG1 κ	-	FN	BioLegend
Cytokeratin	KL1	mouse IgG1	AF647 (Zenon)	IF	Beckman Coulter
Mouse IgG H+L	polyclonal	donkey	AF555	IF	Molecular Probes
Mouse IgG3	polyclonal	goat	AF488	IF	Molecular Probes
CD68	PGM1	mouse IgG3	-	IF, IHC	Dako
Cytokeratin	KL1	mouse IgG1	-	IHC	Beckman Coulter
WT1	WT49	mouse IgG1	-	IHC	Leica
Anti-mouse Ig	polyclonal	horse	HRP	WB	Cell Signaling

Antigen	Clone	Source/isotype	Label	Use	Manufacturer
Anti-rabbit Ig	polyclonal	goat	HRP	WB	Cell Signaling
β-actin	Poly6221	rabbit	-	WB	BioLegend
HLA-G	4H-84	mouse IgG1	-	WB, IHC, IF	BD Pharmingen

Antigen: all antigens are human, Ig = Immunoglobulin, H+L = heavy and light chain
Labels: AF = AlexaFluor, others see abbreviations, Zenon = labelled with Zenon labelling kit
Uses: FC = flow cytometry, WB = Western Blotting, IHC = immunohistochemistry, IF = immunofluorescence, FN = functional/blocking

2.1.11 Kits

Reagent	Manufacturer
iScript cDNA Synthesis Kit	Bio-Rad Laboratories, Inc.
MACS NK Cell Isolation Kit II, human	Miltenyi Biotec GmbH
MACS anti-CD14 beads, human	Miltenyi Biotec GmbH
MACS $CD8^+$ T Cell Isolation Kit, human	Miltenyi Biotec GmbH
MACS $CD4^+$ T Cell Isolation Kit II, human	Miltenyi Biotec GmbH
TaqMan Platinum® Quantitative PCR SuperMix-UDG	Thermo Fisher
Zenon® Mouse IgG1 Labelling Kit AlexaFluor647	Life Technologies
ADVANCE™ HRP IHC Kit	Dako, Agilent Technologies
Foxp3 / Transcription Factor Staining Buffer Set	eBioscience
Matched IL-4 ELISA antibody pairs	Immunotools
Matched IL-10 ELISA antibody pairs	Immunotools

2.1.12 Oligonucleotides

The following oligonucleotides were used for HLA-G mRNA TaqMan qPCR:

Oligonucleotide	Sequence 5´ -> 3´	Source
18s RNA, fw primer	CGGCTACCACATCCAAGGAA	Eurogentec
18s RNA, rev primer	GCTGGAATTACCGCGGCT	Eurogentec
18s RNA, probe, yakima yellow 5' TAMRA 3'	TGCTGGCACCAGACTTGCCCTC	Eurogentec
mHLA-G RNA, fw primer	CTCTCAGGCTGCAATGTGAA	Sigma
mHLA-G RNA, rev primer	CATGAGGAAGAGGGTCATGG	Sigma
mHLA-G RNA, probe, FAM 5' BHQ1 3'	TGCAGAGACCAGCCCACCCC	Sigma
sHLA-G RNA, fw primer	CCCCTCATGCTGAGTAAGGA	Sigma
sHLA-G RNA, rev primer	GGTGAAGGTGAGGGTCTCTG	Sigma
sHLA-G RNA, probe, Texas Red 5' BHQ2 3'	AGGGTCGGTGGTGAGGCTG	Sigma

2.1.13 Standards and ladders

Use	Ladder	Manufacturer
Protein	Spectra Multicolor Broad Range	Thermo Fisher Scientific Inc.
RNA	RiboRuler High Range	Thermo Fisher Scientific Inc.

2.1.14 Disinfectants

Use	Reagent	Manufacturer
Skin disinfection	Cutasept	BODE Chemie GmbH, Hamburg, Germany
Work space disinfection	70% Ethanol	Hospital pharmacy

2.2 Methods

In order to improve readability, methods are listed in the same order as results whenever feasible.

2.2.1 Immunofluorescence

FFPE serous ovarian carcinoma and lymph node samples were cut into 4 µm sections with a microtome, mounted on charged microscope slides and dried. Sections from FFPE TMAs were already mounted on microscope slides.

In order make the proteins accessible, all sections were de-waxed for 25 minutes in xylene and rehydrated for 5 minutes each in 100%, 90%, 80%, and 70% ethanol followed by 10 minutes in H_2O. Antigens were retrieved by boiling for 20 minutes in a steamer in citrate buffer pH 7.0. Slides were then transferred into TRIS buffer.

All following steps were carried out in a humid chamber in order to avoid evaporation. Unspecific binding sites were blocked with Antibody Diluent for 15 minutes. HLA-G was stained for 1h with anti HLA-G antibody (clone 4H-84) diluted 1:20 in Antibody Diluent. Slides were then washed 3 times for 5 minutes with TRIS buffer on a shaker. For visualization, AlexaFluor555-labeled donkey anti-mouse IgG was diluted 1:400 in Antibody Diluent and also incubated for 1h, followed by 3 x 5 minutes washing with TRIS buffer.

Slides were then blocked for 1h with mouse serum diluted 1:20, followed by 3 more identical washing steps. CD68 staining was carried out for 1h with antibody clone PGM1 diluted 1:50, followed by identical washing steps and 1h incubation with an AlexaFluor 488 labelled goat antibody specific for mouse IgG3. This secondary antibody was diluted 1:400.

Meanwhile, cytokeratin staining was prepared. For each slide, 10 µl of the pan-cytokeratin antibody KL1 were mixed with 10 µl Zenon AlexaFluor647 for 7 minutes. The labelling reaction was stopped with 10 µl Zenon block (7 min), and 170 µl TRIS-buffer were added. Staining was carried out for 1h, followed by 3 washes. Slides were

then treated with formalin for 10 minutes, washed 3 more times, mounted with Flouromount G and dried at 8°C in the dark over night.

2.2.2 Immunohistochemistry

First steps in immunohistochemistry were carried out as described above for immunofluorescence. However, only one antigen was stained for on each section. WT1 was detected with WT49 antibody. After the primary antibody had been washed off, slides were incubated with 0.3% H_2O_2 in TRIS buffer for 15 minutes. Secondary antibody staining was carried out using the ADVANCE™ HRP kit according the manufacturers protocol. Slides were then counterstained with haematoxylin solution and dehydrated with ascending ethanol concentrations (70%-100%). Sections were embedded in a drop of Vitroclud with a coverslip and sealed in nail varnish.

2.2.3 ELISA

ELISA was used to quantify IL-4, IL-10 and soluble HLA-G in ovarian carcinoma and benign ascites samples. For IL-4 and IL-10 detection, matched ELISA antibody pairs (Immunotools) and standards were used as described by the manufacturer. For HLA-G detection, MEM-G9 was used as a capture antibody (2 µg/ml) and anti-ß2-microglobulin antibody B2-M01 labelled with biotin (1 µg/ml) was used as detection antibody. LCL scHLA-G5 SN diluted in dilution buffer was used as a standard. Highest standard concentration was 400 ng/ml, which was diluted 5 times in 4fold dilutions (400, 100, 25, 6.25, 1.58, 0.39 ng/ml). The following protocol was used:

50 µl of capture antibody diluted in coating buffer was added to each well of a Nunc maxisorp 96-well plate which was stored in a humid box overnight at 4°C. The capture antibody was removed by flicking the plate over a sink and each well was washed twice with 200 µl washing buffer. Remaining protein-binding sites on the plate were blocked for 1h at room temperature in a humid box by adding 300 µl blocking buffer. Each well was washed two more times with washing buffer. 50 µl of standards and samples in appropriate dilutions were added to the wells in duplicates and incubated on the plate in a humid box for 2h at room temperature. The plate was then washed 4x with washing buffer. Then, 50 µl of detection antibody diluted in dilution buffer was added to each well

and incubated at room temperature in a humid box for 1h. Plates were then washed 4 more times with washing buffer, before 50 µl streptavidin-HRP (diluted 1:250 in dilution buffer) were added to each well. The plate was then kept for 30 minutes in a humid at room temperature. After four more washes, 50 µl substrate solution (freshly prepared 5 ml 0.1M sodium acetate pH 6.0, 50 µl TMB, 1 µl 30% H_2O_2) was added. Depending on colour development, plates were kept at room temperature or 37°C for up to 15 minutes before the reaction was stopped by adding 25 µl of 1M H_2SO_4. Absorption at 450 nm and at the reference wavelength 620 nm were measured with the Sunrise reader. Absorption values were normalized to reference values, the mean blank values (dilution buffer only) were subtracted and the concentrations determined by curve-fitting algorithms provided by the Magellan software.

2.2.4 Cell culture

General notes

All steps were carried out under sterile conditions, protective containers were only opened under laminar flow hoods. Unless otherwise indicated, cells were always centrifuged at 350 x g for 5 minutes. All viable cells were maintained in incubators at 37°C, 5% CO_2 and >95% humidity. A water bath set for 37°C was used to prewarm media, PBS or other solutions added to the cells. Neubauer chambers were used for cell counting.

Thawing of cells

Cryopreserved cells were thawed at 37°C and immediately diluted in 15 ml PBS. Cells were centrifuged once to remove DMSO and the pellet was resuspended in complete media. Cells then used for experiments or seeded into appropriate cell culture flasks and cultured in an incubator.

Culturing and subculturing

Depending on cell densities and planned experiments, Jeg-3 cells were cultured in complete RPMI1640 10% FCS (see 2.1.8) in appropriate cell culture flasks and subcultured 2-3 times per week. For subculturing, adherent Jeg-3 cells were first washed with 10 ml PBS. 0.5 to 1ml of trypsin/EDTA solution was added to the flask, which was returned to the incubator until all cells were detached (2-5 min). Trypsin was inactivated

by 5 ml of Complete RPMI1640 10% FCS and the detached cells were usually split 1 to 10 before being transferred into a new cell culture flask for further culture.

PBMC or immune cell subsets were usually cultured in 6-, 12-, or 24-well plates in RPMI1640 medium supplemented with 5% human serotype AB serum, sodium pyruvate and antibiotics (Complete RPM1640 5% hAB serum, see 2.1.8).

Cryopreservation of cells

For cryopreservation, adherent cells were first detached with Trypsin/EDTA and then centrifuged. The cell pellet was resuspended in 1 ml of fresh freezing medium and the solution transferred to cryovials. These were kept in cryogenic boxes at -80°C for 24h. Vials were then transferred to liquid nitrogen tanks.

2.2.5 PBMC isolation

Peripheral blood mononuclear cells (PBMC) were isolated from whole blood of healthy volunteers or leukocytes from whole-blood leukoreduction filters diluted 1:1 with sterile PBS. 10% acid citrate dextrose solution (ACD-A) was added to prevent clotting. 35 ml of such diluted blood were carefully layered over 15 ml Biocoll solution in a 50 ml-Falcon tube and centrifuged at 600 x g for 20 minutes without subsequent braking. PBMC within the “cloudy” interphase were carefully extracted, transferred to a new 50 ml-Falcon tube and washed twice with PBS (standard centrifugation).

2.2.6 Isolation of immune cell subsets

Either freshly isolated PBMCs or thawed PBMCs were used for the isolation of immune cell subsets. $CD4^+$ and $CD8^+$ T cells and NK cells were isolated using negative isolation kits, $CD14^+$ cells were isolated using positive isolation kits (all Miltenyi). Subset isolation was done according to the manufacturers protocols using LC columns and appropriate magnets. Cell purities as verified by flow cytometry were usually 90 to 95%. In some experiments, the flow through (e.g. $CD14^-$ cells or peripheral blood lymphocytes, PBL) was also collected.

In some experiments, monocytes were enriched by adherence. Briefly, PBMC in Complete RPMI1640 10% FCS were cultured for 1 hour on sufficiently large petri

dishes. Then, non-binding cells were thoroughly rinsed off by pipetting PBS onto the dishes. Adherent cells were then detached by trypsin/EDTA and matured into macrophages or dendritic cells.

2.2.7 HLA-G induction

HLA-G protein induction

For Western Blotting, 2 x 10^6 purified cells ($CD14^+$ monocytes or $CD4^+$ or $CD8^+$ T cells or NK cells) were used. 1 x 10^6 PBMCs were used for flow cytometry. Cells were cultured in Complete RPM1640 5% hAB serum alone or in the presence of 10 ng/ml IL-4, 10 ng/ml IL-10 or 10 ng/ml of each cytokine for 48h. Monocytes were not analysed in detail in flow cytometry experiments because no HLA-G was detectable in preliminary experiments and monocytes were highly auto-fluorescent and unspecifically bound high amounts of antibodies irrespective of Fc receptor blocking strategies.

HLA-G mRNA induction

HLA-G mRNA induction was quantified in 5 x 10^5 cells per condition. Purified $CD14^+$ monocytes, $CD4^+$ and $CD8^+$ T cells and NK cells were cultured in Complete RPM1640 5% hAB serum alone or in the presence of 10 ng/ml IL-4 or 10 ng/ml IL-10 for 6h.

2.2.8 Flow cytometry

Protocol

Flow cytometry was used in numerous experiments. Below, cell numbers, antibody combinations and concentrations and individual staining protocols are listed for each experiment. Unless indicated otherwise, cells were kept on ice or at 4°C during all steps. Antibodies were diluted 1:100 in FACS buffer unless indicated differently. All antibodies are abbreviated by the bound antigen and coupled fluorophore, all antibody details are listed in materials. Generally, cells were blocked with 10% hAB serum in FACS buffer for 30 min, stained in 100 µl in 96-well V bottom plates, washed twice with 200 µl FACS buffer and transferred to FACS tubes in 400 µl FACS buffer for analysis. After each step, cells were pelleted at 450 x g for 5 minutes at 4°C, supernatants were removed by flicking. Cells were analysed with the Attune®Acoustic Focusing Cytometer. The

specific fluorescence intensity (SFI) was calculated by dividing the mean fluorescence intensity of the specific antibody by the mean fluorescence intensity obtained with the respective isotype control antibody.

Antibody combinations

Purity assessment after immune cell subset isolation

Number of cells analysed	2-5 x 10^4
Combination of antibodies	CD3 APC-Vio770, CD4 PE, CD8 PE-Cy7, CD14 FITC, CD56 APC

Analysis of HLA-G surface expression

Number of cells analysed	All cells used in experiment/condition
Combination of antibodies	HLA-G (MEM-G9) FITC or isotype FITC, CD3 APC-Vio770, CD4 PE, CD8 PE-Cy7 and CD56 APC

Analysis of ILT4 surface expression

Number of cells analysed	All cells used in experiment/condition
Combination of antibodies (dilution)	Primary antibody: ILT4 rat IgM or isotype rat IgM (1:50) Secondary antibody: anti-rat FITC (1:50) CD3 APC-Vio770, CD4 PE, CD8 PE-Cy7, CD56 APC

After each step, cells were washed twice in 200 µl FACS buffer

T_{reg} staining

Number of cells analysed	All cells used in experiment/condition
Combination of antibodies	Monensin treatment 2mM added for 4h (for IL-10) Surface staining: CD4 PE, CD8 PE-Cy7 Fixation and permeabilisation: FoxP3 staining kit Intracellular staining: FoxP3 APC, IL-10 AlexaFluor488 (IL-10 staining not shown)

T cell proliferation staining

Number of cells analysed	All cells used in experiment/condition
Combination of antibodies	Dye eFluor® 670 staining see 2.2.15 CD4 PE, CD8 PE-Cy7, CD3 FITC, 7-AAD (1:100)

2.2.9 Protein isolation, SDS-PAGE and Western Blotting

Protein isolation and quantification

Cells were washed 3x with cold PBS and lysed for 20 minutes in 50 µl lysis buffer P (with protease and phosphatase inhibitors, see 2.1.8) on ice. Lysates were spun at 1300 x g for 20 minutes to remove debris and the supernatant was transferred to new 1.5 ml tubes. Protein concentration was determined by the Roti®-Quant Bradford Assay according to the manufacturers protocol. Usually, 20 µg proteins were loaded on each lane. 5x loading buffer supplemented with 10% β-mercaptoethanol was added and proteins were denatured for 5 minutes at 95°C. Samples were then cooled down on ice, spun down and kept on ice until being loaded on the gel.

Gradient gel preparation

The Mini-Protean® Tetra Cell system was used for gel casting and Western Blotting. Separating gel solutions where prepared from the following reagents.

Separating gel	15%	12.5%	10%	7.5%	Stacking gel
dd H_2O	2.19 ml	2.1375 ml	2.45 ml	2.763 ml	3.7ml
40% acrylamide mix	2.25 ml	1.5625 ml	1.25 ml	0.938 ml	0.625ml
1.5 M Tris-HCl+SDS pH 8.8	1.56 ml	1.3 ml	1.3 ml	1.3 ml	-
0.1 M Tris-HCl+SDS pH 6.8	-	-	-	-	0.625ml
10% APS	30 µl	25 µl	25 µl	25 µl	50 µl
TEMED	3 µl	2.5 µl	2.5 µl	2.5 µl	10 µl

APS and TEMED were added just before layering. Each gel was layered with about 2 cm 15% polyacrylamide gel solution followed by each about 1.3 cm 12.5%, 10% and 7.5%

gel solutions. Then, 150 µl of isopropanol were added to exclude bubbles. After 30 min, isopropanol was removed with a whatman paper. Then, the stacking gel was added and the comb was inserted.

SDS Gel electrophoresis

The casted gel was inserted into the holder and the buffer tank was filled with 1 x running buffer. The comb was carefully removed and samples and the protein ladder (8µl) were loaded. Constant 30mA per gel (maximum voltage) were applied for 1h for electrophoresis.

Western blotting

The nitrocellulose membrane was activated in methanol, washed in ddH_2O and equilibrated in transfer buffer for 5 minutes each. Whatman papers and sponge pads were soaked in transfer buffer. Gel, membrane and whatman papers were stacked according to the Mini-Protean protocol and proteins were transferred at 100V constant for 1h.

Detection

The remaining protein-binding sites were blocked for 1h with 5% skimmed dry milk in TBS-T. The primary antibody (4h-84 mouse anti-HLA-G) was diluted 1:1000 in 5% skimmed dry milk in TBS-T and incubated over night at 4°C. The membrane was washed three times for 5 minutes with TBS-T. The polyclonal HRP-coupled secondary antibody was diluted 1:5000 in TBS-T containing 5% skimmed dry milk and incubated for 1h. The membrane was then washed three more times.

Luminol-based developmment solution (here ECL) was prepared by mixing 1 ml ECL A, 100 µl ECL B and 1 µl 30% H_2O_2. The membrane was incubate for 1 minutes in ECL solution and transferred to an X-ray film cassette. Luminescence was detected by X-ray film which was developed and fixed in the dark.

For re-probing, membranes were stripped with stripping buffer followed by neutralization with neutralizing buffer (10 minutes each). Membranes were then blocked and incubated with anti-β-actin (1h) and corresponding secondary antibodies (1h) for normalisation as described above.

X-ray films were subsequently labelled, scanned and bands were quantified with ImageJ.

2.2.10 RNA isolation and reverse transcription

All immune cells treated as described in 2.2.7 were collected and washed once in PBS. The cell pellet was resuspended, lysed in 0.5 ml TriFast reagent and RNA was isolated according to the manufacturers protocol. Briefly, each sample was lysed for 15 minutes at room temperature. 100 µl chloroform was added followed by vigorous vortexing. Samples were kept for 10 minutes at room temperature before phases were separated by centrifugation for 10 minutes at 12000 x g. The clear phase was transferred to a new 1.5 ml tube and RNA was precipitated at 4°C with 0.25 ml isopropanol. The RNA was pelleted and washed twice with 1 ml 75% ethanol (centrifugation 10 min, 12000 x g, 4°C). Ethanol was removed and the RNA pellets air-dried at room temperature. The RNA was resuspended in 20 µl ddH_2O.

Quality control

RNA concentration and quality were measured by photometry. RNA was diluted 1:100 and absorbance was measured at 260 nm and 280 nm. The concentration was determined according to the following formula:

C_{RNA} [µg/ml] = OD_{260} nm x 100 (dilution factor) x 40

Only RNA with a 260 nm/280 nm ratio >1.6 was used for further experiments.

1µg of RNA from each sample was reversely transcribed into complementary DNA (cDNA) with the iScript kit according to the manufacturers protocol. cDNA was diluted 1:10 in nuclease-free ddH_2O.

2.2.11 mHLA-G and sHLA-G TaqMan qPCR

Several semiquantitative protocols for detecting different isoforms of HLA-G mRNA via northern blotting have been described (Paul *et al.* 2000). Additionally, HLA-G TaqMan quantitative PCR (qPCR) kits are commercially available, but lack detailed information regarding primer and probe sequences. Thus, we developed a probe-based qPCR protocol that allows for quantifying membrane-bound (mHLA-G) and soluble (sHLA-G) isoforms separately. Primers and probe for soluble HLA-G were located on exon 4 and intron 4, primers and probe for membrane-bound isoforms on exon 6 and 7. Multiple alignments of HLA-G, HLA-A and HLA-F generated with ClustalW (standard DNA settings, http://www.ebi.ac.uk/Tools/msa/clustalw2/) were used to detect stretches in the mRNA sequence that were as HLA-G-specific as possible. Primers and probes were then designed using the frodo/primer3 homepage. Melting temperatures of primers and probes were designed to match a published 18s TaqMan primer and probe set (Mjosberg *et al.* 2009). Multiple alignment and primer and probe locations for mHLA-G are shown in Figure 6.

```
                    Exon 6
HLA-A   AAAGGAGGGAGCTACTCTAAGGCTGAGTGGAGCGACAGTGCCCAGGGGTC 1184
HLA-G   AAAGGAGGGAGCTACTCTCAG---------------------------- 1216
HLA-F   AACAGAGGGAGCTACTCTCAGG--------------------------- 1154
       **..**************.**
                                      Exon 7
HLA-A   TGAGTCTCACAGCTTGTAAAGCCTGAGACAGCTGCCTTGTGTGCGACTGA 1234
HLA-G   ----------------------------GCTGCAATGTG--------- 1227
HLA-F   ---------------------------CTGCAGCCTACTCAG------- 1169
                                    **:**.:: *

HLA-A   GATGCACAGCTG--CCTTGTGTGCGACTGAGATG-CAGGATTTCCTCACG 1281
HLA-G   ---AAACAGCTG--CCCTGTGTGGGACTGAGTGG-CAAGT---------- 1261
HLA-F   --TGGTCAGCGGAAACTTGATGATAACATGGTGGTCAAG---------- 1206
           . :**** *  .* **:  . .**: .*: * **.*

HLA-A   CCTCCCCTATGTGTCTTAGGGGACTCTGGCTTCTCTTTTTGCAAGGGCCT 1331
HLA-G   ----CCCTTTGTGACTTCAAGAACCCTGACTCCTCTTTGTGCAGAG---- 1303
HLA-F   ----CTTATTTCTCCTGGGGGTGCTCTTCCAAGGATATTTGGGCTGCCTC 1252
            *  ::*    **  ..* .* **  *:   .*:* ** .  *

HLA-A   CTGAATCTGTCTGTGTCCCTGTTAGCACAATGTGAGGAGGTAGAGAAACA 1381
HLA-G   ---------------------------------------------ACCA 1307
HLA-F   CGGAGTCACAGTG-------------------------------TCTTG 1270
                                                     .  .

HLA-A   GTCCACC--TCTGTGTCTACCATGACCCCCTTCCTCACACTG-ACCTGTG 1428
HLA-G   GCCCACC--CCTGTGCCCACCATGACCCTCTTCCTCATGCTG-AACTGCA 1354
HLA-F   GGCCGCCGGAAGGTGGGTGACATGTGGATCTTGTTTTTTTTGTGGCTGTG 1320
        * **.**   . ***   ..****:  . ***  * :   ** . *** .
```

Figure 6: Multiple HLA alignment and primer/probe locations for mHLA-G
Multiple alignment of HLA-A, -G, and –F mRNA exons 6 and 7 (* = identical nucleotide, other symbols = non-identical nucleotides) as generated using ClustalW and primer and probe locations (bold) are shown.

The following primers and probes were used:

Oligonucleotide	length, T_m, GC-content, location
18s RNA, fw primer	20 bp, 62°C, 55%
18s RNA, rev primer	18 bp, 58°C, 61.1%
18s RNA, probe, yakima yellow 5’ TAMRA 3’	22 bp, 72°C, 63.6%
mHLA-G RNA, fw primer	20 bp, 60°C, 50%, Exon 6/ Exon 7
mHLA-G RNA, rev primer	20 bp, 60°C, 60%, Exon 7
mHLA-G RNA, probe, FAM 5’ BHQ1 3’	20 bp, 70°C, 70%, Exon 7
sHLA-G RNA, fw primer	20 bp, 60°C, 55%, Exon 4/Intron 4
sHLA-G RNA, rev primer	20 bp, 60°C, 60%, Intron 4
sHLA-G RNA, probe, Texas Red 5’ BHQ2 3’	20 bp, 70°C, 70%, Intron 4

fw = forward, rev = revers

TaqMan qPCR was set up according to the Platinum Quantitative PCR SuperMix-UDG kit instructions. Briefly, the following reagents were combined:

Reagent	Amount per well (15 µl)	Final concentration
2x PCR SuperMix-UDG	7.5 µl	1x
10 µM forward primer	0.3 µl	0.4 µM
10 µM reverse primer	0.3 µl	0.4 µM
10 µM TaqMan probe	0.15 µl	0.2 µM
Nuclease-free ddH_2O	To 10 µl	-
Sample cDNA (1:10)	5 µl	~25 ng

We have also tested whether HLA-G and 18s can be quantified within the same well (not shown). This is possible when high HLA-G cDNA concentrations are expected, but 18s primer concentrations should be reduced to 40 nM.

qPCR cycling conditions

The 7500Fast qPCR cycler was used with the following settings

Step	Temperature	Time	Cycles
UDG Incubation	50°C	2 min	
Initial denaturation	95°C	2 min	
Denaturation	95°C	15 sec	45 cycles
Annealing and Elongation	60°C	30 sec	
Holding	4°C	-	

Primer/probe efficiencies were analysed using several Jeg-3 cDNA dilutions (1:10, 1:100, 1:1000, 1:10 000, 1:100 000). sHLA-G cDNA was only detectable in 1:10 and 1:100 dilutions and was therefore not analysed in further experiments. mHLA-G and 18s cDNA quantities were detectable with the used primer/probe sets over 5 $\log_{10}$ scales in an almost linear manner (R^2 = 0.987 and 0.997, respectively. See also Figure 7)

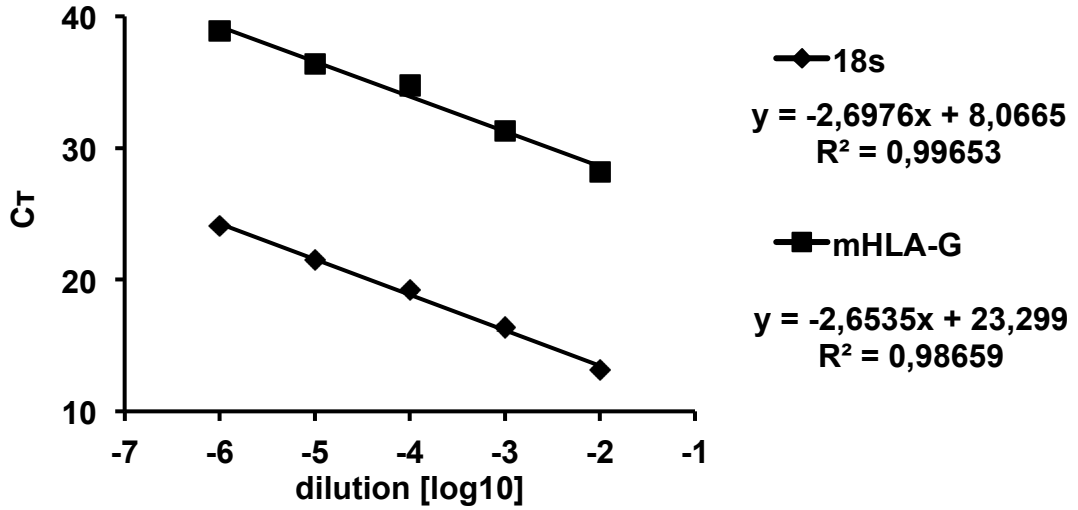

Figure 7: TaqMan qPCR enables the quantification of low levels of mHLA-G mRNAs
Jeg-3 cDNA was diluted in log10 steps and mHLA-G and 18s cDNAs were quantified by TaqMan using the described primer/probe sets and cycling conditions. C_T values plotted against log10 dilutions are shown. mHLA-G cDNA was detectable in $1:10^{-6}$ dilutions of Jeg-3 cDNA from 1 µg of RNA. Primer/probe efficiencies for each experiment were determined via the slope.

Primer/probe efficiencies were calculated for each experiment using the following formula:

efficiency = (10^(-1/slope)-1)·100

These were used to correct measured C_T values and then for determining mHLA-G cDNA concentrations in immune cell samples.

2.2.12 Generation of DC and DC-10

DC and DC-10 were differentiated from bead-purified monocytes from healthy donors. 5 x 10^6 monocytes per ml were cultured for 7 days in Complete RPMI1640 10% FCS supplemented either with 10 ng/ml rhIL-4 and 50 ng/ml rhGM-CSF (DC, elsewhere also referred to as iDC) or 10 ng/ml rhIL-10, 10 ng/ml rhIL-4 and 50 ng/ml rhGM-CSF (DC-10). Media was replaced on day 3 and day 5. After 7 days, cells were analysed by flow cytometry or used for experiments.

2.2.13 Transfer of scHLA-G5 to DC-10

2.5 x 10^5 DC-10 were washed once with PBS, and the cell pellet was resuspended in 250 µl Complete RPMI1640 10% FCS with 10 ng/ml rhIL-10, 10 ng/ml rhIL-4 and 50 ng/ml rhGM-CSF. Then, 250 µl LCL-scHLA-G5 or LCL-ctrl supernatant were added. Unless indicated otherwise, scHLA-G5 was transferred to DC-10 for 4h at 37°C with agitation. DC-10 were then washed 3 times with 1ml PBS and used for further experiments. 10µg/ml anti-HLA-G (cone 87G), anti-ILT-2 (clone HPF1) or anti-ILT-4 (clone 27D6) blocking antibodies were added before the transfer in the experiment shown in 3.4.4.

2.2.14 Induction of regulatory T cells

1 x 10^6 syngeneic PBL were cultured in an incubator alone or with 5 x 10^5 DC-10^{ctrl} or 5 x 10^5 DC-$10^{scHLA\text{-}G5}$ for 7 days in RPMI hABc with IL-2 and TGFβ1 (5ng/ml each). Medium was replaced every second day. FoxP3 or IL-10 expression were then analysed by flow cytometry as described in 2.2.8.

2.2.15 $CD8^+$ T cell proliferation assays

For each setting, 4 x 10^5 syngeneic PBL were stained with 5 µM Cell Proliferation Dye eFluor670 according to the manufacturers instructions. PBL were cultured alone or with 5 x 10^5 DC-10^{ctrl} or 5 x 10^5 DC-$10^{scHLA\text{-}G5}$ for 24h in 100 µl RPMI hABc with IL-2 (20 ng/ml). Then, 1µg/ml PHA was added to all wells except for the negative control. On day 3, 100 µl RPMI hABc with IL-2 were added to each well. On day 5, T cells were stained for additional surface markers and T cell proliferation was assessed by flow cytometry.

2.2.16 Statistical analysis

Graphpad Prism 6 was used for statistical analyses. The respective statistical tests are indicated in the results section. P values ≤ 0.05 were considered statistically significant.

3 Results

3.1 Expression of HLA-G in healthy tissues and ovarian carcinoma

In order to get a more detailed overview of HLA-G expression in physiological conditions and during ovarian carcinoma development, paraffin-embedded ovarian cancer samples of different subtypes and control tissues were stained for HLA-G

3.1.1 HLA-G is expressed in few healthy tissues

A TMA consisting of each three 1mm cores from 50 different FFPE healthy control tissues was immunofluorescently stained for HLA-G, cytokeratin and CD68. The staining, image acquisition and scoring protocols for all FFPE materials were optimized and carried out together with Sabine Roth and Prof. Dr. Eva Geißinger from the Institute of Pathology, University of Würzburg. As expected, a strong expression of HLA-G was detected in the placenta, particularly in the amniotic membrane. However, significant levels of specific HLA-G staining were also detected in the medulla of the adrenal gland and in seminiferous tubules of the testes. In some tissues, fluorescence detected in the HLA-G channel did not correlate with cellular structures and was most likely caused by staining artefacts. Round, spot-like artefacts were detected in spleen, liver, cortex of the adrenal gland and seminal vesicles. Thin, extracellular structures were positively stained in kidney, skin and ectocervix samples. Representative confocal images are shown in Figure 8, a complete overview of HLA-G expression intensities in all screened tissues is shown in Figure 9.

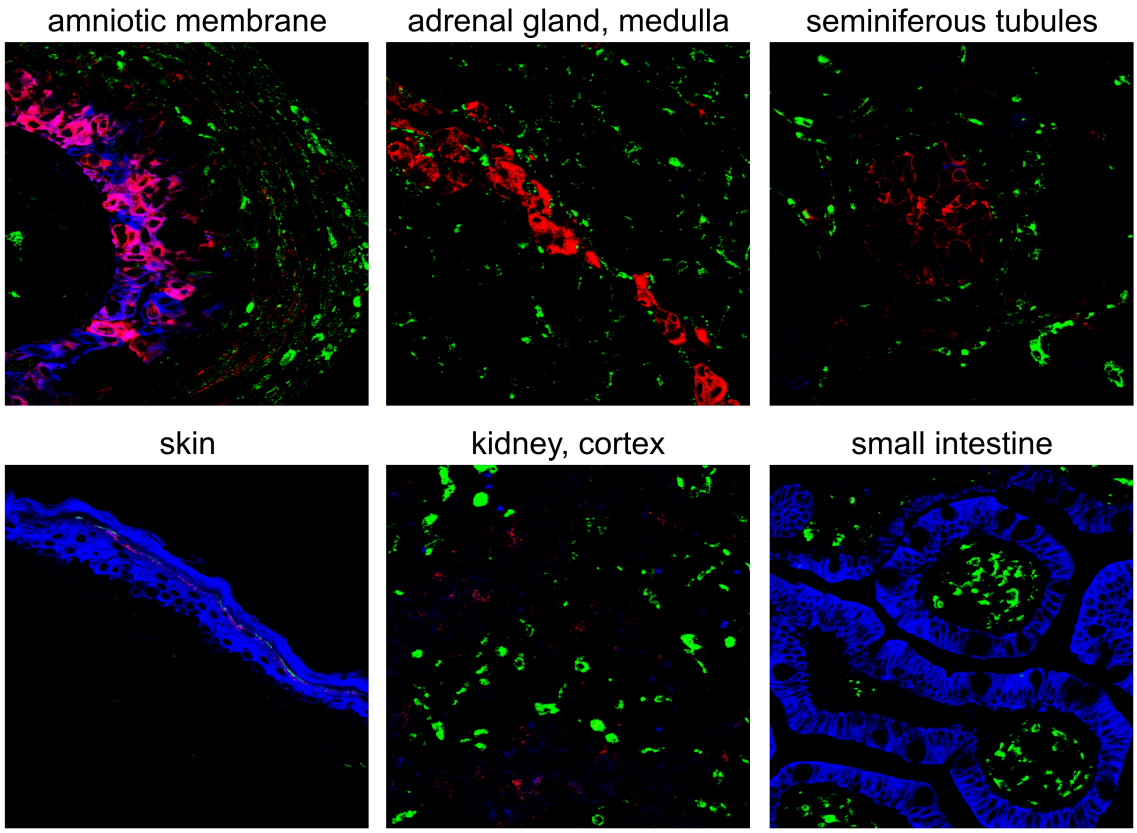

Figure 8: Representative examples of HLA-G expression in healthy control tissues
A tissue microarray containing each three 1mm cores of 30 different FFPE healthy control tissue samples was stained for HLA-G, cytokeratin and CD68. Representative confocal images (60x magnification) from different control tissues are shown. HLA-G, cytokeratin and CD68 are depicted in red, blue and green, respectively. HLA-G was detected in the amniotic membrane, the medulla of the adrenal gland and seminiferous tubules. Weak fluorescence in the HLA-G channel that most likely resulted from staining artefacts was detected in some tissues such as skin and kidney. No specific staining was detected in most tissues, such as small intestine. See Figure 9 for a complete overview of HLA-G expression in all stained tissues.

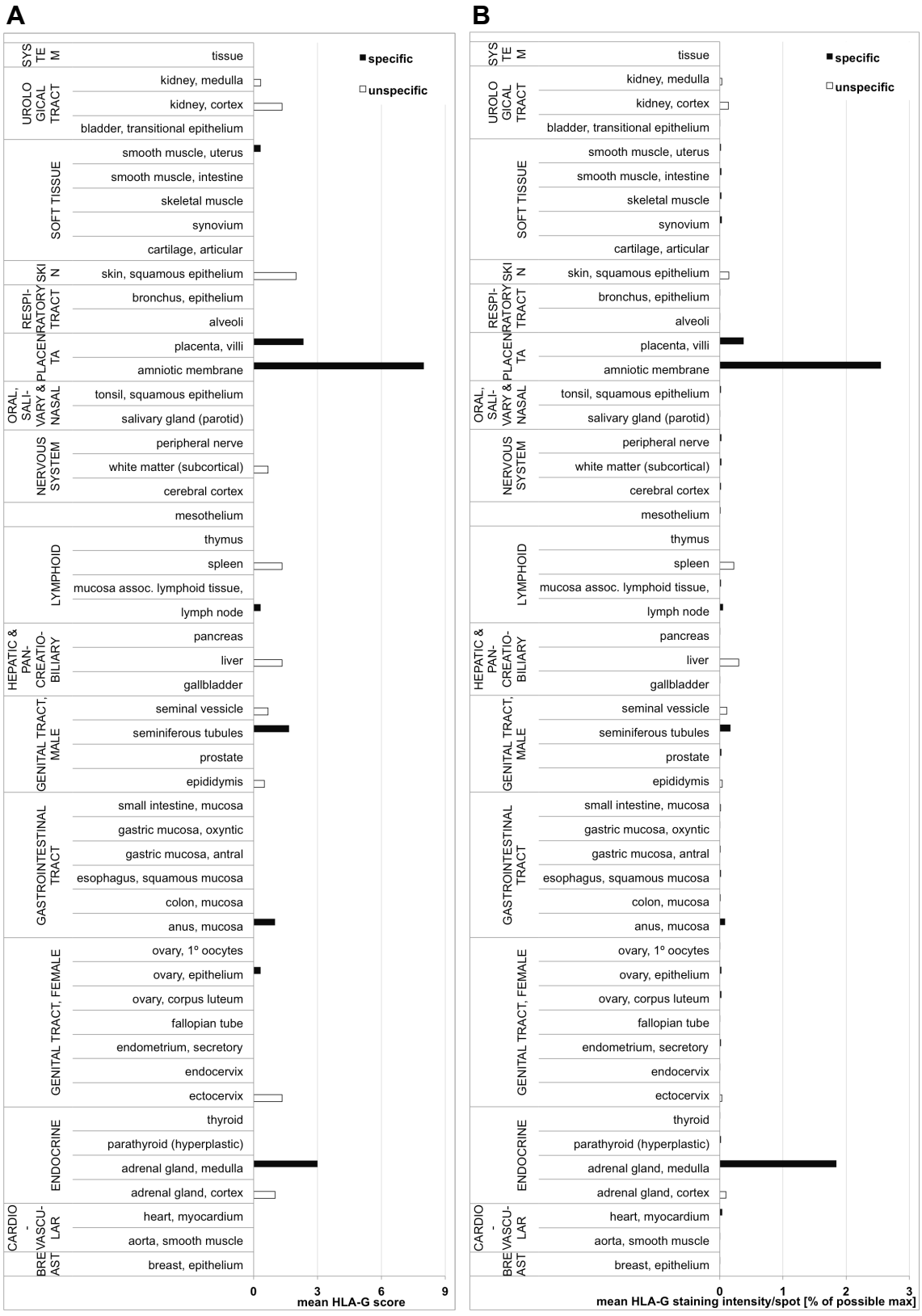

Figure 9: HLA-G expression in healthy control tissues

The tissue microarray described in Figure 8 was screened for the expression of HLA-G. HLA-G expression was either manually scored **(A)** or the average fluorescence intensity in the HLA-G channel of each image was quantified **(B)**. The staining intensity was normalized to the tissue area, and mean values for all three spots are displayed. Specific HLA-G staining is indicated by filled bars, while fluorescence that resulted most likely from staining artefacts such as red blood cells is indicated by unfilled bars.

3.1.2 HLA-G is expressed in different subtypes of ovarian carcinoma

In order to investigate how frequently HLA-G is expressed in different subtypes of ovarian carcinoma, a TMA was immunofluorescently stained as described in 3.1.1. The TMA contained each 4 different 0.6 mm cores from each 20 clear cell, 20 endometrioid, 20 mucinous, 37 serous and 3 undifferentiated ovarian carcinomas. Here, all tumours used in the microarray had been graded according to the older FIGO 4-tier grading system, and no information regarding high-grade or low-grade classification was available. However, in studies comparing the grading systems, all grade 1 tumours were found to be low-grade and most grade 2 and all grade 3 ovarian carcinomas were found to be high-grade tumours (Malpica *et al.* 2004). Each spot in which HLA-G was detectable was both manually scored and scored based on measured fluorescence intensity in the HLA-G channel. Identically stained cores from ovarian epithelium and amniotic membrane of the control TMA were used for negative and positive controls, respectively. Overall, HLA-G was detected by manual scoring in cores 10 out of 37 serous, 4 out of 20 mucinous, 3 out of 20 endometrioid, 3 out of 20 clear cell and 1 out of 3 non-differentiated carcinomas. Compared to the healthy ovarian tissue, elevated levels of HLA-G expression were detected in 7 serous, 1 mucinous, 2 endometrioid and 2 clear cell carcinomas. Among the assessed subtypes, the lowest HLA-G expression was detected in non-differentiated, mucinous and clear cell carcinomas. Manually determined scores nicely correlated with quantified HLA-G fluorescence, which was used as a control. Representative examples of HLA-G immunofluorescence stainings for all subtypes are shown in Figure 10. HLA-G expression scores as well as grade, stage and age are listed for all patients in Table 2.

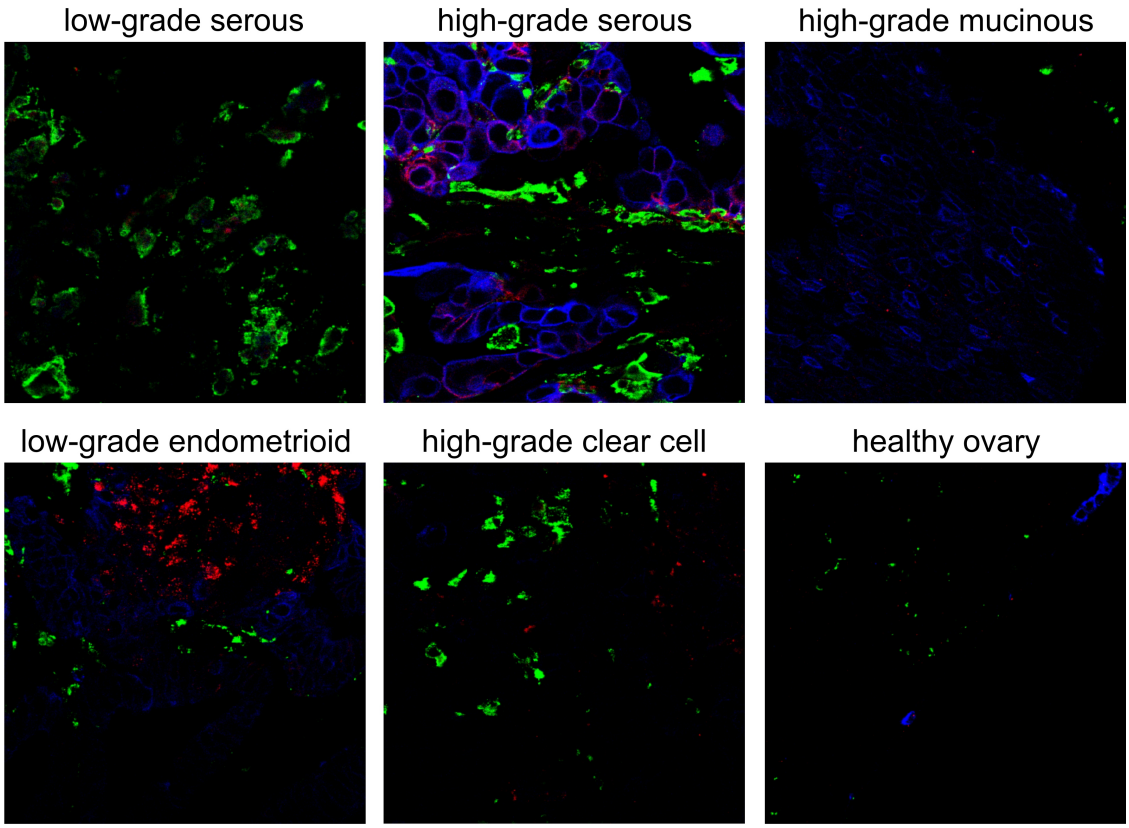

Figure 10: HLA-G is detectable by immunofluorescence in different ovarian carcinoma subtypes
A tissue microarray containing each four 0.6 mm cores of each 20 different FFPE tumour samples of five ovarian carcinoma subtypes was stained for HLA-G, cytokeratin and CD68 (depicted in red, blue and green, respectively). As compared to healthy ovaries, elevated levels of HLA-G were detected in some tumours of each subtype.

Table 2: Results TMA HLA-G expression in ovarian carcinoma subtypes

type	grade	stage	age	score	intens.
serous	G1	T1a	62	1	0.018
		T1b	67	0	0.000
		T3b	53	0	0.000
		T3b	53	0	0.000
	G2	T1a	79	0	0.000
		T1b	32	0	0.000
		T2b	73	0	0.000
		T3a	65	0	0.000
		T3a	52	0	0.002
		T3b	79	0	0.000
		T3b	72	0	0.000
		T3b	48	0	0.000
		T3b	83	0	0.000
		T3b	79	0	0.000
		T3b	47	0	0.000
		T3b	70	0	0.000
		T3b	65	0	0.009
		T3b	75	6	0.282
		T3c	33	0	0.000
		T3c	86	2	0.007
	G3	T1c	71	2	0.079
		T2b	83	4	0.009
		T2b	55	1	0.008
		T2b	44	0	0.000
		T3a	67	1	0.013
		T3b	58	0	0.000
		T3b	55	0	0.000
		T3b	75	0	0.000
		T3b	58	0	0.000
		T3b	73	0	0.000
		T3b	73	0	0.006
		T3b	57	0	0.000
		T3b	52	4	0.193
		T3c	68	0	0.000
		T3c	53	0	0.000
		T3c	62	4	0.096
		T3c	60	2	0.040
mucinous	G1	T1a	52	0	0.000
		T1a	37	0	0.000
		T1a	62	1	0.002
		T1a	62	0	0.000
		T1a	59	0	0.000
		T1a	39	0	0.000
		T1a	42	0	0.000
		T1a	61	0	0.000
		T1a	54	0	0.000
		T1a	63	0	0.000
		T1a	73	0	0.000
		T1c	78	0	0.000
		T2b	40	2	0.017
		T2b	40	0	0.000

type	grade	stage	age	score	intens.
mucinous	G1	T3b	80	0	0.000
		T3c	51	0	0.000
	G2	T1c	40	0	0.000
		T3c	62	0	0.000
	G3	T3a	65	1	0.003
		T3b	59	1	0.005
endometrioid	G1	T1a	73	0	0.000
		T1a	41	0	0.000
		T1a	48	4	0.062
		T1a	38	0	0.000
		T2a	73	0	0.000
	G2	T1a	57	0	0.000
		T1a	52	2	0.006
		T1a	41	0	0.000
		T1a	54	1	0.016
		T1b	68	0	0.000
		T1c	64	0	0.000
		T2a	49	0	0.000
		T2c	72	0	0.000
		T3a	74	0	0.000
		T3b	51	0	0.000
	G3	T1b	52	0	0.000
		T1b	52	0	0.000
		T2a	50	0	0.000
		T2b	59	0	0.000
		T3c	54	0	0.000
clear cell	G1	T1a	50	0	0.000
	G2	T1a	36	0	0.002
		T1a	60	0	0.000
		T1a	49	2	0.030
		T1a	53	0	0.000
		T1c	63	0	0.000
		T2a	63	0	0.000
		T2a	52	0	0.000
		T2b	59	0	0.000
		T3a	65	0	0.000
		T3a	56	1	0.011
		T3c	70	0	0.000
		T3c	55	0	0.000
		T3c	49	0	0.000
	G3	T2a	52	0	0.000
		T3b	53	0	0.000
		T1a	68	0	0.000
		T3a	67	0	0.000
		T3a	83	2	0.028
		T3b	75	0	0.000
ND	G4	T2b	73	0	0.002
		T3b	49	1	0.003
		T3b	76	0	0.000
healthy ovary			49	1	0.033
healthy placenta			21	9	0.601

Each four 0.6 µm cores stained for HLA-G, cytokeratin and CD68 were analysed from each patient; score = highest manually determined HLA-G expression score of one tumour, intens. = mean detected HLA-G fluorescence intensity of all spots [% of maximum detectable intensity]; ND = non-differentiated; healthy ovary = ovarian epithelium from healthy donor; healthy placenta = amniotic membrane from normal term placenta; three 1 µm cores of these control tissues were stained in parallel on a different microarray and included in this table for reference.

3.1.4 Most HLA-G is detectable in high-grade serous carcinomas

In serous carcinomas, moderate to high HLA-G expression levels (score > 1) were detected in none of 4 grade 1 (low-grade) tumours, 2 out of 16 grade 2 tumours (which are mostly high-grade; HLA-G expressing tumours were stage T3b and T3c) and in 5 out of 17 grade 3 (high-grade) tumours. This trend, which has also been reported by others (Menier, Prevot *et al*. 2009, Singer, Rebmann *et al*. 2003), was observed with regards to only serous (see Figure 11) or all carcinoma subtypes (see Figure 12). However, due to the low sample numbers, this difference did not reach statistical significance (P=0.16 and P=0.08, respectively; unpaired Student's t-Test; one-tailed). HLA-G expressing tumours were detected in all stages and patients of all ages (see Figure 12).

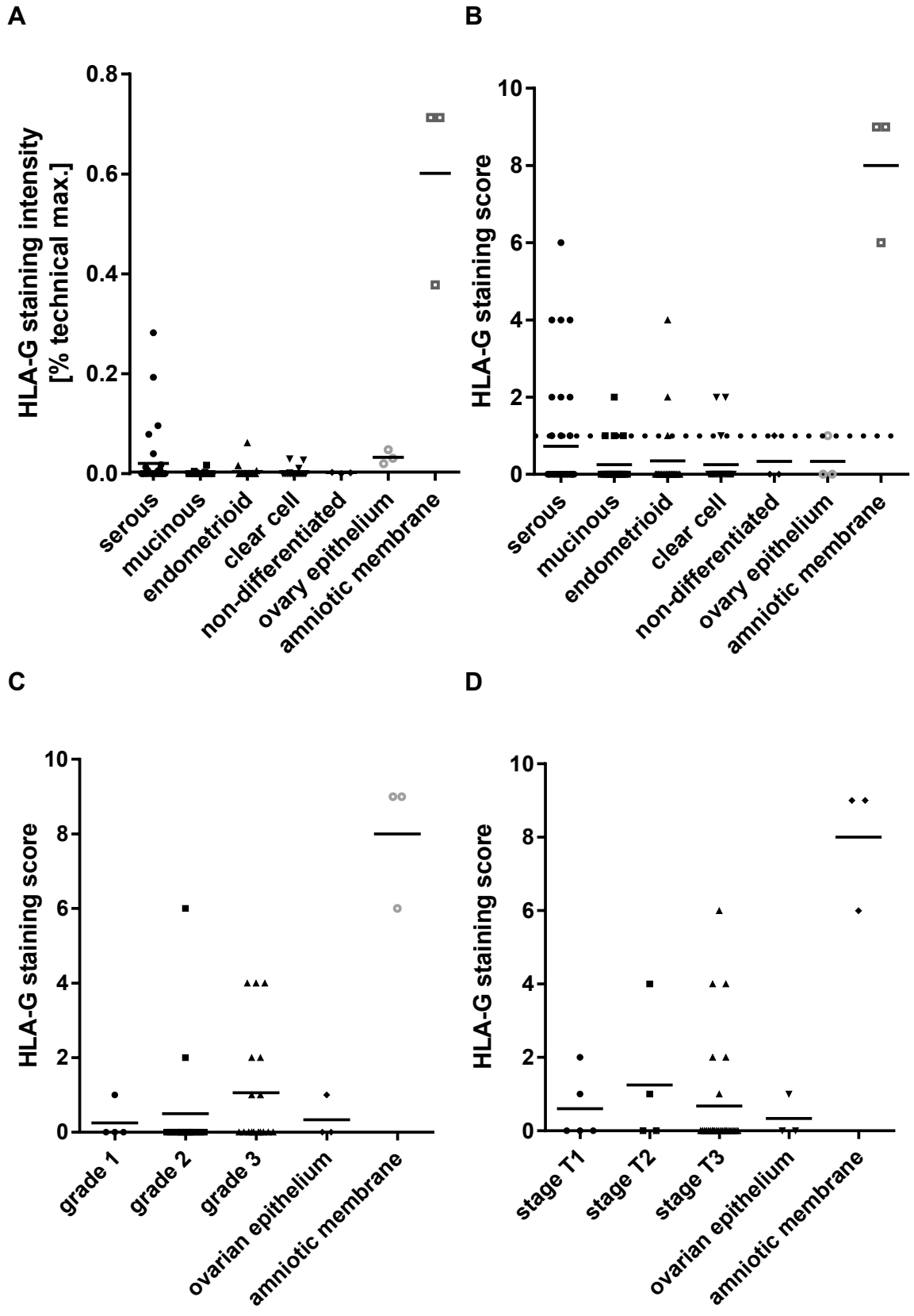

Figure 11: HLA-G may most frequently be expressed by high-grade, serous carcinomas
HLA-G expression was quantified with similar results by **(A)** quantifying the staining intensity or by (**B-D**) manual scoring (highest detected score for each patient is indicated). (**B**) Most of the tumours that expressed high levels of HLA-G (above dashed line) were serous carcinomas **(C)** of grade 2 or 3 and **(D)** stage T2 or T3. Only serous carcinomas are shown in (**C** and **D**).

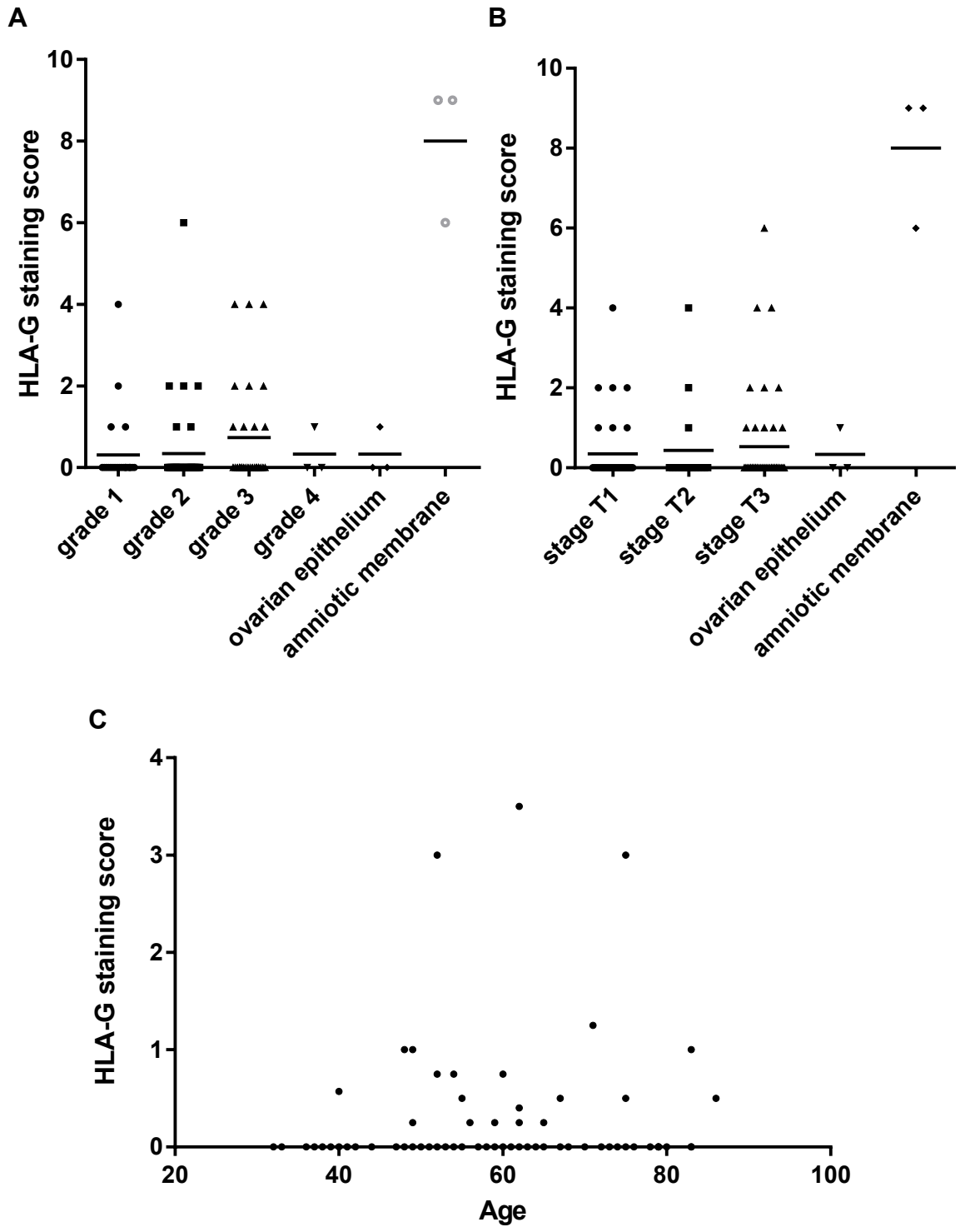

Figure 12: HLA-G is most frequently expressed by grade 3 carcinomas irrespective of stage or patient age
When all ovarian carcinoma samples included in the TMA are analysed together, the trend that grade 3 express most HLA-G is confirmed (**A**). However, no correlation with tumour stage (**B**) or age of the patients at time of surgery (**C**) was found. Samples were from patients between 32 and 86 years of age. HLA-G-expression was detected in carcinomas from patients of age 40 to 86.

3.1.5 In primary lesions, HLA-G is predominantly expressed by malignant cell

In order to confirm HLA-G expression on malignant cells, some consecutive slides were additionally stained for tumour markers Wilms tumour protein (WT1) and cytokeratin. As shown in Figure 13, HLA-G was mostly detected on cytokeratin-positive, WT1-postitive or double-positive tumour cells.

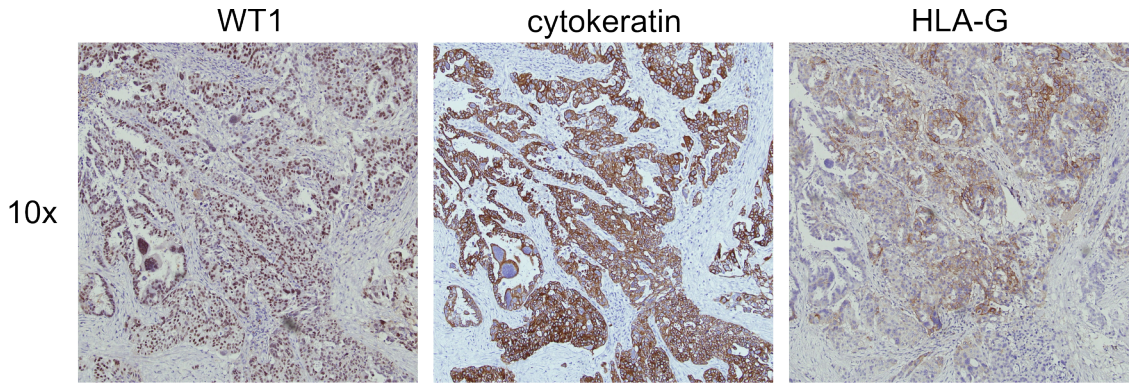

Figure 13: HLA-G is predominantly expressed by ovarian carcinoma cells in primary lesions
Three FFPE sections of the same tumour area were stained by IHC for the tumour markers wilms tumour protein (WT1) and cytokeratin and for HLA-G. In primary tumours, HLA-G was mostly detected in cells that expressed these tumour markers and were of malignant morphology.

3.1.6 HLA-G is detectable in metastases and histiocytes in local lymph nodes

Ovarian carcinomas frequently metastasize into draining lymph nodes within the pelvis or to pelvic organs, such as the omentum majus (Jayson, Kohn *et al*. 2014). In order to investigate whether HLA-G is also expressed in metastases, FFPE primary metastases and lymph node samples were stained for HLA-G. As high-grade serous ovarian carcinomas most frequently expressed HLA-G and due to the availability of FFPE lymph node samples from, only samples of this subtype were analysed here. In contrast to the TMA in which 4 0.6 µm cores from 100 different tumours were analysed on one slide, here only 1 or 2 tumour or lymph node sections were analysed per slide. The sections were mostly between 5 and 15 mm in diameter. Thus, in these samples, a much higher fraction of the tumour was screened for HLA-G expression. Lymph nodes that were assessed here belonged to the nodi lymphatici (Nll) paraaortica, iliaci communes, interni and externi and obturatori (see Figure 14).

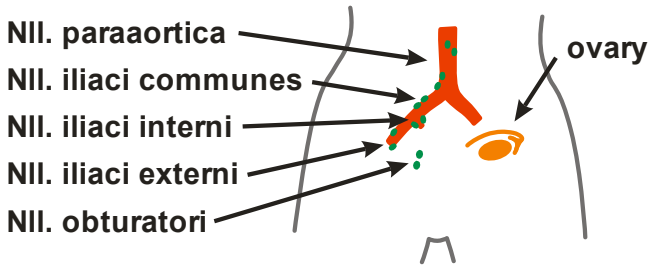

Figure 14: Anatomical sites of patient lymph nodes screened for HLA-G expression
Lymph nodes from high-grade serous carcinoma patients that were screened for HLA-G were from the following sites: nodi lymphatici (Nll) paraaortica, iliaci communes, interni and externi and obturatori. A short part of the aorta is shown in red. Lymph nodes (green) and the ovary (orange) of one side only are depicted.

In tumour sections from primary lesions, significant HLA-G-staining was detected in samples of 9 out of 11 patients with high-grade serous carcinomas (11 out of 13 different sections). HLA-G was also expressed in metastases of 6 out of 7 patients (8 out of 10 sections), although at significantly lower expression levels (P=0.033, unpaired Student's t-Test; two-tailed). HLA-G expression within different areas of one tumour was usually heterogeneous (see Figure 15). Surprisingly, high levels of HLA-G were also detected on histiocytes in lymph nodes with and without metastases, even in cases in which no HLA-G was detectable in the primary lesion (see Table 3). In contrast, no HLA-G was detectable in tonsils from non-malignant donors which were used as a reference tissue for secondary lymphoid organs. Furthermore, only marginal levels of HLA-G were detected in immunofluorescently stained lymph nodes from healthy donors (see Figure 9). Thus, HLA-G may be induced in or transferred to histiocytes in tumour-free lymph nodes. Representative IHC stainings of tonsils from non-malignant patients, primary lesions and lymph nodes with and without metastases and histiocytes from serous carcinoma patients are shown in two different magnifications in Figure 15.

HLA-G staining of malignant cells in primary tumours and metastases and histiocytes in lymph nodes was manually scored in order to be able to compare expression levels in between these tissues. Reference sections that were used for scoring the HLA-G staining intensity on tumour cells and histiocytes are shown in Figure 16. HLA-G expression scores in these tissues are listed for all patients in Table 3 and compiled in Figure 17 where patient-specific symbols are used.

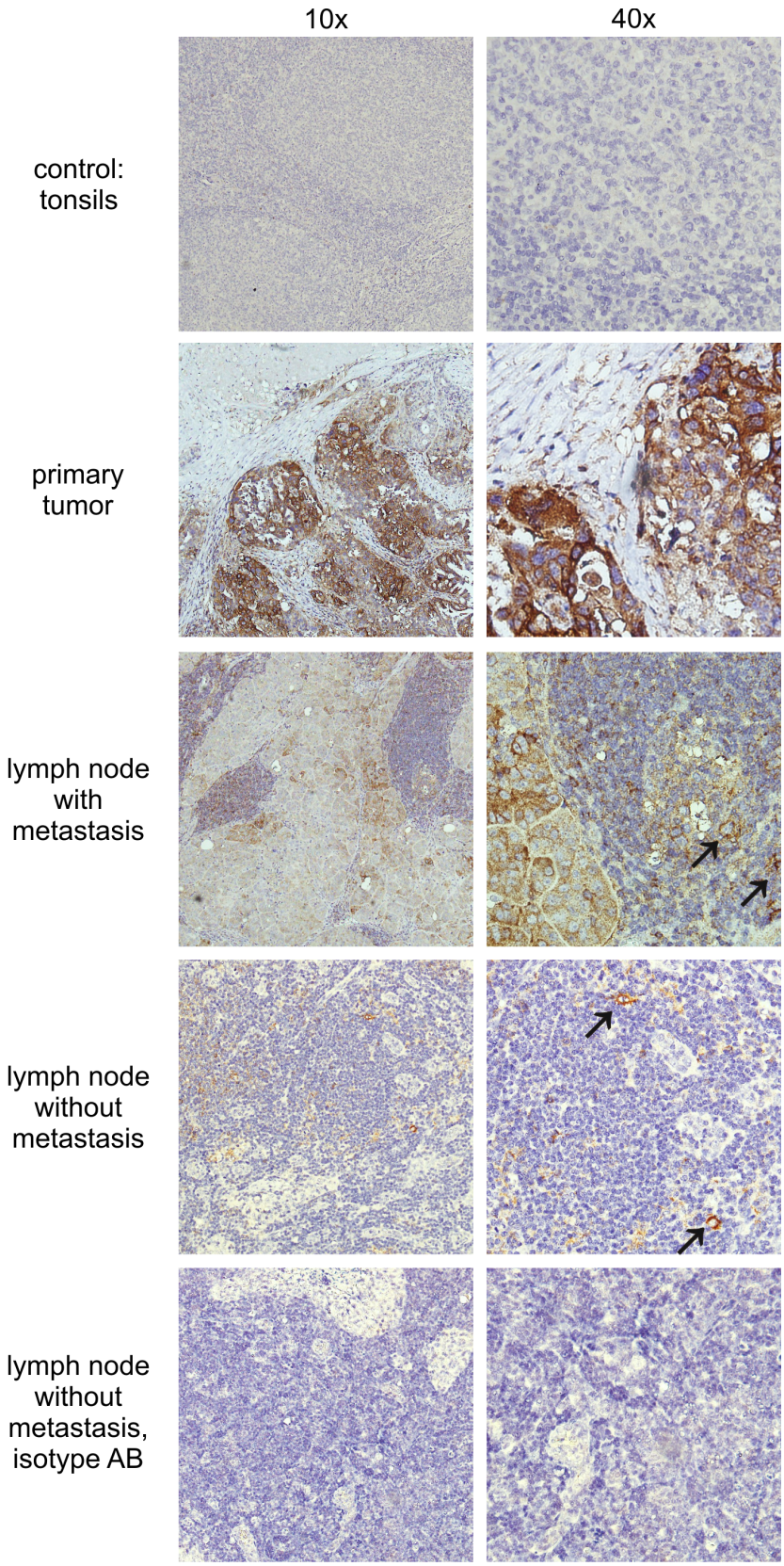

Figure 15: Representative examples of tumours and lymph node sections stained by IHC for HLA-G
FFPE primary tumour, metastases and lymph node samples from high-grade serous carcinoma patients were stained by IHC with the anti-HLA-G antibody 4H84. HLA-G was expressed at high levels in most primary tumours and at lower levels in most metastases. HLA-G was also detected on histiocytes (indicated by arrows) in local tumour-free lymph nodes and lymph nodes with metastases. No HLA-G was detected in tonsils from non-tumour patients or in healthy lymph nodes (see Figure 9).

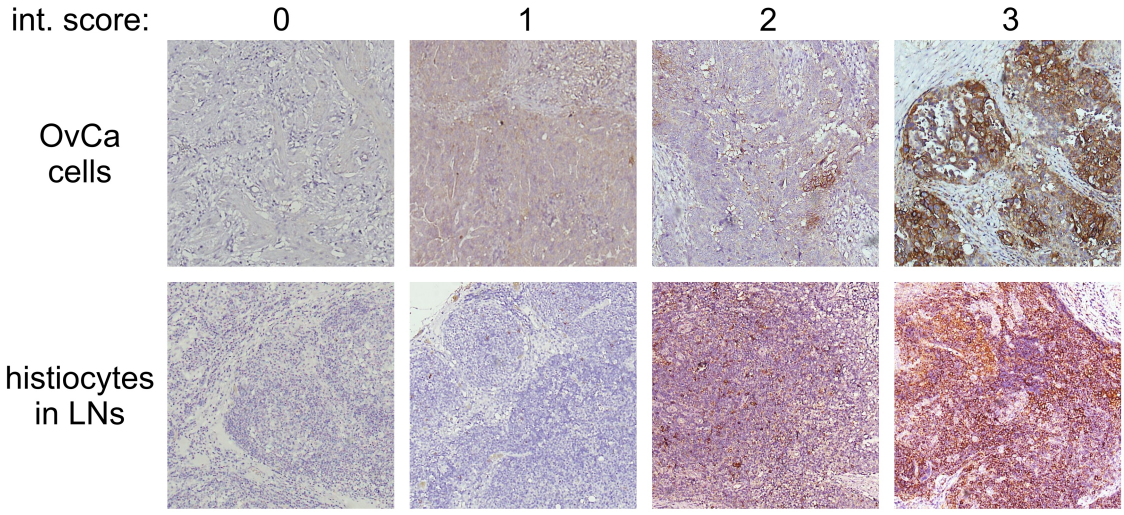

Figure 16: Reference sections for IHC HLA-G intensity scoring

The HLA-G staining intensity in primary tumour and lymph node (LN) sections was manually scored by evaluating the intensity on a scale from 0 to 3. Reference images are shown. For the expression score, this intensity value was multiplied by 0, 1, 2, 3 or 4 when stained cells were found in 0%, 1-10%, 10-25%, 25-50%, or 50-100% of the tumour or lymph node area, respectively. As an example, the highest possible expression score of 12 is given if a very intense HLA-G staining is detected in more than 50% of carcinoma cells or histiocytes.

Table 3: HLA-G expression scores in malignant cells and on histiocytes

patient #	tumour cells primary lesion	tumour cells metastasis	histiocytes in LN without metastases	histiocytes in LN with metastases
1	8			6/9/3/4/3
2	9/6	4/1	6/6	4/6/9
3	6/2	3/0	6	6/3
4	8/6	4/3	12/12	12
5	2	3		6
6	0	2/0	6/3	
7	8/6		6	9
8	6	6	9	1
9	0			2/0

LN = lymph node, expression scores for each available sample are indicated and separated by / symbols. In some cases, several parts of the primary tumour were assessed.

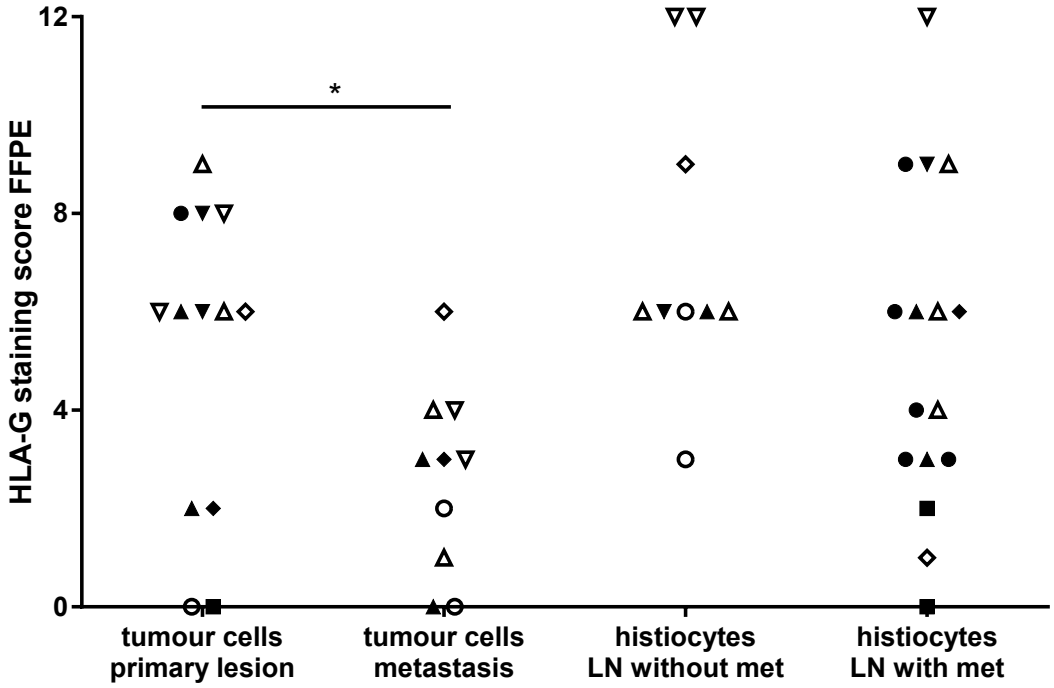

Figure 17: HLA-G is detected in primary tumours, metastases and histiocytes in local lymph nodes.
HLA-G IHC staining intensity was scored in FFPE primary tumour, metastases and lymph node samples from 9 high-grade serous carcinoma patients. In some patients, several tumours or lymph nodes were assessed. Each patient is represented by an individual symbol. Most assessed tumour samples expressed HLA-G both in primary tumours and, in significantly lower amounts, in metastases (P=0.033, unpaired Student's t-Test; two-tailed). HLA-G was detected on histiocytes in at least one lymph node section in all of the assessed patients.

3.2 HLA-G and MHC Ia expression correlate in ovarian carcinomas

In order to investigate whether HLA-G expression may enable otherwise immunogenic ovarian carcinomas to escape from immunosurveillance, a published gene expression dataset was screened for mRNAs which correlate with HLA-G mRNA expression. A dataset from a microarray-based study that included gene expression data from 285 carcinomas of the ovary, peritoneum, and fallopian tube was selected (Tothill *et al.* 2008). The R2 genomics analysis and visualization platform (http://r2.amc.nl) was used to find genes expressed at high levels HLA-G expressing tumours. Interestingly, among the seven mRNAs expressed in highest correlation with HLA-G mRNA (all $P < 10^{-77}$) were, in addition to HLA-E and HLA-F, mRNAs from all classical MHC class Ia genes (HLA-A, -B and -C) and TAP1, which is involved in transporting and loading antigenic peptides to MHC class I molecules (Momburg and Tan 2002, Raghuraman *et al.* 2002) (see also Table 4). Two X-Y plots of these almost linear correlations (indicated by R^2 values ranging form 0.85 to 0.95) are displayed in Figure 18.

Table 4: HLA-G expression correlates with MHC Ia and TAP1 expression in ovarian carcinomas

gene	R^2	P value	Function	Reference
HLA-G	1.000	0.0e+00	see introduction	
HLA-J	0.946	8.6e-137	inactivated gene	(Messer *et al.* 1992)
HLA-F	0.945	3.9e-136	MHC Ib	see introduction
HLA-B	0.897	2.1e-98	antigen presentation	(Neefjes, Jongsma *et al*. 2011, Williams *et al.* 2002)
HLA-E	0.889	3.0e-94	MHC Ib	see introduction
HLA-C	0.887	2.0e-93	antigen presentation	(Neefjes, Jongsma *et al*. 2011, Williams, Peh *et al*. 2002)
HLA-A	0.883	1.1e-91	antigen presentation	(Neefjes, Jongsma *et al*. 2011, Williams, Peh *et al*. 2002)
TAP1	0.852	2.7e-78	peptide transport/ MHC loading	(Momburg and Tan 2002, Raghuraman, Lapinski *et al*. 2002)

Source: (Tothill, Tinker *et al*. 2008) dataset analysed with R2 (http://r2.amc.nl)

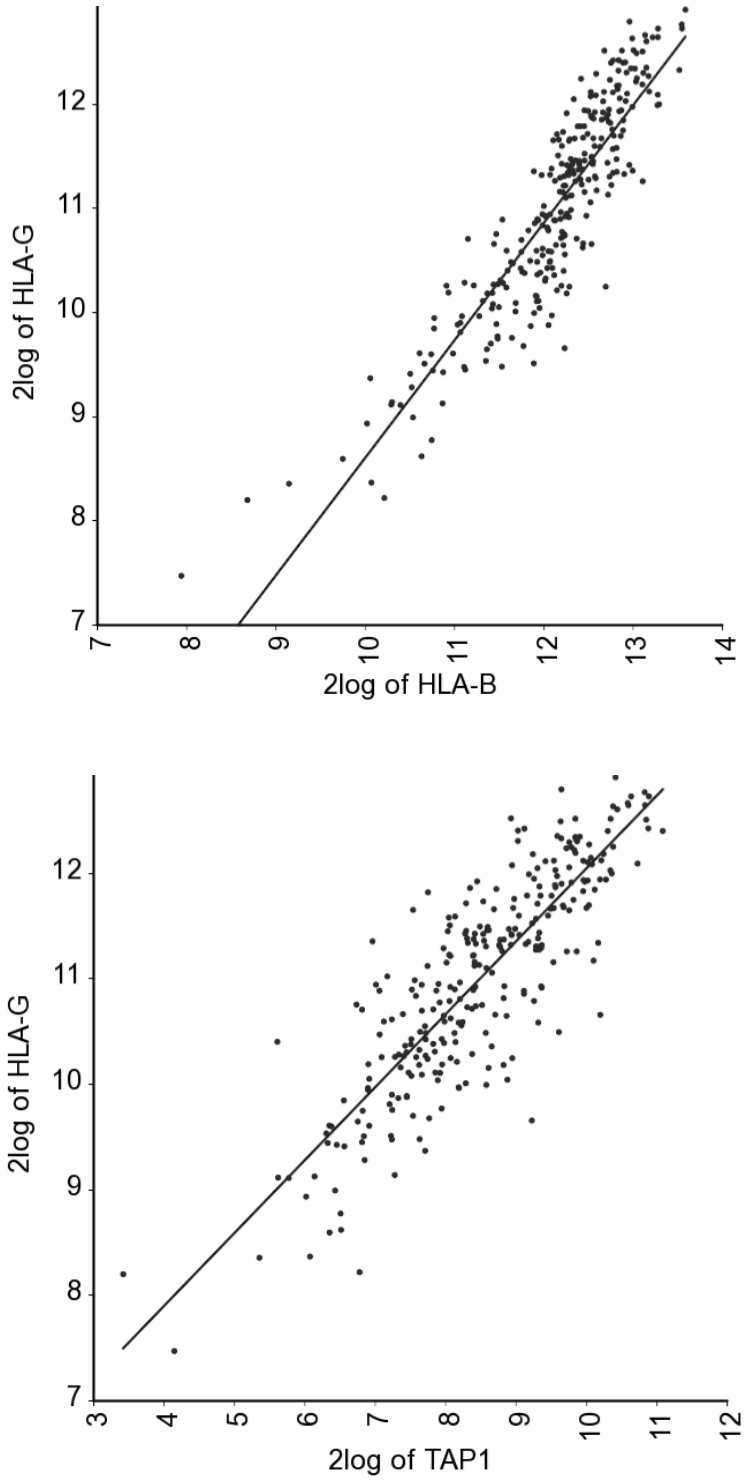

Figure 18: HLA-G and HLA-B and TAP1 gene expression correlate in ovarian cancer
The R2 genomics analysis and visualization platform (http://r2.amc.nl) was used to analyse genes expressed in correlation with HLA-G in ovarian cancer (Tothill, Tinker *et al*. 2008). HLA-B and TAP1 are both involved in antigen presentation and their expression highly correlated with HLA-G expression.

3.3 Induction of HLA-G in immune cells

3.3.1 Ascites of ovarian carcinoma patients often contains high levels of IL-4 and IL-10

It has been reported that dendritic cells that are generated in the presence of IL-10 in addition to IL-4 and GM-CSF (DC-10) express high levels of HLA-G (Gregori, Tomasoni *et al*. 2010). Furthermore, IL-10 has been reported to induce HLA-G in trophoblasts and monocytes of some donors (Moreau *et al.* 1999) and IL-4 may induce the expression of soluble HLA-G5 in T cells (Lombardelli, Aguerre-Girr *et al*. 2013). In order to investigate whether IL-4 and IL-10 may also induce the observed HLA-G expression in dendritic cells in lymph nodes in ovarian cancer, concentrations of both cytokines were measured by ELISA in ascites derived from ovarian carcinoma patients. High concentrations of both cytokines were frequently detected in ascites from OvCa patients, but also in benign ascites (physiological serum levels are indicated by dotted lines in Figure 19).

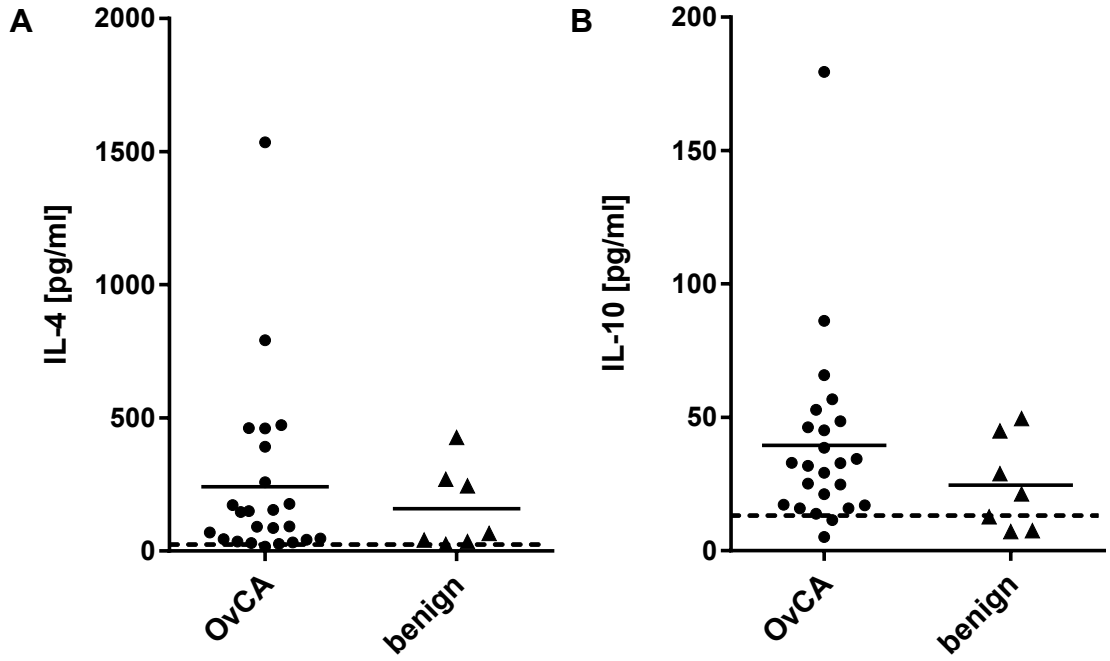

Figure 19: Ovarian carcinoma ascites contains high levels of IL-4 and IL-10
IL-4 **(A)** and IL-10 **(B)** in ascites samples from 24 ovarian carcinoma (OvCA) patients and 7 patients without malignancy were quantified by ELISA. As ascites does not accumulate in healthy individuals, physiological serum levels of each cytokine as reported in the literature (Sheu and Shih Ie 2007) are indicated by the dotted lines for reference. Highly elevated concentrations of both cytokines were detected in some benign and most ovarian carcinoma ascites samples.

3.3.2 IL-4 and IL-10 induce HLA-G expression in lymphocytes, but not in monocytic cells

In order to investigate whether HLA-G expression in histiocytes may be induced due to high levels of IL-4 or IL-10, we tested if these cytokines induce HLA-G in monocytes or monocyte-derived dendritic cells from healthy donors. Monocytes were isolated either by adherence enrichment or via anti-CD14 magnetic beads. Within 48 hours, both IL-4 and IL-10 induced the expression of HLA-G on protein level both in adherence-enriched monocytes and $CD14^-$ lymphocytes. However, no induction or basal expression was detected in bead-purified $CD14^+$ cells. Flow cytometry revealed that only between 25% and 63% of adherence-enriched cells were actually $CD14^+$ monocytes (see Figure 20). Thus, HLA-G detected in adherence-enriched monocytes may be derived from contaminating lymphocytes. Similarly, DC-10 cells derived from bead-purified monocytes did not express HLA-G (see Figure 24A LCL ctrl SN lane).

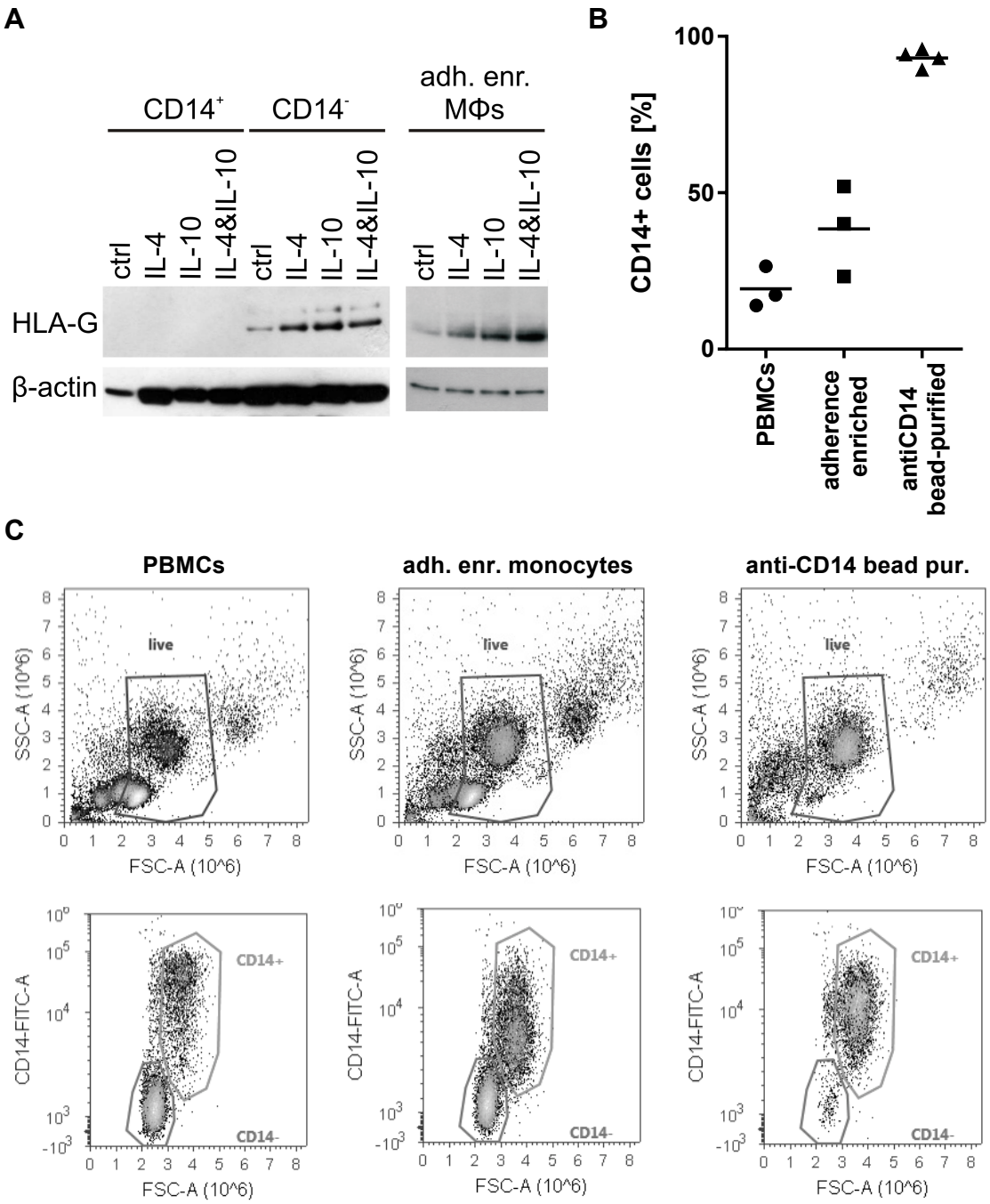

Figure 20: IL-4 and IL-10 induce HLA-G in lymphocytes, but not in monocytes

(A) Adherence-enriched and both $CD14^+$ and $CD14^-$ fractions from bead-purified PBMCs were left untreated or treated with IL-4, IL-10, or both cytokines for 48 hours. HLA-G-expression was quantified by Western Blotting. The experiment was repeated three times, a representative example is shown. **(B)** In different experiments, only 25-65% of adherence-enriched viable cells were $CD14^+$ monocytes, while anti-CD14 bead-based purification repeatedly resulted in purities of more than 90%. **(C)** Gating strategy for one representative example.

3.3.3 IL-4 may induce HLA-G expression in T cells

It has previously been reported that IL-4 (Lombardelli, Aguerre-Girr *et al*. 2013) and IL-10 induce HLA-G expression (Gregori, Tomasoni *et al*. 2010, Moreau, Adrian-Cabestre *et al*. 1999, Urosevic and Dummer 2003). Here, we found that both cytokines induce HLA-G expression on protein level in PBL, but not in monocytic cells. Thus, we set out to investigate whether these cytokines may also upregulate HLA-G expression on mRNA level. HLA-G mRNA was quantified untreated and IL-4 or IL-10 treated immune cell subpopulations. As HLA-G expression had been detected on dendritic cells in lymph nodes, we focussed on membrane-bound HLA-G (mHLA-G) mRNA. To this end, a highly sensitive and quantitative TaqMan PCR assay was developed (see 2.2.11).

$CD14^+$ monocytes, $CD4^+$ and $CD8^+$ T cells and NK cells were then isolated by magnetic beads. These cells were left untreated or treated with 10 ng/ml IL-4 or IL-10 for 6 hours. RNA was isolated, reversely transcribed and mHLA-G cDNA was quantified. In acordance with Western Blotting results, only very low HLA-G mRNA levels were detected in purified $CD14^+$ and NK cells. In contrast, higher mRNA levels were detectable in T cells, which were significantly increased in $CD4^+$ cells in response to IL-4 treatment. Jeg-3 choriocarcinoma cells which were used as positive control expressed more than 100 fold more HLA-G mRNA than untreated T cells (see Figure 21A).

Subsequently, it was investigated whether IL-4 may also induce the expression of HLA-G protein on the cell surface of different lymphoid cells. Here, PBMCs were left untreated or treated with 10 ng/ml IL-4 for 48 hours. HLA-G surface expression was detected by flow cytometry in a small fraction of T and NK cells, and this fraction was increased in response to IL-4 treatment in three independent experiments (see Figure 21B), however, to a highly donor-dependent extent. Here, monocytes were not analysed due to high autofluorescence and unspecific binding of both specific and isotype antibodies, which could not be sufficiently blocked.

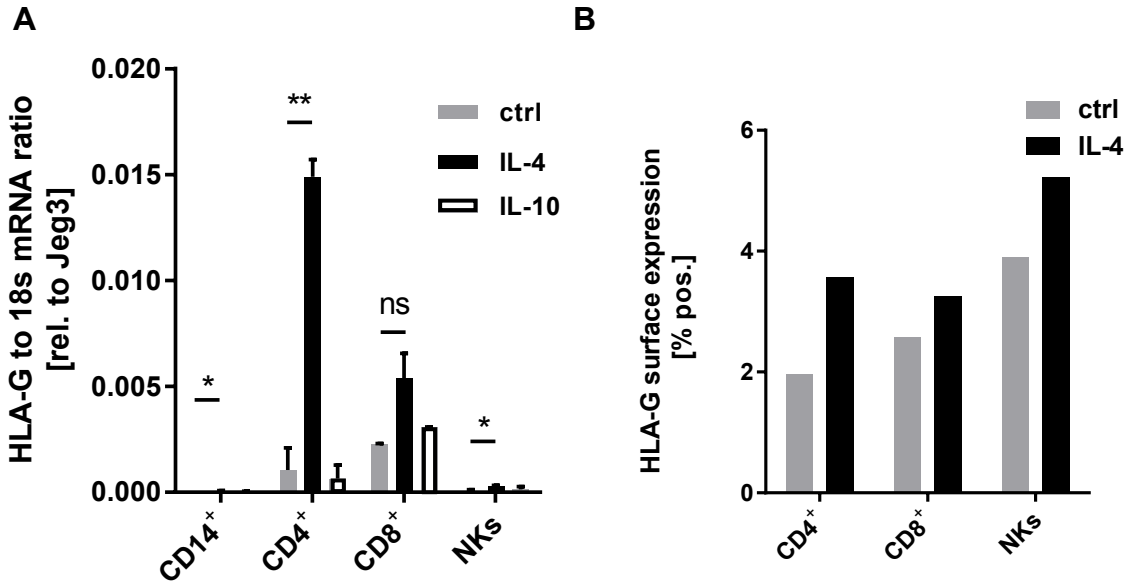

Figure 21: IL-4 may induce HLA-G expression in T cells

(A) Bead-purified $CD14^+$, $CD4^+$, $CD8^+$ and NK cells were left untreated or treated with IL-4 for 6 hours. HLA-G induction on mRNA level was quantified by TaqMan qPCR. Means and standard deviations of technical replicates are shown, mRNA expression was statistically analysed in each cell type by individual T tests. **(B)** PBMCs from healthy donors were treated with IL-4 of left untreated for 48 hours. HLA-G surface expression in different subsets of immune cells was quantified by flow cytometry. All experiments were repeated three times with similar, yet donor-dependent results. Representative examples are shown.

3.4 Transfer of soluble HLA-G to monocytic cells

As HLA-G was not inducible in monocytes or monocyte-derived dendritic cells from healthy donors and basal expression levels were very low, we investigated whether these cells are capable of binding soluble HLA-G that may be produced by tumour cells. Several mechanisms of transfer have been described for HLA-G, such as trogocytosis and transfer via exosomes. Furthermore, monocytes were reported to bind soluble HLA-G tetramers predominantly via the ILT4 receptor (Biancotto *et al.* 2013, Kleiner *et al.* 2013). Thus, we hypothesized that tumour-derived sHLA-G may be specifically transferred to myeloid cells via the ILT4 receptor. In order to test this hypothesis, it was investigated whether soluble HLA-G is present in high concentrations in the tumour microenvironment. Furthermore, the surface expression levels of ILT4 receptors on PBL and DC were quantified. Finally, it was investigated whether DC bind soluble HLA-G derived from supernatants of HLA-G5 transfected tumour cells.

Some experiments in this section were done together with Tamara Kuhfuß and, when indicated, published in part in her Bachelor of Science thesis entitled “Transfer von löslichem HLA-G auf dendritische Zellen – ein neuer immune escape Mechanismus im Ovarialkarzinom?” (transfer of soluble HLA-G to dendritic cells – a novel immune escape mechanism in ovarian cancer?).

3.4.1 Ascites samples from ovarian carcinoma patients contain soluble HLA-G

High levels of soluble HLA-G (sHLA-G) have previously been reported to be present in ascites (Allan *et al.* 1999) and serum (Singer, Rebmann *et al*. 2003) of ovarian carcinoma patients. In order to confirm that sHLA-G is present in the tumour microenvironment, ascites samples from ovarian carcinoma patients were screened for sHLA-G by ELISA. In accordance with the literature, ovarian carcinoma ascites contained significantly more sHLA-G as compared to benign ascites samples (P=0.022, unpaired T Test, one-tailed). In detail, 10 out of 20 ovarian carcinoma ascites samples but none of the benign ascites samples contained more sHLA-G than the arbitrary threshold of 5 ng/ml (see Figure 22).

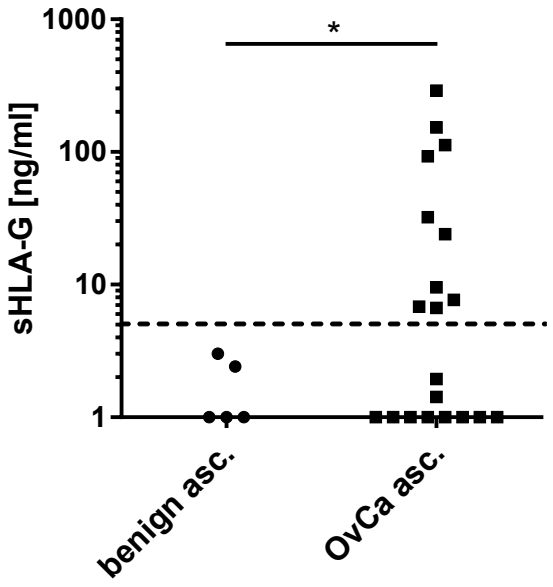

Figure 22: Ascites from ovarian carcinoma patients contains elevated levels of sHLA-G.
sHLA-G was quantified by ELISA in 20 ovarian carcinoma ascites samples and 5 benign ascites samples. sHLA-G levels were found to be elevated in ovarian carcinoma ascites samples as compared to benign ascites (P=0.022, unpaired Student's t-Test, one-tailed). Concentrations above the arbitrary threshold of 5 ng/ml (dashed line) were detected in 10 out of 20 ovarian carcinoma ascites samples but in none of the 5 benign ascites samples. The detection limit was 1 ng/ml.

3.4.2 DC and particularly DC-10 express ILT4

It has been reported that HLA-G tetramers bind to monocytes in an ILT4-dependent manner (Mach *et al.* 2010). In contrast to ILT2 which is expressed in both lymphoid and monocytic cells, ILT4 is reported to be exclusively expressed by monocytes, macrophages and dendritic cells (Allan, Colonna *et al*. 1999). DC-10 cells that are cultured in the presence of not only IL-4 and GM-CSF but also IL-10 for 7 days have been reported to express particularly high levels of ILT4 (Colonna, Samaridis *et al*. 1998). Thus, this receptor could play a role decisive role in the selective transfer of soluble HLA-G to monocytic cells.

In order to confirm these findings, surface expression of ILT4 on $CD4^+$ and $CD8^+$ T cells, NK cells, DC and DC-10 was quantified by flow cytometry. ILT4 was detected on DC cultured with GM-CSF and IL-4 and on $CD11c^+$, $CD68^+$, HLA-DR^+ DC-10 (Gregori, Tomasoni *et al*. 2010). As expected, DC-10 expressed significantly higher levels of ILT4 (see Figure 23). These experiments were done together with Tamara Kuhfuss and have been presented in part in her B.Sc. Thesis.

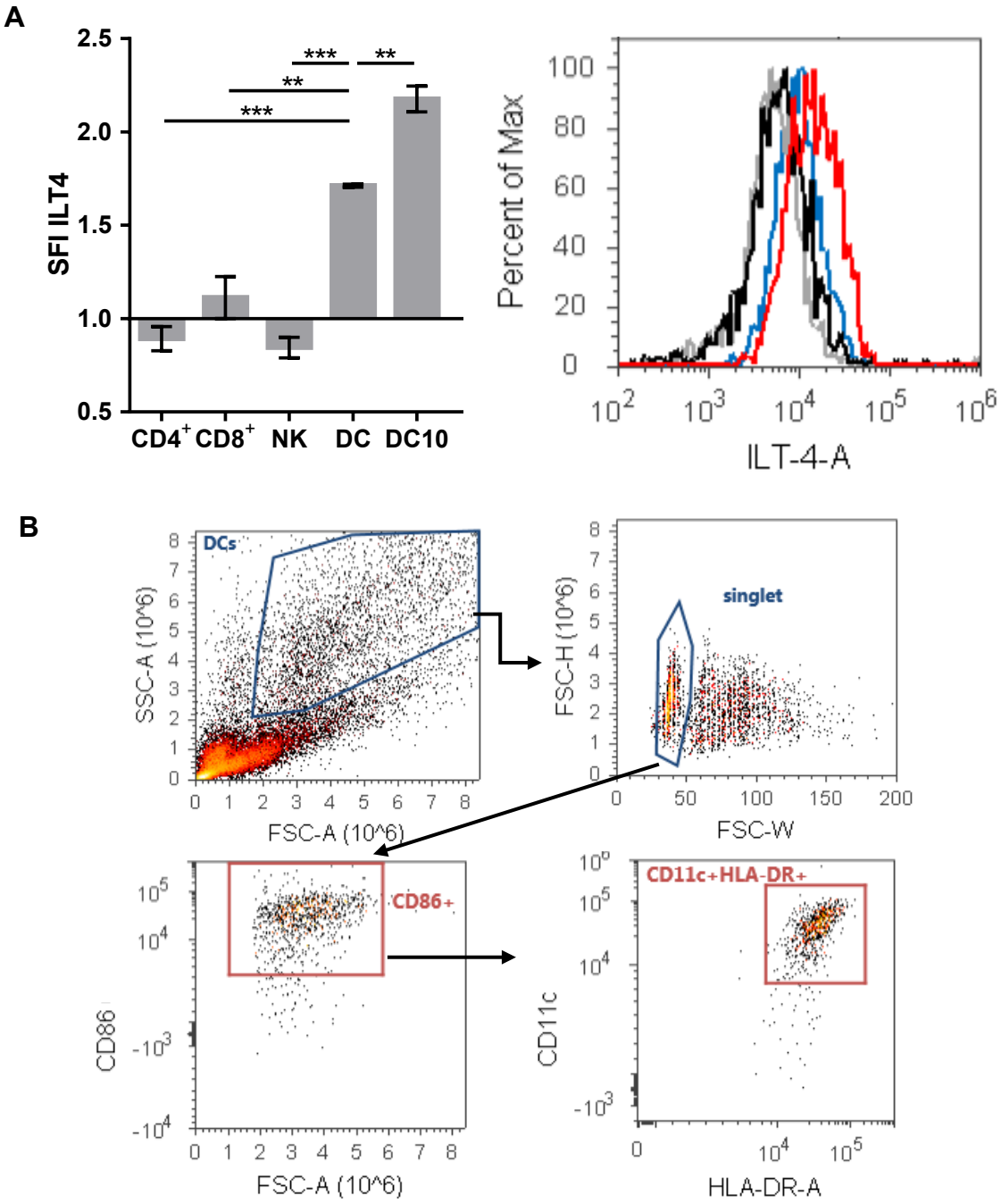

Figure 23: DC-10 express more ILT4 on the cell surface than DC

Anti-CD14 bead-purified monocytes from 2 healthy donors were matured for 7 days in the presence of IL-4 and GM-CSF (DC, elsewere also referred to as immature DC) or IL-4, IL-10 and GM-CSF (DC-10). Freshly isolated PBL were included as controls. DC and DC-10 were stained with fluorescently labelled antibodies for CD11c, CD86, HLA-DR, and ILT4. **(A)** DC-10 (red curve, black=isotype antibody) express significantly more ILT4 as compared to DC (blue curve, grey=isotype antibody, P=0.0011, unpaired T Test, two-tailed, mean and SD from 3 independent experiments are shown), which express significantly more ILT4 than ILT4$^-$ leukocytes. **(B)** DC-10 are CD11c$^+$, CD86$^+$ and HLA-DR$^+$.

3.4.3 DC-10 efficiently bind soluble HLA-G5

Because of the high expression of ILT4 on DC-10 it was subsequently investigated whether these cells may bind soluble HLA-G. Here, supernatant of LCL cells transfected with a single chain construct consisting of HLA-G5, a linker and β2-microglobulin (single chain HLA-G5, here abbreviated scHLA-G5) was used as a source of HLA-G (kind gift of Dr. Joel LeMaoult). Natural isoforms of HLA-G such as HLA-G1 and HLA-G5 dissociate from β2-microglobulin under denaturing conditions and are then detectable by Western Blotting as a 39 kDa band. In contrast, scHLA-G5 can be detected as a 50kDa band and is thus clearly distinguishable from any natural isoform. In three independent experiments, no endogenous HLA-G was detected in DC-10 cells derived from bead-purified monocytes or DC-10 treated with mock-transfected control supernatants (see Figure 24A LCL ctrl SN lane). However, DC-10 cells efficiently bound high amounts of scHLA-G5 from the supernatant, which was detectable by Western Blotting after stringent washing of the cells (see Figure 24A LCL scHLA-G5 SN lanes). 2 hours were sufficient for transferring high amounts of scHLA-G. Transfer occurred both at 37°C and, during shorter incubation periods to a slightly lesser extent, at 4°C. These experiments were done together with Tamara Kuhfuss and have been presented in part in her B.Sc. Thesis.

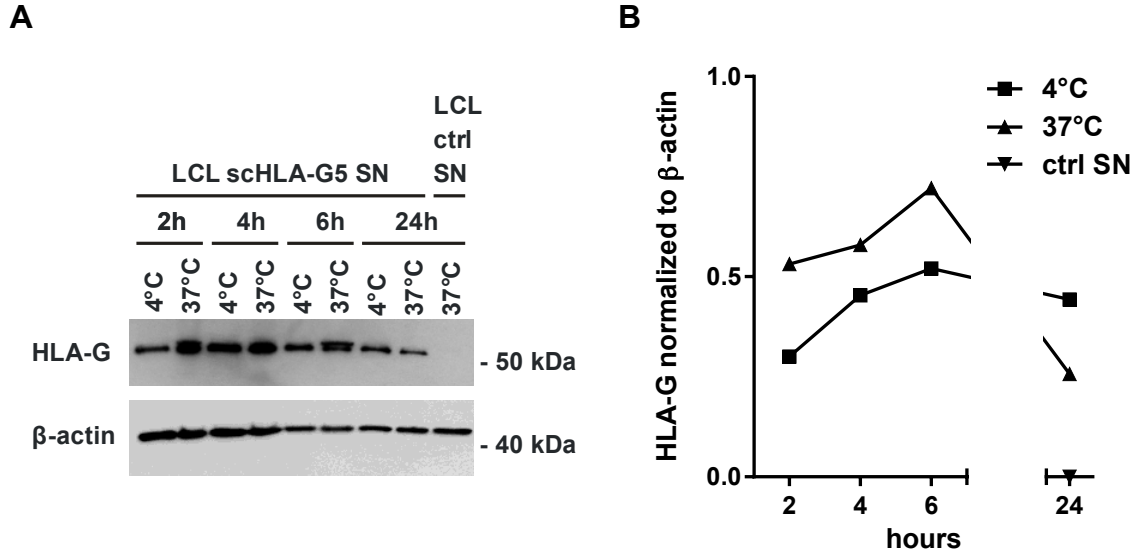

Figure 24: DC-10 cells efficiently bind soluble HLA-G from supernatants at 4°C and 37°C.
2.5 x 10^5 DC-10 cells each were incubated for 2, 4, 6 or 24h at 4°C or 37°C with 100 µl DC medium plus 100 µl LCL scHLA-G5 SN or LCL ctrl SN. Cells were then washed three times with 10 ml prewarmed PBS and cell pellets were lysed in lysis buffer. **(A)** HLA-G and β-actin were detected by Western Blotting and **(B)** quantified by measuring band sizes and intensities with ImageJ.

3.4.4 Blocking of ILT receptors reduces binding of HLA-G5

In order to verify that ILT receptors are involved in the transfer of sHLA-G to DC-10 blocking experiments were subsequently carried out. In three independent experiments, the addition of antibodies that block HLA-G, ILT2 or ILT4 to scHLA-G5 SN reduced the amounts of soluble scHLA-G5 bound by DC-10 cells. A representative example is shown in Figure 25. These experiments were carried out together with Lina Hilscher.

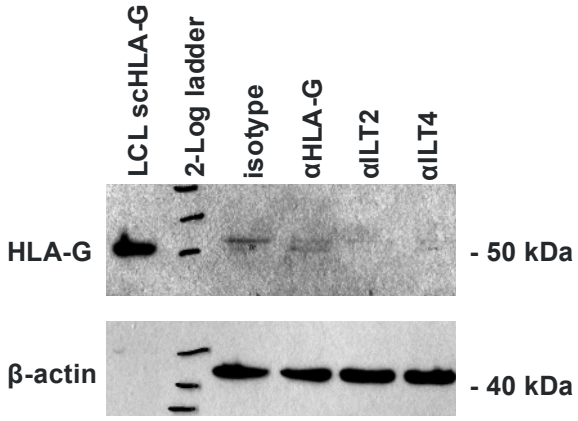

Figure 25: Antibodies directed against HLA-G, ILT2 or ILT4 block the transfer of sHLA-G to DC-10.
2.5 x 10^5 DC-10 cells were incubated for three hours with LCL scHLA-G5 SN plus isotype or blocking antibodies (10µg/ml) at 37°C. Cells were stringently washed, lysed and bound scHLA-G5 and intracellular β-actin were detected by Western Blotting. LCL scHLA-G5 SN containing 5 ng scHLA-G5 was directly loaded on the first lane as a positive control.

3.5 DC-10 loaded with HLA-G5 are more immunosuppressive

As discussed in the introduction, HLA-G is known to exert suppressive effects on various immune cells. Furthermore, we have detected high levels of HLA-G on dendritic cells in tumour-draining lymph nodes, which may be transferred tumour-derived soluble HLA-G. In order to test whether dendritic cells that have absorbed HLA-G may be more immunosuppressive, it was investigated whether DC-10 cells loaded with scHLA-G5 ($DC\text{-}10^{scHLA\text{-}G5}$) may induce regulatory T cells or inhibit $CD8^+$ effector T cell proliferation.

3.5.1 DC-10 loaded with HLA-G5 induce regulatory T cells

It has previously been shown that both HLA-G and DC-10 may contribute to the induction of T_{regs} (Gregori, Tomasoni *et al*. 2010). Thus, it was tested whether transferred HLA-G may amplify DC-10-mediated T_{reg} induction. PBL in T_{reg} medium were either left untreated or DC-10^{ctrl} or DC-$10^{scHLA\text{-}G5}$ from the same healthy donor were added. After 6 days, the percentage of $FoxP3^+$ T_{reg} cells among $CD4^+$ cells was quantified by intracellular staining and flow cytometry. In three independent experiments, a clear induction or expansion of T_{reg} was detected after coculture with DC-10^{ctrl}, and, to a higher extent, after coculture DC-$10^{scHLA\text{-}G5}$ cells. A representative experiment is shown in Figure 26. Some of these experiments were done together with Tamara Kuhfuss and have been presented in part in her B.Sc. Thesis.

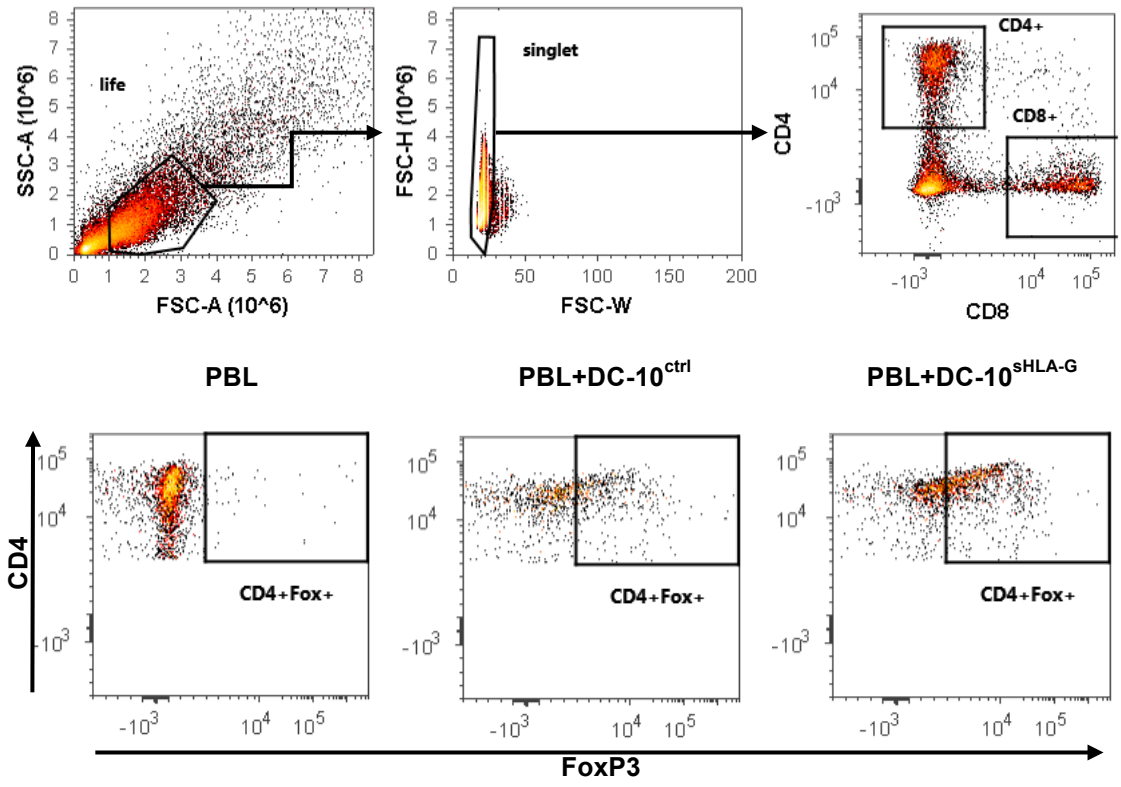

Figure 26: DC-10 and particularly DC-$10^{scHLA\text{-}G5}$ induce $CD4^+$ $FoxP3^+$ regulatory T cells
DC-10 cells were generated as described before, incubated for 3 hours at 37°C with LCL ctrl supernatant (DC-10^{ctrl}) or LCL-scHLA-G5 supernatant (DC-$10^{scHLA\text{-}G5}$) and washed three times with prewarmed PBS. 10^6 PBL in T_{reg} medium were either left untreated or 5 x 10^4 DC-10^{ctrl} or DC-$10^{scHLA\text{-}G5}$ from the same healthy donor were added. At day 6, cells were stained for extracellular markers CD4 and CD8 and for intracellular FoxP3 and analysed by flow cytometry. The percentage of T_{reg} cells (CD4+Fox+ gate) induced was highly donor-depent, but DC-$10^{scHLA\text{-}G5}$ induced most T_{reg} in three independent experiments. A representative experiment is shown.

3.5.2 Fixed DC-10$^{scHLA-G5}$ inhibit CD8^{+} T cell proliferation

sHLA-G bound by DC-10 cells enhances their capacity induce T_{reg}. However, it remained unclear whether these effects on T cells were mediated directly via HLA-G bound to the cell surface of DC-10 or indirectly through ILT-receptor mediated upregulation of immunosuppressive molecules on DC-10 cells. Thus, it was tested whether DC-10$^{scHLA-G5}$ that are fixed with paraformaldehyde and thus incapable of upregulating or secreting any immunosuppressive molecules are also more immunosuppressive as compared to identically treated DC-10^{ctrl}. Here, we tested whether effects on the proliferative capacity of syngeneic CD8^{+} T cells are detectable. In three independent experiments, fixed DC-10$^{scHLA-G5}$ inhibited the PHA-induced proliferation of cell-proliferation dye eFluor 670-stained CD8^{+} T cells to a higher extent as compared to fixed DC-10^{ctrl}. A representative example is shown in Figure 27.

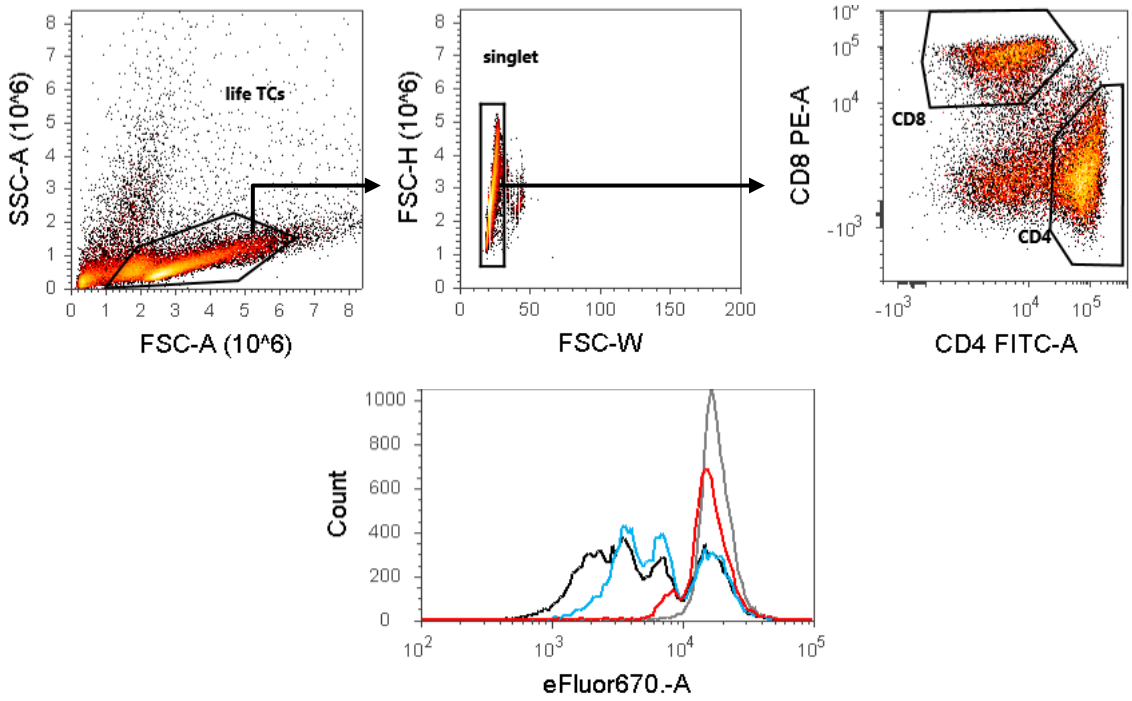

Figure 27: DC-10$^{scHLA-G5}$ strongly inhibit CD8^{+} T cell proliferation
DC-10 cells were generated as described before, incubated for 3 hours at 37°C with LCL ctrl supernatant (DC-10^{ctrl}) or LCL-scHLA-G5 supernatant (DC-10$^{scHLA-G5}$) and washed three times with prewarmed PBS. DC-10 were then fixed for 10 minutes with 1% PFA and washed 3 more times. 4 x 10^5 syngenic PBL from the same healthy donor were stained with eFluor 670 Cell Proliferation Dye and either left untreated (grey line), treated with PHA (2.4ng/ml, black line) or with PHA and 1 x 10^5 fixed DC-10^{ctrl} (blue line) or PHA DC-10$^{scHLA-G5}$ (red line). PHA-induced CD8^{+} T cell proliferation indicated by peaks with diluted eFluor concentrations was inhibited particularly in presence of DC-10$^{scHLA-G5}$ cells. A representative example of three independent experiments is shown.

4 Discussion

Due to its potent immunosuppressive effects, HLA-G possesses the ability to protect altered or foreign tissues from immunological destruction. This effect has been demonstrated in a xenograft study, in which HLA-G transfected human melanoma cells grew for about 3 days in completely immunocompetent mice. Moreover, complete tumour rejection required more than two weeks, while non-transfected melanoma cells were immediately rejected (Agaugue *et al.* 2011). Here, HLA-G most likely interacts with paired immunoglobulin-like inhibitory receptor (PIR-B), the mouse homologue of ILT4 (Liang *et al.* 2002). While some researches have stated that there is no direct homologue for HLA-G in the mouse (Agaugue, Carosella *et al*. 2011), the murine MHC Ib molecule Qa-2 shares many features with HLA-G. It presents nonapeptides, exists in membrane-bound and soluble isoforms, possesses a short cytoplasmic tail and is expressed in preimplantation embryos where it enhances survival and promotes embryonic growth (reviewed by Comiskey *et al.* 2003). Alternatively, blastocyst MHC could be a functional homologue. It is expressed in the placenta and able to protect tumour cells from immunological assault (Tajima *et al.* 2003). Of note, the amino acid sequences of the alpha 3 domains of both molecules are more than 92% identical (alignment see Supplements Table 7).

HLA-G is essential during embryogenesis (Rizzo, Vercammen *et al.* 2011, Verloes, Van de Velde *et al*. 2011), may play an important role in autoimmune diseases (Rizzo *et al.* 2014), could protect pathogens such as viruses (Amiot *et al.* 2014, Rizzo, Bortolotti *et al*. 2014) and is apparently perilous in a high proportion of malignant diseases. In this context, novel insights into the function of HLA-G in physiological and malignant processes that were obtained in this thesis will be discussed.

4.1 Physiological role and expression of HLA-G

Due to the limited availability of tissues from healthy donors, it was decided to use a FFPE tissue microarray to study HLA-G expression. This approach has several advantages. As opposed to staining individual sections, the required time and resources are lowered, and technical variability due to slight alterations during the staining process are less likely. Furthermore, it takes less time to switch in between samples during evaluation, which may lead to a more accurate scoring. However, due to the small size of the cores, small anatomical structures or heterogeneously expressed proteins may not be detectable in all samples. This can be partially compensated for by combining several cores from each tissue in one microarray.

In contrast to ubiquitously expressed MHC class Ia molecules which enable the immune system to detect malignant or infected cells throughout the body, only very few tissues have been reported to physiologically express HLA-G.

In accordance with the literature, we detected the highest physiological HLA-G expression level in the placenta (see Figure 8). This confirms the suitability of the used staining protocol and suggests that HLA-G molecules have been well preserved in microarray tissues obtained from surgery. As discussed in the introduction, HLA-G expression on cytotrophoplast cells is most likely required to prevent the maternal immune system from attacking and rejecting of embryonic tissues. Tolerance towards "self" tissues usually depends on the depletion of autoreactive T cells within the thymus, where also tolerogenic T_{reg} cells are generated. However, embryos express paternal MHC molecules, may have different serotypes and express thousands of paternal proteins which may either contain slightly altered protein sequences or are completely different, such as proteins encoded for by the Y chromosome. As none of these factors are present within the maternal thymus, there should also be no pre-existing tolerance towards embryonic tissues. As observable in skin allograft transplantation experiments in mice (Steinmuller *et al.* 1982), these factors should lead to immediate rejections of non-matched transplanted organs, unless immunosuppressive therapeutics are given (Ruiz *et al.* 2013) or the transplanted organ is from a immunoprivileged site (Streilein 2003). Thus, each successful pregnancy is an enourmous immunological challenge, which has fascinated immunologists for more than 60 years (Medawar 1953). In fact, the risk for

spontaneous pregnancy loss particularly in the first trimester is higher than 10% even in young and healthy parents and increases with parental age (de la Rochebrochard and Thonneau 2002, Garcia-Enguidanos *et al.* 2002).

One of the most important factors to protect embryos from rejection is thought to be HLA-G (Hunt, Langat *et al*. 2006). As previously mentioned, embryonic HLA-G expression correlates with successful pregnancies (Rizzo, Vercammen *et al*. 2011). Reduced soluble HLA-G serum levels during early or late pregnancy (Hackmon *et al.* 2007, Yie *et al.* 2004, Yie *et al.* 2005) and altered HLA-G transcription (O'Brien *et al.* 2001) correlate with preeclampsia, which usually occurs during the last trimester (Steegers *et al.* 2010). Preeclampsia may be triggered by maternal Th1 immune reactions towards embryonic tissues (Visser *et al.* 2007), occurs in 5%-10% of all pregnancies (Le Bouteiller *et al.* 2003) and is the leading cause of infant and maternal death during pregnancies.

In addition to the immunological challenge, significant anatomical changes must be induced during a successful pregnancy. First, the blastocyst must implant in the endometrium of the uterus, and the trophoectoderm cells must further invade this tissue to form a placenta that ensures sufficient transport of nutrients towards the fetus. Interestingly, HLA-G may also promote vascularisation through interactions with decidual NK cells (Rajagopalan *et al.* 2006, Rajagopalan and Long 2012). Furthermore, the knockdown of HLA-G mRNA in zygotes significantly slowed down embryonic development (Yao, Shu *et al*. 2014).

From this perspective, it makes sense that HLA-G is also expressed within testicular tissues such as seminiferous tubules (see Figure 9). HLA-G has previously been detected in seminal fluids (Verloes, Van de Velde *et al*. 2011, Yao, Shu *et al*. 2014), and may thus help to prevent maternal immune reactions towards antigens on sperm cells. Thus, the most important physiological function of HLA-G may be the protection of embryonal tissues.

However, HLA-G has also been detected in adult tissues. One of them is the cornea (Le Discorde, Moreau *et al*. 2003), which is widely recognised as an immune privileged tissue. Corneas have first been successfully transplanted more than hundred years ago, and are often not rejected even when donors and recipients are not matched (Moffatt *et al.* 2005). Unfortunately, cornea tissue was not included in the microarray.

Furthermore, HLA-G has been detected in the thymus (Mallet, Blaschitz *et al*. 1999) and in the pancreas (Cirulli, Zalatan *et al*. 2006). HLA-G was not detectable in either of these tissues in the FFPE cores included in the microarray. However, in the thymus, HLA-G has been described to be present in medullary thymic epithelial cells only. These cells express the autoimmune regulator AIRE and produce protein fragments from most proteins in the human genome which are required for negative T cell selection and T_{reg} induction (Coquet *et al.* 2013, Leavy 2013). Soluble HLA-G could play an important role in these processes, as soluble HLA-G induces regulatory T cells (Le Rond *et al.* 2006) and may induce apoptosis in $CD8^+$ effector cells (Contini, Ghio *et al*. 2003). On the other hand, HLA-G expression could be randomly induced under control of the AIRE complex.

In the pancreas, HLA-G has been detected only on islet cells (Cirulli, Zalatan *et al*. 2006). These islets produce insulin and other hormones. In our study, HLA-G may have not been detectable in both the pancreas and the thymus because the comparatively rare relevant cell subsets were not present in the small microarray cores.

However, we have found a significant HLA-G expression within the adrenal medulla. In analogy to the islet cells in the pancreas, this endocrine tissue mostly produces hormones such as adrenalin and noradrenalin, but it is not immediately obvious why immunosuppressive molecules such as HLA-G are expressed here. To our knowledge, HLA-G expression in the adrenal medulla has not been previously described. However, moderate levels of mRNA of Mamu-AG, the rhesus monkey homologue of HLA-G (Gregori *et al.* 2009, Moreau, Adrian-Cabestre *et al*. 1999, Naji *et al.* 2007) have been detected in rhesus monkey adrenal glands (Slukvin *et al.* 1999).

4.2 HLA-G expression in ovarian carcinomas

High expression levels of HLA-G have been detected in a wide variety of cancers (Amiot, Ferrone *et al*. 2011), including ovarian carcinomas (Lin, Yan *et al*. 2007, Menier, Prevot *et al*. 2009). Due to its unique functions during pregnancies, HLA-G may also contribute to several tumourigenic processes. In fact, clinically detectable tumours have overcome several challenges that resemble the ones present during embryonic development. Tumours contain altered genetic material (Schumacher and Schreiber 2015) which must be shielded from immunological assault, undergo rapid cell divisions, grow invasively and induce neovascularisation. As described in 4.1, HLA-G may contribute to all of these processes.

Our microarray analysis confirmed that high levels of HLA-G are expressed particularly by high-grade serous tumours (see Table 2), which account for more than 50% of all ovarian cancers (Table 2). Here, significant expression levels were detected in 5 out of 17 (29%) high-grade tumours (excluding grade 2 tumours due to unclear high/low status). However, only four 0.6 µm cores from each tumour were analysed here. When larger fractions of primary tumours were screened for HLA-G expression on individual sections, expression levels within one tumour were frequently very heterogeneous, and HLA-G was often detected only in distinct parts of the tumour. Thus, the frequency of HLA-G positive tumours may be underestimated when tumours are assessed only by tissue microarrays. In line with this, HLA-G was detected in 7 out of 9 (78%) individual sections from high-grade serous tumours. Furthermore, HLA-G was detected in lymph nodes of 9 out of 9 patients (100%).

Tissue microarrays nevertheless remain very efficient tools for initial screenings of large amounts of samples. Overall, a trend towards higher HLA-G expression levels in grade 3 as opposed to grade 1 tumours was observed (see Figure 12). However, this trend did not reach statistical significance, which may be ascribed to the limited number of samples. Furthermore, HLA-G expression did not significantly correlate with tumour stage or patient age (see Figure 12). To our knowledge, the presented tissue microarray screening has resulted in the first description of HLA-G expression in mucinous or endometrioid ovarian carcinomas. Nonetheless, these findings should be confirmed in further studies.

Although an overwhelming amount of evidence suggests that HLA-G is an immunosuppressive molecule and may promote tumour growth, patients with high-grade ovarian carcinomas that express HLA-G were reported to have a better clinical prognosis as compared to patients with HLA-G negative high-grade tumours (Rutten, Dijk *et al*. 2014).

One aim of this thesis was to investigate whether two immunologically distinct subgroups as suggested by Gajewski *et al.* (Gajewski, Schreiber *et al*. 2013) may exist in ovarian carcinoma. This may in fact be the case, as almost all ovarian carcinomas in which *HLA-G* is transcribed also transcribed genes coding for classical MHC molecules or proteins involved in antigen processing, such as TAP1 (see Table 4). This may be due to the fact that all these genes are encoded in the MHC region on chromosome 6. In addition, expression of HLA-G can be induced in response to inflammatory cytokines (Wiendl, Mitsdoerffer *et al*. 2002). Thus, some ovarian carcinomas may escape from immunosurveillance by compensating for the presentation of tumour antigens on MHC class Ia through the expression of immunosuppressive MHC class Ib molecules including HLA-G, while others escape from adaptive immune responses because the MHC locus is silenced completely. A link between immune cell infiltration and expression of non-classical MHC molecules has also been shown for HLA-E in glioma (Mittelbronn *et al.* 2007).

4.3 Induction of HLA-G in immune cells

We and others have observed heterogeneous HLA-G expression in primary high-grade ovarian carcinomas. When larger tumour sections where screened for HLA-G expression, we did not detect any HLA-G in 2 out 9 tumours, and 1 only expressed low levels (expression score 2). In contrast, high levels of HLA-G (expression score 6 or higher) were detected on histiocytes in at least 1 regional lymph node from each patient (see Table 3). Histiocytes are extravascular cells of the monocytic line, such as tissue macrophages. Within lymph nodes, dendritic cells are the major subpopulation of histiocytes. To our knowledge, HLA-G has not previously been detected in local lymph nodes in ovarian cancer. However, dendritic cells in regional lymph nodes play a crucial role in tumour immunosurveillance (Strioga *et al.* 2013) and have been successfully used in cancer vaccination approaches (Palucka and Banchereau 2012). Dendritic cells take up tumour antigens and present them to T cells in regional lymph nodes, thereby priming adaptive anti-tumour immune responses. In fact, individual dendritic cells have been shown to interact with up to 5000 T cells per hour (Miller *et al.* 2004). Thus, cancer cells often inactivate dendritic cells to interfere with immunosurveillance (Vicari *et al.* 2002).

In the context of HLA-G, recent reports have suggested that monocyte-derived dendritic cells that are cultured with IL-4, IL-10 and GM-CSF (DC-10) express both high levels of ILT4 and HLA-G (Amodio *et al.* 2013, Gregori, Tomasoni *et al*. 2010). DC-10 also secrete IL-10, are tolerogenic in an ILT4/HLA-G-dependent manner and induce regulatory $CD8^+$ T cells (Tr1 cells) (Amodio *et al.* 2015, Gregori, Tomasoni *et al*. 2010). DC-10 and HLA-G^+ $CD4^+$ cells have also been detected in the decidua during pregnancy (Amodio, Mugione *et al*. 2013). Furthermore, IL-10 has been reported to induce HLA-G expression in monocytes (Moreau, Adrian-Cabestre *et al*. 1999) and to be present in high concentrations in ascites from ovarian cancer patients (Gotlieb, Abrams *et al*. 1992).

Thus, we set out to investigate if IL-10 and possibly also IL-4 induce HLA-G expression in monocytic cells. First, IL-4 and IL-10 concentrations in benign and ovarian cancer ascites samples were quantified by ELISA. Both cytokines were detectable in partially very high concentrations particularly in ascites samples from ovarian cancer patients (see Figure 19). In accordance with published protocols (Gregori, Tomasoni *et al*. 2010), adherence enriched monocytes were used initially. These monocytes were matured for 5

days in complete RPMI1640 5% hAB serum before IL-4, IL-10 or both cytokines were added for 48h. In this setting, we have observed robust HLA-G inductions in numerous independent experiments both on protein (see Figure 20) and on mRNA level (data not shown). However, when monocytes where purified with anti-CD14 beads, no basal expression or induction in response to IL-4 or IL-10 was observed. In contrast, IL-4 and IL-10 induced HLA-G expression in the $CD14^-$ fraction (PBL). These findings were confirmed on mRNA level, where HLA-G was significantly upregulated in T cells (see Figure 21). HLA-G mRNA expression in monocytes and NK cells was very low, but also significantly increased in response to IL-4. However, these bead-purified monocytes were only 90% to 95% pure, and it is thus likely that the detected HLA-G mRNA was derived from few contaminating T cells.

Similar reasons may have led to the description of HLA-G expression in monocytes or dendritic cells. Here, purity analyses revealed that only 25% to 60% of adherence-enriched cells were actually $CD14^+$ monocytes (Figure 20). Thus, all evidence suggests that HLA-G expression in adherence-enriched cells may be due to contaminating PBL. Of note, as discussed below, monocytes or dendritic cells may still acquire HLA-G from other immune cells. Overall, the HLA-G mRNA to 18S rRNA ratio in untreated T cells was more than 100 fold lower as in Jeg-3 cells (see Figure 20). On protein level, this was not systematically investigated, however, 1 µg of Jeg-3 lysate usually resulted in stronger signals than 20 µg of lysate from 2 x 10^6 immune cells (not shown).

4.4 Transfer of soluble HLA-G to dendritic cells

As HLA-G was not inducible in monocytes or DC-10, we speculated that dendritic cells might take up tumour-derived soluble HLA-G. Monocytic cells had been shown to bind HLA-G tetramers through HLA-G receptors such as ILT4 (Biancotto, Wank *et al*. 2013, Kleiner, Marcuzzi *et al*. 2013). In accordance with the literature (Singer, Rebmann *et al*. 2003), we detected high levels of soluble HLA-G in ascites samples from ovarian carcinoma patients (see Figure 22). Then, we quantified ILT4 surface expression on different immune cells. As reported by others (Gregori, Tomasoni *et al*. 2010, LeMaoult *et al.* 2005, Shiroishi, Tsumoto *et al*. 2003), ILT4 was detectable on dendritic cells that had been cultured for 7 days with IL-4 and GM-CSF (also often referred to as immature dendritic cells or iDC) and expressed at even higher levels on DC-10 (see Figure 23). In order to test whether DC-10 absorb soluble HLA-G from the microenvironment, DC-10 were incubated with supernatants from a cell line transfected with a plasmid coding for a single chain HLA-G5 construct. Here, HLA-G5 and β2-microglobulin are linked with a flexible peptide linker. Thus, the construct has a molecular weight of about 50 kDa and is thereby distinguishable from all natural isoforms of HLA-G by Western Blotting. We found that DC-10 quickly and efficiently bind high amounts of scHLA-G-5 both at 4°C or at 37°C. In contrast, no HLA-G was detectable on DC-10 that were incubated with supernatant from mock transfected cells (see Figure 24). Cells were washed three times in order to ensure that no unbound HLA-G from the supernatant had been carried over into the protein lysates. Here, 2.5×10^5 DC-10 cells were sufficient to demonstrate HLA-G transfer by Western Blotting. Binding of HLA-G by DC-10 was clearly reduced in presence of antibodies that block HLA-G, ILT2 or ILT4 (see Figure 25), which highlights the importance of these receptors during HLA-G transfer. At this point, it is unclear why blocking of the ILT2 receptor also decreased binding of soluble HLA-G. Both receptors could be involved in the transfer process in a cooperative manner. In some lymph nodes with very intense HLA-G staining, it was difficult to determine if other immune cells had also taken up HLA-G (see Figure 16). Thus, it cannot be excluded that sHLA-G may to some extent bind to ILT2. Alternatively, blocking one receptor with a relatively large antibody could also interfere with HLA-G binding to the other type of receptor for steric reasons if both are localized in close proximity. Furthermore, as both receptors are closely related, the blocking antibodies may cross-react to a certain extent.

4.5 Soluble HLA-G increases the immunosuppressive capacity of DC-10

The next obvious step was to investigate which effects the transfer of HLA-G to dendritic cells may have in local lymph nodes. It is known that a high frequency of tumour infiltrating $CD8^+$ T cells and particularly a high $CD8^+$ to $CD4^+$ T_{reg} ratio are associated with favourable clinical outcomes in ovarian cancer (Sato, Olson *et al*. 2005). We have shown that DC-10 which are loaded with soluble HLA-G ($DC\text{-}10^{scHLA\text{-}G5}$) efficiently induce $CD4^+FoxP3^+$ regulatory T cells (see Figure 26). However, in this setting, it was not clear whether T_{reg} cells were induced because of effects directly mediated by soluble HLA-G on the surface of DC-10 cells, or because of secondary effects such as DC-10 derived cytokines or surface molecules induced by HLA-G. Thus, in the next set of experiments, $DC\text{-}10^{scHLA\text{-}G5}$ and DC-10 incubated with control supernatant were fixed in 1% paraformaldehyde. We have observed that Jeg-3 cells fixed by the same protocol inhibit T cell proliferation in a HLA-G dependant manner.

After several washes, syngeneic PBL stained with cell proliferation dye were added and T cell proliferation was induced by PHA. Here, $CD8^+$ T cell proliferation was most effectively suppressed by fixed DC-10 loaded with HLA-G in three independent experiments (see Figure 27). Again, substantial donor-dependent differences were observed.

4.6 Conclusion

We have shown that HLA-G is expressed in various subtypes of ovarian cancer, and in the majority of high-grade serous tumours. However, HLA-G expressing tumours may also frequently express classical HLA molecules while others may escape from immunosurveillance by downregulating all MHC molecules. Thus, HLA-G expression is not necessarily associated with a poor clinical prognosis. HLA-G was also detectable on dendritic cells in lymph nodes from all assessed patients. Our experiments suggest that dendritic cells may not express HLA-G, but are capable of binding tumour-derived soluble HLA-G. Such HLA-G loaded dendritic cells are highly immunosuppressive. Thus, soluble HLA-G may enable serous ovarian carcinomas to remotely inhibit anti-tumour immune responses in regional lymph nodes (see Figure 28). This novel

immunosuppressive mechanism may also protect other solid tumours that secrete HLA-G and could play an important role during embryogenesis.

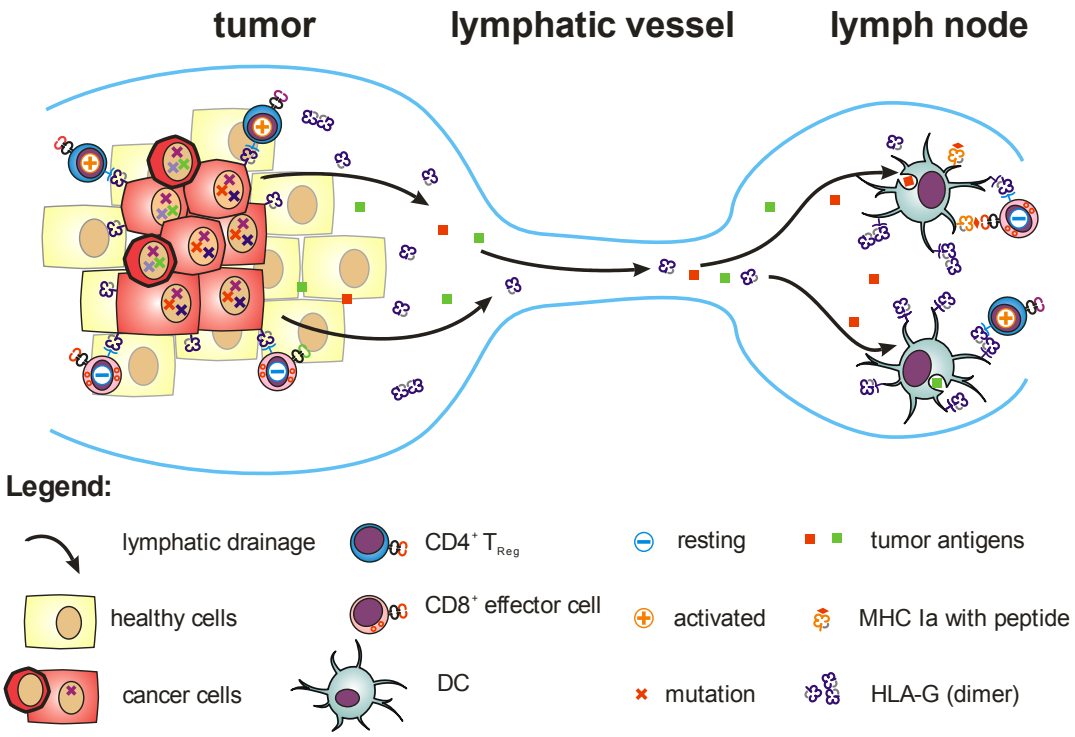

Figure 28: Soluble HLA-G may remotely suppress anti-tumour immune responses in regional lymph nodes
Ovarian carcinomas and other tumours express altered proteins that should in principle initiate anti-tumour immune responses. Dendritic cells in regional lymph nodes are, however, critical for priming such a response. They may enter malignant tissues and take up tumour antigens before they migrate to lymph nodes (not shown). Alternatively, dendritic cells within a lymph node may take up tumour antigens via pinocytosis. These antigens are then presented to T cells, which start proliferating if they express cognate T cell receptors. Such cytotoxic $CD8^+$ T cells effectively detect and eliminate malignant cells. However, dendritic cells also bind tumour-derived soluble HLA-G. In this case, $CD8^+$ T cell proliferation is inhibited and regulatory T cells are induced, which may migrate into the tumours and suppress further immune responses. This mechanism may have evolved to protect semi-allogeneic embryos from adaptive immune responses (see main text for references).

Figures

Tables

References

Agaugue, S., E. D. Carosella and N. Rouas-Freiss (2011). "Role of HLA-G in tumor escape through expansion of myeloid-derived suppressor cells and cytokinic balance in favor of Th2 versus Th1/Th17." Blood **117**(26): 7021-7031.

Aghajanian, C., S. V. Blank, B. A. Goff, P. L. Judson, M. G. Teneriello, A. Husain, M. A. Sovak, J. Yi and L. R. Nycum (2012). "OCEANS: a randomized, double-blind, placebo-controlled phase III trial of chemotherapy with or without bevacizumab in patients with platinum-sensitive recurrent epithelial ovarian, primary peritoneal, or fallopian tube cancer." J Clin Oncol **30**(17): 2039-2045.

Aguirre-Ghiso, J. A. (2007). "Models, mechanisms and clinical evidence for cancer dormancy." Nat Rev Cancer **7**(11): 834-846.

Alegre, E., V. Rebmann, J. Lemaoult, C. Rodriguez, P. A. Horn, A. Diaz-Lagares, J. I. Echeveste and A. Gonzalez (2013). "In vivo identification of an HLA-G complex as ubiquitinated protein circulating in exosomes." Eur J Immunol **43**(7): 1933-1939.

Allan, D. S., M. Colonna, L. L. Lanier, T. D. Churakova, J. S. Abrams, S. A. Ellis, A. J. McMichael and V. M. Braud (1999). "Tetrameric complexes of human histocompatibility leukocyte antigen (HLA)-G bind to peripheral blood myelomonocytic cells." J Exp Med **189**(7): 1149-1156.

Allan, D. S., A. J. McMichael and V. M. Braud (2000). "The ILT family of leukocyte receptors." Immunobiology **202**(1): 34-41.

Amiot, L., S. Ferrone, H. Grosse-Wilde and B. Seliger (2011). "Biology of HLA-G in cancer: a candidate molecule for therapeutic intervention?" Cell Mol Life Sci **68**(3): 417-431.

Amiot, L., N. Vu and M. Samson (2014). "Immunomodulatory properties of HLA-G in infectious diseases." J Immunol Res **2014**: 298569.

Amodio, G., M. Comi, D. Tomasoni, M. E. Gianolini, R. Rizzo, J. LeMaoult, M. G. Roncarolo and S. Gregori (2015). "HLA-G expression levels influence the tolerogenic activity of human DC-10." Haematologica **100**(4): 548-557.

Amodio, G., A. Mugione, A. M. Sanchez, P. Vigano, M. Candiani, E. Somigliana, M. G. Roncarolo, P. Panina-Bordignon and S. Gregori (2013). "HLA-G expressing DC-10 and CD4(+) T cells accumulate in human decidua during pregnancy." Hum Immunol **74**(4): 406-411.

Artyomov, M. N., M. Lis, S. Devadas, M. M. Davis and A. K. Chakraborty (2010). "CD4 and CD8 binding to MHC molecules primarily acts to enhance Lck delivery." Proc Natl Acad Sci U S A **107**(39): 16916-16921.

Baba, T., P. A. Convery, N. Matsumura, R. S. Whitaker, E. Kondoh, T. Perry, Z. Huang, R. C. Bentley, S. Mori, S. Fujii, J. R. Marks, A. Berchuck and S. K. Murphy (2009). "Epigenetic regulation of CD133 and tumorigenicity of CD133+ ovarian cancer cells." Oncogene **28**(2): 209-218.

Bamberger, A. M., S. Jenatschke, H. M. Schulte, T. Loning and M. C. Bamberger (2000). "Leukemia inhibitory factor (LIF) stimulates the human HLA-G promoter in JEG3 choriocarcinoma cells." J Clin Endocrinol Metab **85**(10): 3932-3936.

Banerjee, S. and S. B. Kaye (2013). "New strategies in the treatment of ovarian cancer: current clinical perspectives and future potential." Clin Cancer Res **19**(5): 961-968.

Barber, E. K., J. D. Dasgupta, S. F. Schlossman, J. M. Trevillyan and C. E. Rudd (1989). "The CD4 and CD8 antigens are coupled to a protein-tyrosine kinase (p56lck) that phosphorylates the CD3 complex." Proc Natl Acad Sci U S A **86**(9): 3277-3281.

Berger, S., A. Siegert, C. Denkert, M. Kobel and S. Hauptmann (2001). "Interleukin-10 in serous ovarian carcinoma cell lines." Cancer Immunol Immunother **50**(6): 328-333.

Bhutta, M. F. (2007). "Sex and the nose: human pheromonal responses." J R Soc Med **100**(6): 268-274.

Biancotto, A., A. Wank, S. Perl, W. Cook, M. J. Olnes, P. K. Dagur, J. C. Fuchs, M. Langweiler, E. Wang and J. P. McCoy (2013). "Baseline levels and temporal stability of 27 multiplexed serum cytokine concentrations in healthy subjects." PLoS One **8**(12): e76091.

Boyson, J. E., R. Erskine, M. C. Whitman, M. Chiu, J. M. Lau, L. A. Koopman, M. M. Valter, P. Angelisova, V. Horejsi and J. L. Strominger (2002). "Disulfide bond-mediated dimerization of HLA-G on the cell surface." Proc Natl Acad Sci U S A **99**(25): 16180-16185.

Braud, V. M., D. S. Allan and A. J. McMichael (1999). "Functions of nonclassical MHC and non-MHC-encoded class I molecules." Curr Opin Immunol **11**(1): 100-108.

Brown, R., E. Curry, L. Magnani, C. S. Wilhelm-Benartzi and J. Borley (2014). "Poised epigenetic states and acquired drug resistance in cancer." Nat Rev Cancer **14**(11): 747-753.

Bruttel, V. S. and J. Wischhusen (2014). "Cancer stem cell immunology: key to understanding tumorigenesis and tumor immune escape?" Front Immunol **5**: 360.

Burnet, F. M. (1970). "The concept of immunological surveillance." Prog Exp Tumor Res **13**: 1-27.

Burt, D., D. Johnston, T. Rinke de Wit, P. Van den Elsen and P. L. Stern (1991). "Cellular immune recognition of HLA-G-expressing choriocarcinoma cell line Jeg-3." Int J Cancer Suppl **6**: 117-122.

Buys, S. S., E. Partridge, A. Black, C. C. Johnson, L. Lamerato, C. Isaacs, D. J. Reding, R. T. Greenlee, L. A. Yokochi, B. Kessel, E. D. Crawford, T. R. Church, G. L. Andriole, J. L. Weissfeld, M. N. Fouad, D. Chia, B. O'Brien, L. R. Ragard, J. D. Clapp, J. M. Rathmell, T. L. Riley, P. Hartge, P. F. Pinsky, C. S. Zhu, G. Izmirlian, B. S. Kramer, A. B. Miller, J. L. Xu, P. C. Prorok, J. K. Gohagan, C. D. Berg and P. P. Team (2011). "Effect of screening on ovarian cancer mortality: the Prostate, Lung, Colorectal and Ovarian (PLCO) Cancer Screening Randomized Controlled Trial." JAMA **305**(22): 2295-2303.

Carosella, E. D., B. Favier, N. Rouas-Freiss, P. Moreau and J. Lemaoult (2008). "Beyond the increasing complexity of the immunomodulatory HLA-G molecule." Blood **111**(10): 4862-4870.

Carosella, E. D., P. Moreau, J. Le Maoult, M. Le Discorde, J. Dausset and N. Rouas-Freiss (2003). "HLA-G molecules: from maternal-fetal tolerance to tissue acceptance." Adv Immunol **81**: 199-252.

Carosella, E. D., P. Moreau, J. Lemaoult and N. Rouas-Freiss (2008). "HLA-G: from biology to clinical benefits." Trends Immunol **29**(3): 125-132.

Caumartin, J., B. Favier, M. Daouya, C. Guillard, P. Moreau, E. D. Carosella and J. LeMaoult (2007). "Trogocytosis-based generation of suppressive NK cells." EMBO J **26**(5): 1423-1433.

Chaix, R., C. Cao and P. Donnelly (2008). "Is mate choice in humans MHC-dependent?" PLoS Genet **4**(9): e1000184.

Cirulli, V., J. Zalatan, M. McMaster, R. Prinsen, D. R. Salomon, C. Ricordi, B. E. Torbett, P. Meda and L. Crisa (2006). "The class I HLA repertoire of pancreatic islets comprises the nonclassical class Ib antigen HLA-G." Diabetes **55**(5): 1214-1222.

Clarke-Pearson, D. L. (2009). "Clinical practice. Screening for ovarian cancer." N Engl J Med **361**(2): 170-177.

Clements, C. S., L. Kjer-Nielsen, L. Kostenko, H. L. Hoare, M. A. Dunstone, E. Moses, K. Freed, A. G. Brooks, J. Rossjohn and J. McCluskey (2005). "Crystal structure of HLA-G: a nonclassical MHC class I molecule expressed at the fetal-maternal interface." Proc Natl Acad Sci U S A **102**(9): 3360-3365.

Collaborative Group on Epidemiological Studies of Ovarian, C., V. Beral, K. Gaitskell, C. Hermon, K. Moser, G. Reeves and R. Peto (2012). "Ovarian cancer and smoking: individual participant meta-analysis including 28,114 women with ovarian cancer from 51 epidemiological studies." Lancet Oncol **13**(9): 946-956.

Colonna, M., F. Navarro, T. Bellon, M. Llano, P. Garcia, J. Samaridis, L. Angman, M. Cella and M. Lopez-Botet (1997). "A common inhibitory receptor for major histocompatibility complex class I molecules on human lymphoid and myelomonocytic cells." J Exp Med **186**(11): 1809-1818.

Colonna, M., J. Samaridis, M. Cella, L. Angman, R. L. Allen, C. A. O'Callaghan, R. Dunbar, G. S. Ogg, V. Cerundolo and A. Rolink (1998). "Human myelomonocytic cells express an inhibitory receptor for classical and nonclassical MHC class I molecules." J Immunol **160**(7): 3096-3100.

Comiskey, M., C. Y. Goldstein, S. R. De Fazio, M. Mammolenti, J. A. Newmark and C. M. Warner (2003). "Evidence that HLA-G is the functional homolog of mouse Qa-2, the Ped gene product." Hum Immunol **64**(11): 999-1004.

Consuegra, S. and C. Garcia de Leaniz (2008). "MHC-mediated mate choice increases parasite resistance in salmon." Proc Biol Sci **275**(1641): 1397-1403.

Contini, P., M. Ghio, A. Poggi, G. Filaci, F. Indiveri, S. Ferrone and F. Puppo (2003). "Soluble HLA-A,-B,-C and -G molecules induce apoptosis in T and NK CD8+ cells and inhibit cytotoxic T cell activity through CD8 ligation." Eur J Immunol **33**(1): 125-134.

Cooper, M. A., T. A. Fehniger and M. A. Caligiuri (2001). "The biology of human natural killer-cell subsets." Trends Immunol **22**(11): 633-640.

Coquet, J. M., J. C. Ribot, N. Babala, S. Middendorp, G. van der Horst, Y. Xiao, J. F. Neves, D. Fonseca-Pereira, H. Jacobs, D. J. Pennington, B. Silva-Santos and J. Borst (2013). "Epithelial and dendritic cells in the thymic medulla promote CD4+Foxp3+ regulatory T cell development via the CD27-CD70 pathway." J Exp Med **210**(4): 715-728.

Cosman, D., N. Fanger, L. Borges, M. Kubin, W. Chin, L. Peterson and M. L. Hsu (1997). "A novel immunoglobulin superfamily receptor for cellular and viral MHC class I molecules." Immunity **7**(2): 273-282.

Crisa, L., M. T. McMaster, J. K. Ishii, S. J. Fisher and D. R. Salomon (1997). "Identification of a thymic epithelial cell subset sharing expression of the class Ib HLA-G molecule with fetal trophoblasts." J Exp Med **186**(2): 289-298.

Dahl, M., T. L. Perin, S. Djurisic, M. Rasmussen, J. Ohlsson, S. Buus, A. Lindhard and T. V. Hviid (2014). "Soluble human leukocyte antigen-G in seminal plasma is associated with HLA-G genotype: possible implications for fertility success." Am J Reprod Immunol **72**(1): 89-105.

Davidson, B., M. B. Elstrand, M. T. McMaster, A. Berner, R. J. Kurman, B. Risberg, C. G. Trope and M. Shih Ie (2005). "HLA-G expression in effusions is a possible marker of tumor susceptibility to chemotherapy in ovarian carcinoma." Gynecol Oncol **96**(1): 42-47.

Davis, D. M. (2007). "Intercellular transfer of cell-surface proteins is common and can affect many stages of an immune response." Nat Rev Immunol **7**(3): 238-243.

de la Rochebrochard, E. and P. Thonneau (2002). "Paternal age and maternal age are risk factors for miscarriage; results of a multicentre European study." Hum Reprod **17**(6): 1649-1656.

Delon, J., C. Gregoire, B. Malissen, S. Darche, F. Lemaitre, P. Kourilsky, J. P. Abastado and A. Trautmann (1998). "CD8 expression allows T cell signaling by monomeric peptide-MHC complexes." Immunity **9**(4): 467-473.

Diefenbach, A. and D. H. Raulet (2002). "The innate immune response to tumors and its role in the induction of T-cell immunity." Immunol Rev **188**: 9-21.

Dunn, G. P., A. T. Bruce, H. Ikeda, L. J. Old and R. D. Schreiber (2002). "Cancer immunoediting: from immunosurveillance to tumor escape." Nat Immunol **3**(11): 991-998.

Dunn, G. P., L. J. Old and R. D. Schreiber (2004). "The three Es of cancer immunoediting." Annu Rev Immunol **22**: 329-360.

Eisenkop, S. M., R. L. Friedman and H. J. Wang (1998). "Complete cytoreductive surgery is feasible and maximizes survival in patients with advanced epithelial ovarian cancer: a prospective study." Gynecol Oncol **69**(2): 103-108.

Eisenthal, A., N. Polyvkin, L. Bramante-Schreiber, F. Misonznik, A. Hassner and B. Lifschitz-Mercer (2001). "Expression of dendritic cells in ovarian tumors correlates with clinical outcome in patients with ovarian cancer." Hum Pathol **32**(8): 803-807.

Fevrier, B. and G. Raposo (2004). "Exosomes: endosomal-derived vesicles shipping extracellular messages." Curr Opin Cell Biol **16**(4): 415-421.

Fons, P., S. Chabot, J. E. Cartwright, F. Lenfant, F. L'Faqihi, J. Giustiniani, J. P. Herault, G. Gueguen, F. Bono, P. Savi, M. Aguerre-Girr, S. Fournel, F. Malecaze, A. Bensussan, J. Plouet and P. Le Bouteiller (2006). "Soluble HLA-G1 inhibits angiogenesis through an apoptotic pathway and by direct binding to CD160 receptor expressed by endothelial cells." Blood **108**(8): 2608-2615.

Gajewski, T. F., H. Schreiber and Y. X. Fu (2013). "Innate and adaptive immune cells in the tumor microenvironment." Nat Immunol **14**(10): 1014-1022.

Garcia, A. and H. Singh (2013). "Bevacizumab and ovarian cancer." Ther Adv Med Oncol **5**(2): 133-141.

Garcia-Enguidanos, A., M. E. Calle, J. Valero, S. Luna and V. Dominguez-Rojas (2002). "Risk factors in miscarriage: a review." Eur J Obstet Gynecol Reprod Biol **102**(2): 111-119.

Geraghty, D. E., B. H. Koller and H. T. Orr (1987). "A human major histocompatibility complex class I gene that encodes a protein with a shortened cytoplasmic segment." Proc Natl Acad Sci U S A **84**(24): 9145-9149.

Gobin, S. J. and P. J. van den Elsen (2000). "Transcriptional regulation of the MHC class Ib genes HLA-E, HLA-F, and HLA-G." Hum Immunol **61**(11): 1102-1107.

Goff, B. (2012). "Symptoms associated with ovarian cancer." Clin Obstet Gynecol **55**(1): 36-42.

Gonen-Gross, T., H. Achdout, T. I. Arnon, R. Gazit, N. Stern, V. Horejsi, D. Goldman-Wohl, S. Yagel and O. Mandelboim (2005). "The CD85J/leukocyte inhibitory receptor-1 distinguishes between conformed and beta 2-microglobulin-free HLA-G molecules." J Immunol **175**(8): 4866-4874.

Goodridge, J. P., A. Burian, N. Lee and D. E. Geraghty (2013). "HLA-F and MHC class I open conformers are ligands for NK cell Ig-like receptors." J Immunol **191**(7): 3553-3562.

Goodridge, J. P., C. S. Witt, F. T. Christiansen and H. S. Warren (2003). "KIR2DL4 (CD158d) genotype influences expression and function in NK cells." J Immunol **171**(4): 1768-1774.

Gotlieb, W. H., J. S. Abrams, J. M. Watson, T. J. Velu, J. S. Berek and O. Martinez-Maza (1992). "Presence of interleukin 10 (IL-10) in the ascites of patients with ovarian and other intra-abdominal cancers." Cytokine **4**(5): 385-390.

Gregori, S., C. F. Magnani and M. G. Roncarolo (2009). "Role of human leukocyte antigen-G in the induction of adaptive type 1 regulatory T cells." Hum Immunol **70**(12): 966-969.

Gregori, S., D. Tomasoni, V. Pacciani, M. Scirpoli, M. Battaglia, C. F. Magnani, E. Hauben and M. G. Roncarolo (2010). "Differentiation of type 1 T regulatory cells (Tr1) by tolerogenic DC-10 requires the IL-10-dependent ILT4/HLA-G pathway." Blood **116**(6): 935-944.

Gruen, J. R. and S. M. Weissman (2001). "Human MHC class III and IV genes and disease associations." Front Biosci **6**: D960-972.

Hackmon, R., A. Koifman, H. Hyodo, H. Glickman, E. Sheiner and D. E. Geraghty (2007). "Reduced third-trimester levels of soluble human leukocyte antigen G protein in severe preeclampsia." Am J Obstet Gynecol **197**(3): 255 e251-255.

Han, L. Y., M. S. Fletcher, D. L. Urbauer, P. Mueller, C. N. Landen, A. A. Kamat, Y. G. Lin, W. M. Merritt, W. A. Spannuth, M. T. Deavers, K. De Geest, D. M. Gershenson, S. K. Lutgendorf, S. Ferrone and A. K. Sood (2008). "HLA class I antigen processing machinery component expression and intratumoral T-Cell infiltrate as independent prognostic markers in ovarian carcinoma." Clin Cancer Res **14**(11): 3372-3379.

Hanahan, D. and R. A. Weinberg (2000). "The hallmarks of cancer." Cell **100**(1): 57-70.

Hanahan, D. and R. A. Weinberg (2011). "Hallmarks of cancer: the next generation." Cell **144**(5): 646-674.

Harris, S. G., J. Padilla, L. Koumas, D. Ray and R. P. Phipps (2002). "Prostaglandins as modulators of immunity." Trends Immunol **23**(3): 144-150.

Harrison, M. L., C. Jameson and M. E. Gore (2008). "Mucinous ovarian cancer." Int J Gynecol Cancer **18**(2): 209-214.

Hausler, S. F., I. Montalban del Barrio, J. Strohschein, P. A. Chandran, J. B. Engel, A. Honig, M. Ossadnik, E. Horn, B. Fischer, M. Krockenberger, S. Heuer, A. A. Seida, M. Junker, H. Kneitz, D. Kloor, K. N. Klotz, J. Dietl and J. Wischhusen (2011). "Ectonucleotidases CD39 and CD73 on OvCA cells are potent adenosine-generating enzymes responsible for adenosine receptor 2A-dependent suppression of T cell function and NK cell cytotoxicity." Cancer Immunol Immunother **60**(10): 1405-1418.

Horton, R., L. Wilming, V. Rand, R. C. Lovering, E. A. Bruford, V. K. Khodiyar, M. J. Lush, S. Povey, C. C. Talbot, Jr., M. W. Wright, H. M. Wain, J. Trowsdale, A. Ziegler and S. Beck (2004). "Gene map of the extended human MHC." Nat Rev Genet **5**(12): 889-899.

Hoskins, P. J., N. Le, B. Gilks, A. Tinker, J. Santos, F. Wong and K. D. Swenerton (2012). "Low-stage ovarian clear cell carcinoma: population-based outcomes in British Columbia, Canada, with evidence for a survival benefit as a result of irradiation." J Clin Oncol **30**(14): 1656-1662.

Hunt, J. S., D. K. Langat, R. H. McIntire and P. J. Morales (2006). "The role of HLA-G in human pregnancy." Reprod Biol Endocrinol **4 Suppl 1**: S10.

Ivanova-Todorova, E., M. Mourdjeva, D. Kyurkchiev, I. Bochev, E. Stoyanova, R. Dimitrov, T. Timeva, M. Yunakova, D. Bukarev, A. Shterev, P. Tivchev and S. Kyurkchiev (2009). "HLA-G expression is up-regulated by progesterone in mesenchymal stem cells." Am J Reprod Immunol **62**(1): 25-33.

Jayson, G. C., E. C. Kohn, H. C. Kitchener and J. A. Ledermann (2014). "Ovarian cancer." Lancet **384**(9951): 1376-1388.

Jemal, A., F. Bray, M. M. Center, J. Ferlay, E. Ward and D. Forman (2011). "Global cancer statistics." CA Cancer J Clin **61**(2): 69-90.

Joly, E. and D. Hudrisier (2003). "What is trogocytosis and what is its purpose?" Nat Immunol **4**(9): 815.

Juch, H., A. Blaschitz, C. Daxbock, C. Rueckert, K. Kofler and G. Dohr (2005). "A novel sandwich ELISA for alpha1 domain based detection of soluble HLA-G heavy chains." J Immunol Methods **307**(1-2): 96-106.

Jung, Y. W., Y. T. Kim, S. W. Kim, S. Kim, J. H. Kim, N. H. Cho and J. W. Kim (2009). "Correlation of human leukocyte antigen-G (HLA-G) expression and disease progression in epithelial ovarian cancer." Reprod Sci **16**(11): 1103-1111.

Kandalaft, L. E., G. T. Motz, J. Duraiswamy and G. Coukos (2011). "Tumor immune surveillance and ovarian cancer: lessons on immune mediated tumor rejection or tolerance." Cancer Metastasis Rev **30**(1): 141-151.

King, M. C., J. H. Marks, J. B. Mandell and G. New York Breast Cancer Study (2003). "Breast and ovarian cancer risks due to inherited mutations in BRCA1 and BRCA2." Science **302**(5645): 643-646.

Kleiner, G., A. Marcuzzi, V. Zanin, L. Monasta and G. Zauli (2013). "Cytokine levels in the serum of healthy subjects." Mediators Inflamm **2013**: 434010.

Koebel, C. M., W. Vermi, J. B. Swann, N. Zerafa, S. J. Rodig, L. J. Old, M. J. Smyth and R. D. Schreiber (2007). "Adaptive immunity maintains occult cancer in an equilibrium state." Nature **450**(7171): 903-907.

Krockenberger, M., Y. Dombrowski, C. Weidler, M. Ossadnik, A. Honig, S. Hausler, H. Voigt, J. C. Becker, L. Leng, A. Steinle, M. Weller, R. Bucala, J. Dietl and J. Wischhusen (2008). "Macrophage migration inhibitory factor contributes to the immune escape of ovarian cancer by down-regulating NKG2D." J Immunol **180**(11): 7338-7348.

Kurman, R. J. (2013). "Origin and molecular pathogenesis of ovarian high-grade serous carcinoma." Ann Oncol **24 Suppl 10**: x16-21.

Landen, C. N., Jr., B. Goodman, A. A. Katre, A. D. Steg, A. M. Nick, R. L. Stone, L. D. Miller, P. V. Mejia, N. B. Jennings, D. M. Gershenson, R. C. Bast, Jr., R. L. Coleman, G. Lopez-Berestein and A. K. Sood (2010). "Targeting aldehyde dehydrogenase cancer stem cells in ovarian cancer." Mol Cancer Ther **9**(12): 3186-3199.

Le Bouteiller, P., N. Pizzato, A. Barakonyi and C. Solier (2003). "HLA-G, pre-eclampsia, immunity and vascular events." J Reprod Immunol **59**(2): 219-234.

Le Discorde, M., P. Moreau, P. Sabatier, J. M. Legeais and E. D. Carosella (2003). "Expression of HLA-G in human cornea, an immune-privileged tissue." Hum Immunol **64**(11): 1039-1044.

Le Page, M. E., J. P. Goodridge, E. John, F. T. Christiansen and C. S. Witt (2014). "Response to comment on "killer Ig-like receptor 2DL4 does not mediate NK cell IFN-gamma responses to soluble HLA-G preparations"." J Immunol **192**(9): 4003-4004.

Le Rond, S., C. Azéma, I. Krawice-Radanne, A. Durrbach, C. Guettier, E. D. Carosella and N. Rouas-Freiss (2006). "Evidence to Support the Role of HLA-G5 in Allograft Acceptance through Induction of Immunosuppressive/ Regulatory T Cells." The Journal of Immunology **176**(5): 3266-3276.

Leavy, O. (2013). "Regulatory T cells: the thymic medulla - a cradle for TReg cell development." Nat Rev Immunol **13**(5): 304.

Lee, Y., A. Miron, R. Drapkin, M. R. Nucci, F. Medeiros, A. Saleemuddin, J. Garber, C. Birch, H. Mou, R. W. Gordon, D. W. Cramer, F. D. McKeon and C. P. Crum (2007). "A candidate precursor to serous carcinoma that originates in the distal fallopian tube." J Pathol **211**(1): 26-35.

LeMaoult, J., J. Caumartin, M. Daouya, B. Favier, S. Le Rond, A. Gonzalez and E. D. Carosella (2007). "Immune regulation by pretenders: cell-to-cell transfers of HLA-G make effector T cells act as regulatory cells." Blood **109**(5): 2040-2048.

LeMaoult, J., K. Zafaranloo, C. Le Danff and E. D. Carosella (2005). "HLA-G up-regulates ILT2, ILT3, ILT4, and KIR2DL4 in antigen presenting cells, NK cells, and T cells." FASEB J **19**(6): 662-664.

Levy, G. and K. Purcell (2013). Premalignant & Malignant Disorders of the Ovaries & Oviducts. CURRENT Diagnosis & Treatment: Obstetrics & Gynecology.
Li, L. and W. B. Neaves (2006). "Normal stem cells and cancer stem cells: the niche matters." Cancer Res **66**(9): 4553-4557.

Liang, S., B. Baibakov and A. Horuzsko (2002). "HLA-G inhibits the functions of murine dendritic cells via the PIR-B immune inhibitory receptor." Eur J Immunol **32**(9): 2418-2426.

Lin, A., H. H. Xu, D. P. Xu, X. Zhang, Q. Wang and W. H. Yan (2013). "Multiple steps of HLA-G in ovarian carcinoma metastasis: alter NK cytotoxicity and induce matrix metalloproteinase-15 (MMP-15) expression." Hum Immunol **74**(4): 439-446.

Lin, A., W. H. Yan, H. H. Xu, M. F. Gan, J. F. Cai, M. Zhu and M. Y. Zhou (2007). "HLA-G expression in human ovarian carcinoma counteracts NK cell function." Ann Oncol **18**(11): 1804-1809.

Lin, A., X. Zhang, H. H. Xu, D. P. Xu, Y. Y. Ruan and W. H. Yan (2012). "HLA-G expression is associated with metastasis and poor survival in the Balb/c nu/nu murine tumor model with ovarian cancer." Int J Cancer **131**(1): 150-157.

Lindaman, A., A. Dowden and N. Zavazava (2006). "Soluble HLA-G molecules induce apoptosis in natural killer cells." Am J Reprod Immunol **56**(1): 68-76.

Lobo, N. A., Y. Shimono, D. Qian and M. F. Clarke (2007). "The biology of cancer stem cells." Annu Rev Cell Dev Biol **23**: 675-699.

Lodish H, Berk A, Matsudaira P, Kaiser CA, Krieger M, Scott MP, Zipursky SL and D. J (2004). Molecular Biology of the Cell. New York, WH Freeman.
Loercher, A. E., M. A. Nash, J. J. Kavanagh, C. D. Platsoucas and R. S. Freedman (1999). "Identification of an IL-10-producing HLA-DR-negative monocyte subset in the malignant ascites of patients with ovarian carcinoma that inhibits cytokine protein expression and proliferation of autologous T cells." J Immunol **163**(11): 6251-6260.

Lombardelli, L., M. Aguerre-Girr, F. Logiodice, O. Kullolli, Y. Casart, B. Polgar, A. Berrebi, S. Romagnani, E. Maggi, P. Le Bouteiller and M. P. Piccinni (2013). "HLA-G5 induces IL-4 secretion critical for successful pregnancy through differential expression of ILT2 receptor on decidual CD4(+) T cells and macrophages." J Immunol **191**(7): 3651-3662.

Mach, P., P. Blecharz, P. Basta, P. Marianowski, J. Skret-Magierlo, Z. Kojs, M. Grabiec and L. Wicherek (2010). "Differences in the soluble HLA-G blood serum concentration levels in patients with ovarian cancer and ovarian and deep endometriosis." Am J Reprod Immunol **63**(5): 387-395.

Mallet, V., A. Blaschitz, L. Crisa, C. Schmitt, S. Fournel, A. King, Y. W. Loke, G. Dohr and P. Le Bouteiller (1999). "HLA-G in the human thymus: a subpopulation of medullary epithelial but not CD83(+) dendritic cells expresses HLA-G as a membrane-bound and soluble protein." Int Immunol **11**(6): 889-898.

Malpica, A., M. T. Deavers, K. Lu, D. C. Bodurka, E. N. Atkinson, D. M. Gershenson and E. G. Silva (2004). "Grading ovarian serous carcinoma using a two-tier system." Am J Surg Pathol **28**(4): 496-504.

McMaster, M. T., C. L. Librach, Y. Zhou, K. H. Lim, M. J. Janatpour, R. DeMars, S. Kovats, C. Damsky and S. J. Fisher (1995). "Human placental HLA-G expression is restricted to differentiated cytotrophoblasts." J Immunol **154**(8): 3771-3778.

Medawar, P. B. (1953). "Some immunological and endocrinological problems raised by the evolution of viviparity in vertebrates." Symp Soc Exp Biol **44**: 320–338.

Menendez, L., L. D. Walker, L. V. Matyunina, K. A. Totten, B. B. Benigno and J. F. McDonald (2008). "Epigenetic changes within the promoter region of the HLA-G gene in ovarian tumors." Mol Cancer **7**: 43.

Menier, C., S. Prevot, E. D. Carosella and N. Rouas-Freiss (2009). "Human leukocyte antigen-G is expressed in advanced-stage ovarian carcinoma of high-grade histology." Hum Immunol **70**(12): 1006-1009.

Messer, G., J. Zemmour, H. T. Orr, P. Parham, E. H. Weiss and J. Girdlestone (1992). "HLA-J, a second inactivated class I HLA gene related to HLA-G and HLA-A. Implications for the evolution of the HLA-A-related genes." J Immunol **148**(12): 4043-4053.

MHC sequencing consortium (1999). "Complete sequence and gene map of a human major histocompatibility complex. The MHC sequencing consortium." Nature **401**(6756): 921-923.

Miki, Y., J. Swensen, D. Shattuck-Eidens, P. A. Futreal, K. Harshman, S. Tavtigian, Q. Liu, C. Cochran, L. M. Bennett, W. Ding and *et al*. (1994). "A strong candidate for the breast and ovarian cancer susceptibility gene BRCA1." Science **266**(5182): 66-71.

Miller, M. J., A. S. Hejazi, S. H. Wei, M. D. Cahalan and I. Parker (2004). "T cell repertoire scanning is promoted by dynamic dendritic cell behavior and random T cell motility in the lymph node." Proc Natl Acad Sci U S A **101**(4): 998-1003.

Mittal, D., M. M. Gubin, R. D. Schreiber and M. J. Smyth (2014). "New insights into cancer immunoediting and its three component phases--elimination, equilibrium and escape." Curr Opin Immunol **27**: 16-25.

Mittelbronn, M., P. Simon, C. Loffler, D. Capper, B. Bunz, P. Harter, H. Schlaszus, A. Schleich, G. Tabatabai, B. Goeppert, R. Meyermann, M. Weller and J. Wischhusen (2007). "Elevated HLA-E levels in human glioblastomas but not in grade I to III astrocytomas correlate with infiltrating CD8+ cells." J Neuroimmunol **189**(1-2): 50-58.

Mjosberg, J., J. Svensson, E. Johansson, L. Hellstrom, R. Casas, M. C. Jenmalm, R. Boij, L. Matthiesen, J. I. Jonsson, G. Berg and J. Ernerudh (2009). "Systemic reduction of functionally suppressive CD4dimCD25highFoxp3+ Tregs in human second trimester pregnancy is induced by progesterone and 17beta-estradiol." J Immunol **183**(1): 759-769.

Moffatt, S. L., V. A. Cartwright and T. H. Stumpf (2005). "Centennial review of corneal transplantation." Clin Experiment Ophthalmol **33**(6): 642-657.

Momburg, F. and P. Tan (2002). "Tapasin-the keystone of the loading complex optimizing peptide binding by MHC class I molecules in the endoplasmic reticulum." Mol Immunol **39**(3-4): 217-233.

Moreau, P., F. Adrian-Cabestre, C. Menier, V. Guiard, L. Gourand, J. Dausset, E. D. Carosella and P. Paul (1999). "IL-10 selectively induces HLA-G expression in human trophoblasts and monocytes." Int Immunol **11**(5): 803-811.

Moreau, P., E. Carosella, M. Teyssier, S. Prost, E. Gluckman, J. Dausset and M. Kirszenbaum (1995). "Soluble HLA-G molecule. An alternatively spliced HLA-G mRNA form candidate to encode it in peripheral blood mononuclear cells and human trophoblasts." Hum Immunol **43**(3): 231-236.

Moreau, P., O. Faure, S. Lefebvre, E. C. Ibrahim, M. O'Brien, L. Gourand, J. Dausset, E. D. Carosella and P. Paul (2001). "Glucocorticoid hormones upregulate levels of HLA-G transcripts in trophoblasts." Transplant Proc **33**(3): 2277-2280.

Mouillot, G., C. Marcou, P. Rousseau, N. Rouas-Freiss, E. D. Carosella and P. Moreau (2005). "HLA-G gene activation in tumor cells involves cis-acting epigenetic changes." Int J Cancer **113**(6): 928-936.

Mouillot, G., C. Marcou, I. Zidi, C. Guillard, D. Sangrouber, E. D. Carosella and P. Moreau (2007). "Hypoxia modulates HLA-G gene expression in tumor cells." Hum Immunol **68**(4): 277-285.

Mustea, A., D. Konsgen, E. I. Braicu, C. Pirvulescu, P. Sun, D. Sofroni, W. Lichtenegger and J. Sehouli (2006). "Expression of IL-10 in patients with ovarian carcinoma." Anticancer Res **26**(2C): 1715-1718.

Naji, A., S. Le Rond, A. Durrbach, I. Krawice-Radanne, C. Creput, M. Daouya, J. Caumartin, J. LeMaoult, E. D. Carosella and N. Rouas-Freiss (2007). "CD3+CD4low and CD3+CD8low are induced by HLA-G: novel human peripheral blood suppressor T-cell subsets involved in transplant acceptance." Blood **110**(12): 3936-3948.

Neefjes, J., M. L. Jongsma, P. Paul and O. Bakke (2011). "Towards a systems understanding of MHC class I and MHC class II antigen presentation." Nat Rev Immunol **11**(12): 823-836.

O'Brien, M., T. McCarthy, D. Jenkins, P. Paul, J. Dausset, E. D. Carosella and P. Moreau (2001). "Altered HLA-G transcription in pre-eclampsia is associated with allele specific inheritance: possible role of the HLA-G gene in susceptibility to the disease." Cell Mol Life Sci **58**(12-13): 1943-1949.

O'Callaghan, C. A. and J. I. Bell (1998). "Structure and function of the human MHC class Ib molecules HLA-E, HLA-F and HLA-G." Immunol Rev **163**: 129-138.

O'Dwyer, T. W. and G. A. Nevitt (2009). "Individual odor recognition in procellariiform chicks: potential role for the major histocompatibility complex." Ann N Y Acad Sci **1170**: 442-446.

Palucka, K. and J. Banchereau (2012). "Cancer immunotherapy via dendritic cells." Nat Rev Cancer **12**(4): 265-277.

Partridge, E., A. R. Kreimer, R. T. Greenlee, C. Williams, J. L. Xu, T. R. Church, B. Kessel, C. C. Johnson, J. L. Weissfeld, C. Isaacs, G. L. Andriole, S. Ogden, L. R. Ragard, S. S. Buys and P. P. Team (2009). "Results from four rounds of ovarian cancer screening in a randomized trial." Obstet Gynecol **113**(4): 775-782.

Passos, G. A., D. A. Mendes-da-Cruz and E. H. Oliveira (2015). "The Thymic Orchestration Involving Aire, miRNAs, and Cell-Cell Interactions during the Induction of Central Tolerance." Front Immunol **6**: 352.

Paul, P., N. Rouas-Freiss, P. Moreau, F. A. Cabestre, C. Menier, I. Khalil-Daher, C. Pangault, M. Onno, R. Fauchet, J. Martinez-Laso, P. Morales, A. A. Villena, P. Giacomini, P. G. Natali, G. Frumento, G. B. Ferrara, M. McMaster, S. Fisher, D. Schust, S. Ferrone, J. Dausset, D. Geraghty and E. D. Carosella (2000). "HLA-G, -E, -F preworkshop: tools and protocols for analysis of non-classical class I genes transcription and protein expression." Hum Immunol **61**(11): 1177-1195.

Perren, T. J., A. M. Swart, J. Pfisterer, J. A. Ledermann, E. Pujade-Lauraine, G. Kristensen, M. S. Carey, P. Beale, A. Cervantes, C. Kurzeder, A. du Bois, J. Sehouli, R. Kimmig, A. Stahle, F. Collinson, S. Essapen, C. Gourley, A. Lortholary, F. Selle, M. R. Mirza, A. Leminen, M. Plante, D. Stark, W. Qian, M. K. Parmar, A. M. Oza and I. Investigators (2011). "A phase 3 trial of bevacizumab in ovarian cancer." N Engl J Med **365**(26): 2484-2496.

Pistoia, V., F. Morandi, X. Wang and S. Ferrone (2007). "Soluble HLA-G: Are they clinically relevant?" Semin Cancer Biol **17**(6): 469-479.

Prat, J. (2012). "New insights into ovarian cancer pathology." Ann Oncol **23 Suppl 10**: x111-117.

Prat, J. and F. C. o. G. Oncology (2014). "Staging classification for cancer of the ovary, fallopian tube, and peritoneum." Int J Gynaecol Obstet **124**(1): 1-5.

Prat, J. and F. C. o. G. Oncology (2015). "FIGO's staging classification for cancer of the ovary, fallopian tube, and peritoneum: abridged republication." J Gynecol Oncol **26**(2): 87-89.

Pujade-Lauraine, E., F. Hilpert, B. Weber, A. Reuss, A. Poveda, G. Kristensen, R. Sorio, I. Vergote, P. Witteveen, A. Bamias, D. Pereira, P. Wimberger, A. Oaknin, M. R. Mirza, P. Follana, D. Bollag and I. Ray-Coquard (2014). "Bevacizumab combined with

chemotherapy for platinum-resistant recurrent ovarian cancer: The AURELIA open-label randomized phase III trial." J Clin Oncol **32**(13): 1302-1308.

Qian, F., J. Villella, P. K. Wallace, P. Mhawech-Fauceglia, J. D. Tario, Jr., C. Andrews, J. Matsuzaki, D. Valmori, M. Ayyoub, P. J. Frederick, A. Beck, J. Liao, R. Cheney, K. Moysich, S. Lele, P. Shrikant, L. J. Old and K. Odunsi (2009). "Efficacy of levo-1-methyl tryptophan and dextro-1-methyl tryptophan in reversing indoleamine-2,3-dioxygenase-mediated arrest of T-cell proliferation in human epithelial ovarian cancer." Cancer Res **69**(13): 5498-5504.

Raghuraman, G., P. E. Lapinski and M. Raghavan (2002). "Tapasin interacts with the membrane-spanning domains of both TAP subunits and enhances the structural stability of TAP1 x TAP2 Complexes." J Biol Chem **277**(44): 41786-41794.

Rajagopalan, S., Y. T. Bryceson, S. P. Kuppusamy, D. E. Geraghty, A. van der Meer, I. Joosten and E. O. Long (2006). "Activation of NK cells by an endocytosed receptor for soluble HLA-G." PLoS Biol **4**(1): e9.

Rajagopalan, S. and E. O. Long (1999). "A human histocompatibility leukocyte antigen (HLA)-G-specific receptor expressed on all natural killer cells." J Exp Med **189**(7): 1093-1100.

Rajagopalan, S. and E. O. Long (2012). "KIR2DL4 (CD158d): An activation receptor for HLA-G." Front Immunol **3**: 258.

Raulet, D. H. and N. Guerra (2009). "Oncogenic stress sensed by the immune system: role of natural killer cell receptors." Nat Rev Immunol **9**(8): 568-580.

Rebmann, V., M. Switala, I. Eue and H. Grosse-Wilde (2010). "Soluble HLA-G is an independent factor for the prediction of pregnancy outcome after ART: a German multi-centre study." Hum Reprod **25**(7): 1691-1698.

Reya, T., S. J. Morrison, M. F. Clarke and I. L. Weissman (2001). "Stem cells, cancer, and cancer stem cells." Nature **414**(6859): 105-111.

Ries, L. Y., JL; Keel, GE; Eisner, MP; Lin, YD; Horner, M-J (2007). SEER Survival Monograph: Cancer Survival Among Adults: U.S. SEER Program, 1988-2001, Patient and Tumor Characteristics.

Riteau, B., F. Faure, C. Menier, S. Viel, E. D. Carosella, S. Amigorena and N. Rouas-Freiss (2003). "Exosomes bearing HLA-G are released by melanoma cells." Hum Immunol **64**(11): 1064-1072.

Rizzo, R., D. Bortolotti, S. Bolzani and E. Fainardi (2014). "HLA-G Molecules in Autoimmune Diseases and Infections." Front Immunol **5**: 592.

Rizzo, R., A. Trentini, D. Bortolotti, M. C. Manfrinato, A. Rotola, M. Castellazzi, L. Melchiorri, D. Di Luca, F. Dallocchio, E. Fainardi and T. Bellini (2013). "Matrix metalloproteinase-2 (MMP-2) generates soluble HLA-G1 by cell surface proteolytic shedding." Mol Cell Biochem **381**(1-2): 243-255.

Rizzo, R., M. Vercammen, H. van de Velde, P. A. Horn and V. Rebmann (2011). "The importance of HLA-G expression in embryos, trophoblast cells, and embryonic stem cells." Cell Mol Life Sci **68**(3): 341-352.

Rodgers, J. R. and R. G. Cook (2005). "MHC class Ib molecules bridge innate and acquired immunity." Nat Rev Immunol **5**(6): 459-471.

Rodriguez, G. C., J. T. Soper, A. Berchuck, J. Oleson, R. Dodge, G. Montana and D. L. Clarke-Pearson (1992). "Improved palliation of cerebral metastases in epithelial ovarian cancer using a combined modality approach including radiation therapy, chemotherapy, and surgery." J Clin Oncol **10**(10): 1553-1560.

Rouas-Freiss, N., S. Bruel, C. Menier, C. Marcou, P. Moreau and E. D. Carosella (2005). "Switch of HLA-G alternative splicing in a melanoma cell line causes loss of HLA-G1 expression and sensitivity to NK lysis." Int J Cancer **117**(1): 114-122.

Rouas-Freiss, N., P. Moreau, S. Ferrone and E. D. Carosella (2005). "HLA-G proteins in cancer: do they provide tumor cells with an escape mechanism?" Cancer Res **65**(22): 10139-10144.

Ruiz, P., P. Maldonado, Y. Hidalgo, A. Gleisner, D. Sauma, C. Silva, J. J. Saez, S. Nunez, M. Rosemblatt and M. R. Bono (2013). "Transplant tolerance: new insights and strategies for long-term allograft acceptance." Clin Dev Immunol **2013**: 210506.

Rutten, M. J., F. Dijk, C. D. Savci-Heijink, M. R. Buist, G. G. Kenter, M. J. van de Vijver and E. S. Jordanova (2014). "HLA-G expression is an independent predictor for improved survival in high grade ovarian carcinomas." J Immunol Res **2014**: 274584.

Sato, E., S. H. Olson, J. Ahn, B. Bundy, H. Nishikawa, F. Qian, A. A. Jungbluth, D. Frosina, S. Gnjatic, C. Ambrosone, J. Kepner, T. Odunsi, G. Ritter, S. Lele, Y. T. Chen, H. Ohtani, L. J. Old and K. Odunsi (2005). "Intraepithelial CD8+ tumor-infiltrating lymphocytes and a high CD8+/regulatory T cell ratio are associated with favorable prognosis in ovarian cancer." Proc Natl Acad Sci U S A **102**(51): 18538-18543.

Schumacher, T. N. and R. D. Schreiber (2015). "Neoantigens in cancer immunotherapy." Science **348**(6230): 69-74.

Sensi, M. and A. Anichini (2006). "Unique tumor antigens: evidence for immune control of genome integrity and immunogenic targets for T cell-mediated patient-specific immunotherapy." Clin Cancer Res **12**(17): 5023-5032.

Shaw, P. A., M. Rouzbahman, E. S. Pizer, M. Pintilie and H. Begley (2009). "Candidate serous cancer precursors in fallopian tube epithelium of BRCA1/2 mutation carriers." Mod Pathol **22**(9): 1133-1138.

Shepherd, J. H. (1989). "Revised FIGO staging for gynaecological cancer." Br J Obstet Gynaecol **96**(8): 889-892.

Sheu, J. J. and M. Shih Ie (2007). "Clinical and biological significance of HLA-G expression in ovarian cancer." Semin Cancer Biol **17**(6): 436-443.

Shih Ie, M. and R. J. Kurman (2004). "Ovarian tumorigenesis: a proposed model based on morphological and molecular genetic analysis." Am J Pathol **164**(5): 1511-1518.

Shiroishi, M., K. Kuroki, T. Ose, L. Rasubala, I. Shiratori, H. Arase, K. Tsumoto, I. Kumagai, D. Kohda and K. Maenaka (2006). "Efficient leukocyte Ig-like receptor signaling and crystal structure of disulfide-linked HLA-G dimer." J Biol Chem **281**(15): 10439-10447.

Shiroishi, M., K. Tsumoto, K. Amano, Y. Shirakihara, M. Colonna, V. M. Braud, D. S. Allan, A. Makadzange, S. Rowland-Jones, B. Willcox, E. Y. Jones, P. A. van der Merwe, I. Kumagai and K. Maenaka (2003). "Human inhibitory receptors Ig-like transcript 2 (ILT2) and ILT4 compete with CD8 for MHC class I binding and bind preferentially to HLA-G." Proc Natl Acad Sci U S A **100**(15): 8856-8861.

Silverberg, S. G. (2000). "Histopathologic grading of ovarian carcinoma: a review and proposal." Int J Gynecol Pathol **19**(1): 7-15.

Singer, G., V. Rebmann, Y. C. Chen, H. T. Liu, S. Z. Ali, J. Reinsberg, M. T. McMaster, K. Pfeiffer, D. W. Chan, E. Wardelmann, H. Grosse-Wilde, C. C. Cheng, R. J. Kurman and M. Shih Ie (2003). "HLA-G is a potential tumor marker in malignant ascites." Clin Cancer Res **9**(12): 4460-4464.

Siva, A., H. Xin, F. Qin, D. Oltean, K. S. Bowdish and A. Kretz-Rommel (2008). "Immune modulation by melanoma and ovarian tumor cells through expression of the immunosuppressive molecule CD200." Cancer Immunol Immunother **57**(7): 987-996.

Slukvin, II, D. I. Watkins and T. G. Golos (1999). "Tissue distribution of the mRNA for a rhesus monkey major histocompatibility class Ib molecule, Mamu-AG." Tissue Antigens **53**(3): 282-291.

Smith, L. H. (2006). "Early clinical detection of ovarian cancer: a review of the evidence." Expert Rev Anticancer Ther **6**(7): 1045-1052.

Spinella, F., L. Rosano, V. Di Castro, P. G. Natali and A. Bagnato (2004). "Endothelin-1-induced prostaglandin E2-EP2, EP4 signaling regulates vascular endothelial growth factor production and ovarian carcinoma cell invasion." J Biol Chem **279**(45): 46700-46705.

Steegers, E. A., P. von Dadelszen, J. J. Duvekot and R. Pijnenborg (2010). "Pre-eclampsia." Lancet **376**(9741): 631-644.

Steinmuller, D., J. D. Tyler, K. G. Waddick and W. J. Burlingham (1982). "Epidermal alloantigen and the survival of mouse skin allografts." Transplantation **33**(3): 308-313.

Streilein, J. W. (2003). "Ocular immune privilege: therapeutic opportunities from an experiment of nature." Nat Rev Immunol **3**(11): 879-889.

Strioga, M., V. Schijns, D. J. Powell, Jr., V. Pasukoniene, N. Dobrovolskiene and J. Michalek (2013). "Dendritic cells and their role in tumor immunosurveillance." Innate Immun **19**(1): 98-111.

Tajima, A., T. Tanaka, T. Ebata, K. Takeda, A. Kawasaki, J. M. Kelly, P. K. Darcy, R. E. Vance, D. H. Raulet, K. Kinoshita, K. Okumura, M. J. Smyth and H. Yagita (2003). "Blastocyst MHC, a putative murine homologue of HLA-G, protects TAP-deficient tumor cells from natural killer cell-mediated rejection in vivo." J Immunol **171**(4): 1715-1721.

Tan, D. S. and S. Kaye (2007). "Ovarian clear cell adenocarcinoma: a continuing enigma." J Clin Pathol **60**(4): 355-360.

Tothill, R. W., A. V. Tinker, J. George, R. Brown, S. B. Fox, S. Lade, D. S. Johnson, M. K. Trivett, D. Etemadmoghadam, B. Locandro, N. Traficante, S. Fereday, J. A. Hung, Y. E. Chiew, I. Haviv, G. Australian Ovarian Cancer Study, D. Gertig, A. DeFazio and D. D. Bowtell (2008). "Novel molecular subtypes of serous and endometrioid ovarian cancer linked to clinical outcome." Clin Cancer Res **14**(16): 5198-5208.

Tsilidis, K. K., N. E. Allen, T. J. Key, L. Dossus, A. Lukanova, K. Bakken, E. Lund, A. Fournier, K. Overvad, L. Hansen, A. Tjonneland, V. Fedirko, S. Rinaldi, I. Romieu, F. Clavel-Chapelon, P. Engel, R. Kaaks, M. Schutze, A. Steffen, C. Bamia, A. Trichopoulou, D. Zylis, G. Masala, V. Pala, R. Galasso, R. Tumino, C. Sacerdote, H. B. Bueno-de-Mesquita, F. J. van Duijnhoven, M. G. Braem, N. C. Onland-Moret, I. T. Gram, L. Rodriguez, N. Travier, M. J. Sanchez, J. M. Huerta, E. Ardanaz, N. Larranaga, K. Jirstrom, J. Manjer, A. Idahl, N. Ohlson, K. T. Khaw, N. Wareham, T. Mouw, T. Norat and E. Riboli (2011). "Oral contraceptive use and reproductive factors and risk of ovarian cancer in the European Prospective Investigation into Cancer and Nutrition." Br J Cancer **105**(9): 1436-1442.

Urosevic, M. and R. Dummer (2003). "HLA-G and IL-10 expression in human cancer--different stories with the same message." Semin Cancer Biol **13**(5): 337-342.

Vang, R., M. Shih Ie and R. J. Kurman (2009). "Ovarian low-grade and high-grade serous carcinoma: pathogenesis, clinicopathologic and molecular biologic features, and diagnostic problems." Adv Anat Pathol **16**(5): 267-282.

Verloes, A., H. Van de Velde, J. LeMaoult, I. Mateizel, G. Cauffman, P. A. Horn, E. D. Carosella, P. Devroey, M. De Waele, V. Rebmann and M. Vercammen (2011). "HLA-G expression in human embryonic stem cells and preimplantation embryos." J Immunol **186**(4): 2663-2671.

Vicari, A. P., C. Caux and G. Trinchieri (2002). "Tumour escape from immune surveillance through dendritic cell inactivation." Semin Cancer Biol **12**(1): 33-42.

Visser, N., B. B. van Rijn, G. T. Rijkers, A. Franx and H. W. Bruinse (2007). "Inflammatory changes in preeclampsia: current understanding of the maternal innate and adaptive immune response." Obstet Gynecol Surv **62**(3): 191-201.

Vitale, M., G. Pelusi, B. Taroni, G. Gobbi, C. Micheloni, R. Rezzani, F. Donato, X. Wang and S. Ferrone (2005). "HLA class I antigen down-regulation in primary ovary carcinoma lesions: association with disease stage." Clin Cancer Res **11**(1): 67-72.

Wiendl, H., M. Mitsdoerffer, V. Hofmeister, J. Wischhusen, A. Bornemann, R. Meyermann, E. H. Weiss, A. Melms and M. Weller (2002). "A functional role of HLA-G expression in human gliomas: an alternative strategy of immune escape." J Immunol **168**(9): 4772-4780.

Williams, A., C. A. Peh and T. Elliott (2002). "The cell biology of MHC class I antigen presentation." Tissue Antigens **59**(1): 3-17.

Woo, E. Y., C. S. Chu, T. J. Goletz, K. Schlienger, H. Yeh, G. Coukos, S. C. Rubin, L. R. Kaiser and C. H. June (2001). "Regulatory CD4(+)CD25(+) T cells in tumors from patients with early-stage non-small cell lung cancer and late-stage ovarian cancer." Cancer Res **61**(12): 4766-4772.

Wooster, R., G. Bignell, J. Lancaster, S. Swift, S. Seal, J. Mangion, N. Collins, S. Gregory, C. Gumbs and G. Micklem (1995). "Identification of the breast cancer susceptibility gene BRCA2." Nature **378**(6559): 789-792.

Yang, H. P., B. Trabert, M. A. Murphy, M. E. Sherman, J. N. Sampson, L. A. Brinton, P. Hartge, A. Hollenbeck, Y. Park and N. Wentzensen (2012). "Ovarian cancer risk factors by histologic subtypes in the NIH-AARP Diet and Health Study." Int J Cancer **131**(4): 938-948.

Yao, G. D., Y. M. Shu, S. L. Shi, Z. F. Peng, W. Y. Song, H. X. Jin and Y. P. Sun (2014). "Expression and potential roles of HLA-G in human spermatogenesis and early embryonic development." PLoS One **9**(3): e92889.

Yie, S. M., L. H. Li, Y. M. Li and C. Librach (2004). "HLA-G protein concentrations in maternal serum and placental tissue are decreased in preeclampsia." Am J Obstet Gynecol **191**(2): 525-529.

Yie, S. M., R. N. Taylor and C. Librach (2005). "Low plasma HLA-G protein concentrations in early gestation indicate the development of preeclampsia later in pregnancy." Am J Obstet Gynecol **193**(1): 204-208.

Yigit, R., L. F. Massuger, C. G. Figdor and R. Torensma (2010). "Ovarian cancer creates a suppressive microenvironment to escape immune elimination." Gynecol Oncol **117**(2): 366-372.

Yusa, S., T. L. Catina and K. S. Campbell (2002). "SHP-1- and phosphotyrosine-independent inhibitory signaling by a killer cell Ig-like receptor cytoplasmic domain in human NK cells." J Immunol **168**(10): 5047-5057.

Zhang, S., C. Balch, M. W. Chan, H. C. Lai, D. Matei, J. M. Schilder, P. S. Yan, T. H. Huang and K. P. Nephew (2008). "Identification and characterization of ovarian cancer-initiating cells from primary human tumors." Cancer Res **68**(11): 4311-4320.

Zitvogel, L., A. Tesniere and G. Kroemer (2006). "Cancer despite immunosurveillance: immunoselection and immunosubversion." Nat Rev Immunol **6**(10): 715-727.

Supplements

Table 5: Characteristics of tissue donors included in the FFPE Norm2 TMA

Tissue	Age	Sex	Tissue	Age	Sex
breast, epithelium	47	F	liver	76	M
aorta, smooth muscle	44	M	pancreas	67	F
heart, myocardium	51	M	lymph node	6	F
adrenal gland, cortex	51	M	mucosa assoc. lymph. tissue, appendix	66	F
adrenal gland, medulla	51	F	spleen	70	M
parathyroid (hyperplastic)	45	F	thymus	48	F
thyroid	38	F	cerebral cortex	64	M
esophagus, squamous mucosa	58	M	white matter (subcortical)	33	F
gastric mucosa, antral	59	F	peripheral nerve	50	F
gastric mucosa, oxyntic	53	F	salivary gland (parotid)	40	M
small intestine, mucosa	85	F	tonsil, squamous epithelium	24	M
colon, mucosa	66	M	amniotic membrane	21	F
anus, mucosa	39	F	placenta, villi	24	F
ectocervix	43	F	alveoli	43	M
endocervix	43	F	bronchus, epithelium	52	M
endometrium, secretory	45	F	skin, squamous epithelium	61	F
fallopian tube	49	F	cartilage, articular	43	M
ovary, oocytes	54	F	skeletal muscle	48	F
ovary, corpus luteum	49	F	smooth muscle, intestine	82	F
ovary, mesothelium	44	F	smooth muscle, uterus	56	F
seminiferous tubules	36	M	synovium	30	F
epididymis	66	M	kidney, cortex	47	F
seminal vessicle	44	M	kidney, medulla	61	M
prostate	52	M	bladder, transitional epithelium	49	M
gallbladder	56	M			

Table 6: Manufacturing company locations

Company	Location
Applied Biosystems	see Life Technologies
BD Pharmingen/BD Biosciences	see Becton, Dickinson and Company
Beckman Coulter	Brea, CA, USA
Becton, Dickinson and Company	Franklin Lakes, NJ, USA
Bio-Rad Laboratories, Inc.	Hercules, CA, USA
BioLegend	San Diego, CA, USA
Carl Roth GmbH & Co. KG	Karlsruhe, Germany
Cell Signaling Technologies	Danvers, MA, USA
Dako, Agilent Technologies	Santa Clara, CA, USA
Eastman Kodak	Rochester, NY, USA
eBioscience	San Diego, CA, USA
ExBio	ExBio, Praha, Czech Republic
ImmunoTools	Friesoythe, Germany
Leica Camera AG	Wetzlar, Germany
Life Technologies	Carlsbad, CA, USA
Miltenyi Biotec GmbH	Bergisch Gladbach, Germany
Molecular Probes	see Thermo Fisher
Sigma-Aldrich	St. Louis, MO, USA
Southern Biotech	Birmingham, AL, USA
Tecan Trading AG	Männedorf, Switzerland
Thermo Fisher Scientific Inc.	Waltham, MA, USA
Leica Biosystems Newcastle Ltd	Newcastle Upon Tyne, UK

Table 7: Alignment Qa-2 (H-2Q7) and Blastocyst MHC (H-2Bl)

```
H-2Q7 RTDPPKAHVTHHPRSYGAVTLRCWALGFYPADITLTWQLNGEELTQDMEL
      |||||||||||.|||..|.||||||||||||||||||||||||||||||||
H-2Bl RTDPPKAHVTRHPRPAGDVTLRCWALGFYPADITLTWQLNGEELTQDMEL

H-2Q7 VETRPAGDGTFQKWASVVVPLGKEQNYTCHVNHEGLPEPLTLRW
      |||||||||||||||:|||||||||||||.|:||||||||||||
H-2Bl VETRPAGDGTFQKWAAVVVPLGKEQNYTCRVHHEGLPEPLTLRW
```

Alpha 3 domains of Qa-2 and Blastocyst MHC were aligned using ClustalW.

Affidavit / Eidesstattliche Erklärung

Affidavit

I hereby confirm that my thesis entitled "Soluble HLA-G binds to dendritic cells which likely suppresses anti-tumour immune responses in regional lymph nodes in ovarian carcinoma" is the result of my own work. I did not receive any help or support from commercial consultants. All sources and / or materials applied are listed and specified in the thesis.

Furthermore, I confirm that this thesis has not yet been submitted as part of another examination process neither in identical nor in similar form.

Place, Date Signature

Eidesstattliche Erklärung

Hiermit erkläre ich an Eides statt, die Dissertation mit dem Titel " Lösliches HLA-G wird von dendritischen Zellen gebunden, was beim Ovarialkarzinom zur Hemmung von Immunraktionen in regionalen Lymphknoten führen kann" eigenständig, d.h. insbesondere selbständig und ohne Hilfe eines kommerziellen Promotionsberaters, angefertigt und keine anderen als die von mir angegebenen Quellen und Hilfsmittel verwendet zu haben.

Ich erkläre außerdem, dass die Dissertation weder in gleicher noch in ähnlicher Form bereits in einem anderen Prüfungsverfahren vorgelegen hat.

Ort, Datum Unterschrift

Acknowledgements

This thesis would not have been possible without substantial scientific, financial and family support.

First, I would like to thank my supervisor, Prof. Dr. Jörg Wischhusen, for providing the topic and giving me the opportunity to work in his lab. I am thankful for a great amount of scientific freedom that allowed me to develop and pursue different scientific ideas. For having always time for questions and for scientific discussions. For funding when my scholarship ran out. For establishing contacts to important cooperation partners. And for being supportive when I had to reschedule working hours because I had to look after a sick child during the day.

I would also like to thank Prof. Dr. Johannes Dietl and Prof. Dr. Achim Wöckel for giving me the opportunity to work in the Department for Gynaecology and Obstetrics of the University Hospital of Würzburg.

I would also like to thank Prof. Dr. Thomas Rudel and Dr. Thomas Joos for their advice and interest in my thesis and for contributing to this work as supervisors in my thesis committee.

Next, I would like to thank Prof. Dr. Eva Geißinger and Sabine Roth from the Institute of Pathology. Without your great help and expertise this project would not have been possible.

I would also like to express my appreciation to Lina Hilscher and Tamara Kuhfuß. It has been a pleasure to work with you during your internships and to supervise your Master's or Bachelor's theses. Here, I would like to also include Clemens Weiss who joined our lab for an internship. It was a great experience to work with such talented and motivated young scientists and I wish you best of luck for your future careers.

A very special thanks also goes to all my other colleagues in the lab. In no particular order, these include Birgitt Fischer, Itsaso Montalban, Evi Horn, Dr. Tina Schäfer, Dr. Laura Schlahsa, Franziska Grän, Kathrin Becker, Anna Schmidt, Petra Hauck, Anastasia Kuzkina, Dr. Anoop Chandran, Markus Junker, Dr. Dirk Pühringer, Dr. Achmed Seida, Dr. Joachim Diessner, Dr. Sebastian Häusler, Dr. Roland Stein, Dr. Markus Haake, Dr.

Stefan Ebert, Igor Vögele, Dr. Stefan Heuer, Raphael Hechinger and Tobias Kluge (I hope I have not forgotten anyone!). I would like to thank you for scientific discussions and advice in the lab and non-scientific discussions during lunch breaks and lab excursions. It was a pleasure to get to know all of you!

Furthermore, I would like to express my gratitude to Prof. Dr. Thomas Hünig and all members of the graduate program “immunomodulation” for vivid scientific discussions, help and advice, and good times particularly during retreats.

I am particularly grateful to the Deutsche Forschungsgemeinschaft (DFG) and the Graduate School of Life Sciences (GSLS) Würzburg for providing funding for my research for four years. I would also like to thank Dr. Gabriele Blum-Oehler for her patience and help in organisational or financial questions. Additionally, I would like to express my gratitude to the interdisciplinary center for clinical research (IZKF) Würzburg for further funding.

Finally, I am most grateful to Anna Nienaber for her encouragement, for keeping me grounded and focussed, for listening to my worries, for reducing her own working hours for the cause and for always being there for me and for our children when I needed her. This work would not have been possible without you. I also want to thank my and Anna’s family, particularly our parents and my sister Julika for their unconditional love and support for our young family during the last years. Last but not least, I want to thank Linus, Elea and Jorin for their smiles, their agility and their talent to deviate my thoughts, which at times can be very helpful.